



**US Army Corps  
of Engineers**

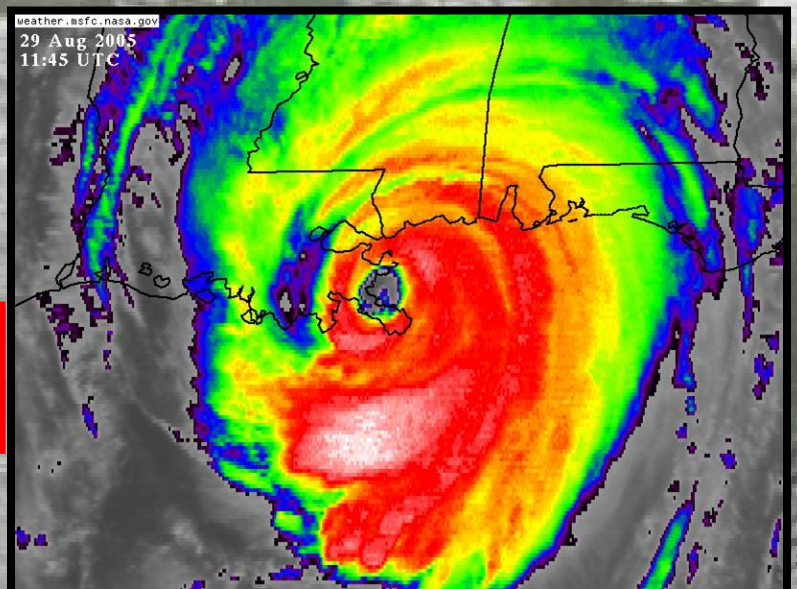
# **Performance Evaluation of the New Orleans and Southeast Louisiana Hurricane Protection System**

## **Final Report of the Interagency Performance Evaluation Task Force**

### **Volume V – The Performance — Levees and Floodwalls**

**June 2007**

**FINAL**



Volume I – Executive Summary and Overview  
Volume II – Geodetic Vertical and Water Level Datums  
Volume III – The Hurricane Protection System  
Volume IV – The Storm  
Volume V – The Performance – Levees and Floodwalls  
Volume VI – The Performance – Interior Drainage and Pumping  
Volume VII – The Consequences  
Volume VIII – Engineering and Operational Risk and Reliability Analysis  
Volume IX – General Appendices

**DISCLAIMER:** The contents of this report are not to be used for advertising, publication, or promotional purposes. Citation of trade names does not constitute an official endorsement or approval of the use of such commercial products. All product names and trademarks cited are the property of their respective owners. The findings of this report are not to be construed as an official Department of the Army position unless so designated by other authorized documents.

**Volume V**  
**The Performance — Levees and**  
**Floodwalls**

---

# Contents

Contents .....	ii
Executive Summary .....	1
Performance Analysis Team.....	2
Historical Data Collection Team .....	3
Perishable Data Collection Team .....	3
Physical Modeling Team.....	4
Floodwall and Levee Performance Analysis.....	5
Hurricane Protection System .....	7
Geology of the New Orleans Area.....	9
Physiography and Setting .....	10
Geologic History.....	12
Geologic Structure and Faulting.....	16
Holocene Environments of Deposition.....	16
Subsidence and Settlement.....	20
17th Street Canal Breach .....	21
Soil Conditions and Soil Properties.....	32
Shear Strength Assessment for Analysis of the 17th Street Canal Breach.....	35
Limit Equilibrium Stability Assessment.....	41
Centrifuge Modeling Results for the 17th Street Canal Breach .....	43
Finite Element Soil-Structure Interaction Results for the 17th Street Canal Breach.....	45
Summary of 17th Street Canal Breach Assessment .....	53
Assessment of London Avenue Canal Breaches.....	54
Seepage and Stability Analyses of the London Avenue Canal Breaches.....	58
Centrifuge Modeling Results for the London Avenue Canal Breaches .....	60
Finite Element Soil-Structure Interaction Results for London Avenue Canal Breaches.....	62
Summary of Assessment of the London Avenue Canal Breaches.....	67
Assessment of Inner Harbor Navigation Canal Breaches .....	67
Assessment of Orleans Canal and Michoud Canal I-Walls .....	74
Analysis of the Performance of the Orleans Canal I-Walls.....	75
Centrifuge Modeling Results for the Orleans Canal I-Wall .....	79
Analysis of the Performance of the Michoud Canal I-Walls.....	82
Levee Erosion and Scour from Overtopping .....	89
Failure Patterns.....	91
Levees.....	104
Transitions .....	122
Floodwall and Levee Performance Findings and Lessons Learned.....	123
Findings.....	123
Lessons Learned .....	124
Other Studies .....	125

- Appendix 1. Soil Data Report
- Appendix 2. Description of New Orleans Area Geology, Environments of Deposition, and General Engineer Properties of these Environments
- Appendix 3. 17th Street Canal Shear Strength Evaluation
- Appendix 4. 17th Street Canal Slope Stability Analyses
- Appendix 5. IPET Centrifuge Model Test Report
- Appendix 6. Soil-Structure Interaction Analysis of the Floodwall at 17th Street
- Appendix 7. Interim Data Report, London Avenue Outfall Canal
- Appendix 8. Analysis of the London Avenue Canal I-Wall Breaches
- Appendix 9. Soil-Structure Interaction Analysis of the Floodwalls at London Avenue Canal
- Appendix 10. Analysis of Performance of the Orleans Canal I-Walls
- Appendix 11. Analysis of Performance of the Inner Harbor Navigation Canal
- Appendix 12. Levee Damage Report – Geotechnical Investigation – New Orleans East (Orleans Parish)
- Appendix 13. Levee and Floodwall Erosion and Scour from Overtopping Storm Surge
- Appendix 14. General Description of New Orleans Basins and Damage from Hurricane Katrina
- Appendix 15. Concrete I-Wall and Sheet Piling Material Recovery, Sampling and Testing: 17th Street Canal Levee Breach
- Appendix 16. Concrete I-Wall and Sheet Piling Material Recovery, Sampling and Testing: IHNC
- Appendix 17. Finite Element Seepage Study
- Appendix 18. Erosion of New Orleans and St. Bernard Levees
- Appendix 19. FLAC Numerical Analyses of Floodwalls of New Orleans Flood Protection System
- Appendix 20. Glossary for Performance of Levees and Floodwalls
- Appendix 21. Regional Geology and History Overview
- Appendix 22. Response to NRC Comments on 17th Street Canal Geology
- Appendix 23. Analysis of the Stability of Michoud Canal

## Executive Summary

This report summarizes a comprehensive investigation of the performance of floodwalls and levees in New Orleans during Hurricane Katrina. In all, about 50 locations were studied, where breaches in the hurricane protection system (HPS) occurred due to overtopping and erosion, or due to structural instability.

The majority of the breaches resulted from erosion following overtopping of floodwalls or levees. Overtopping and erosion led to failure of I-walls when water cascading over the top of the walls scoured and eroded the soil on the protected side of the wall, eventually eroding away so much of the soil supporting the wall that the wall became unstable. Overtopping and erosion led to breaching of levees when the soils of which the levees were constructed had insufficient resistance to erosion to withstand the velocity of the water flowing down the protected side of the levee embankment, eventually cutting through the levee crest, washing out the levee.

Most alarming were the failures of I-walls that occurred before overtopping, as a result of foundation instability. Breaches resulting from failures of this type occurred at the 17th Street Canal and the Inner Harbor Navigation Canal (IHNC), where the failure occurred in weak foundation clay, and at the London Avenue Canal, where the instability resulted from intense seepage and high uplift water pressures in the sand foundation. A common element in these I-wall failures was development of a gap between the wall and the soil on the canal side of the wall. Water entered these gaps, increasing the water loads on the walls. Limit equilibrium stability analyses indicate that the factors of safety against instability dropped by about 25% when the gaps formed and water flowed into them. Limit equilibrium stability analyses, centrifuge model tests, and finite element soil-structure interaction analyses all indicated that gap formation played a key role in the instability of the walls. At the London Avenue I-wall, with sand beneath the levee and I-wall, the opening of the gap allowed water to flow down the back of the I-wall, introducing high water pressures into the sand, resulting in high uplift water pressures, increased hydraulic gradients, and greatly increased likelihood of subsurface erosion and piping on the protected side of the wall.

The clay in the foundations of the 17th Street Canal I-wall and the IHNC I-wall was found to be normally consolidated, with undrained shear strength that was lower beneath the levee slopes and beyond the toe than beneath the levee crest, where the clay had been compressed under higher pressure. This variation of the undrained strength of the clay with pressure was determined to be an important aspect of the foundation soil behavior, and a key factor in evaluation of stability.

The ability of levees to withstand overtopping without suffering extensive erosion varied significantly throughout the New Orleans area. The areas where the levees were made of clay performed well in spite of the fact that the levees were overtopped. In other areas, the levees were completely washed away after being overtopped. The difference in performance appears to depend on the type of material that was used to construct the levees. Grass covered semi-compacted clay levees withstood overtopping the best, and levees constructed of sand and silt by hydraulic filling suffered far more erosion from overtopping.

The investigations described in this report provide a basis for more reliable designs for floodwalls and levees, and the lessons learned from these studies have been incorporated in the design work of the Task Force Guardian team. The findings are also useful in assessing the current conditions and stability of the unfailed sections of the levees and floodwalls.

## Performance Analysis Team

<b>Name</b>	<b>Assignment</b>	<b>Organization</b>
Reed Mosher, PhD	<b>Co-Leader</b>	ERDC/GSL
Mike Duncan, PhD, PE	<b>Co-Leader</b>	Virginia Tech
George Sills, PE	Geotechnical	ERDC/GSL
Noah Vroman	Geotechnical	ERDC/GSL
Joe Dunbar	Geologist	ERDC/GSL
Ron Wahl, PE	Geotechnical Modeling	ERDC/GSL
Maureen Corcoran, PhD	Geologist	ERDC/GSL
Robert Ebeling, PhD, PE	Geotechnical Modeling	ERDC/ITL
Don Yule	Geotechnical Modeling	ERDC/GSL
Eileen Glynn	Geotechnical	ERDC/GSL
L. Tommy Lee	Geotechnical	ERDC/GSL
Paul Mlakar, PhD, PE	Structural	ERDC/GSL
Joe Padula, PhD, PE	Structural	ERDC/GSL
Kevin Abraham	Geotechnical Modeling	ERDC/ITL
Mike Pace	Geotechnical Modeling	ERDC/ITL
Benita Abraham	Data Support	ERDC/GSL
Tony Young, PE	Geotechnical	MVD
Ken Klaus, PE	Geotechnical	MVD
Richard Pinner, PE	Geotechnical	MVD
Pete Cali, PhD, PE	Geotechnical	MVD
Tom Brandon, PhD, PE	Geotechnical	Virginia Tech
Steve Wright, PhD, PE	Slope Stability	University of Texas
Allen Marr, PhD, PE	PLAXIS Analysis	GeoComp
Thomas McGill	GIS Analysis	ERDC/GSL
Laurel Gorman	GIS Analysis	ERDC/ITL
Johannes L. Wibowo	Geotechnical	ERDC/GSL
Perry A. Taylor	Geotechnical	ERDC/GSL

## Historical Data Collection Team

<b>Name</b>	<b>Assignment</b>	<b>Organization</b>
Maureen Corcoran, PhD	<b>Co-Leader</b>	ERDC-GSL
Reed Mosher, PhD	<b>Co-Leader</b>	ERDC-GSL
Benita Abraham	Data Collection	ERDC-GSL
Bernice Bass	Data Collection	ERDC-GSL
Glenda Brandon	Data Collection	ERDC-GSL
Vickey Davis	Data Collection	ERDC-GSL
Beverly DiPaolo, PhD	Data Collection	ERDC-GSL
Vikki Edwards	Data Collection	ERDC-GSL
Eileen Glynn	Data Collection	ERDC-GSL
Blaise Grden	Data Collection	ERDC-ITL
Tina Holmes	Data Collection	ERDC-GSL
Edward Huell	Data Collection	ERDC-ITL
Bob Larson	Data Collection	ERDC-GSL
L. Tommy Lee	Data Collection	ERDC-GSL
Cheri Loden	Data Collection	ERDC-GSL
Sharon McBride	Data Collection	ERDC-GSL
Tiffany Mims	Data Collection	ERDC-GSL
Hattie Smith	Data Collection	ERDC-GSL
Charlie Whitten	Data Collection	ERDC-GSL
Sue Wolfe	Data Collection	ERDC-GSL

## Perishable Data Collection Team

<b>Name</b>	<b>Assignment</b>	<b>Organization</b>
Reed Mosher, PhD	<b>Task Leader</b>	ERDC-GSL
Paul Mlakar, PhD, PE	<b>Onsite Leader</b>	ERDC-GSL
Beverly DiPaolo, PhD	Structural	ERDC-GSL
Joe Dunbar	Geology	ERDC-GSL
Eileen Glynn	Geotechnical	ERDC-GSL
Rick Haskins	Parallel Seismic	ERDC-ITL
Ken Klaus	Geotechnical	MVD
Rick Olsen	Geotechnical	ERDC-GSL
Joe Padula, PhD, PE	Structural	ERDC-GSL
Guillermo Riveros	Structural	ERDC-ITL
George Sills, PE	Geotechnical	ERDC-GSL



Evelyn Villanueva	Geology	ERDC-GSL
Noah Vroman	Geotechnical	ERDC-GSL
Don Yule	Geotechnical	ERDC-GSL

### Physical Modeling Team

<b>Name</b>	<b>Assignment</b>	<b>Organization</b>
Michael K. Sharp, PhD, PE	<b>Co-Leader</b>	USACE-ERDC
R. Scott Steedman, PhD, FREng	<b>Co-Leader</b>	Steedman & Associates, LTD
Henry Blake	Instrumentation	USACE-ERDC
David Carnell	Instrumentation	USACE-ERDC
David Daily	Instrumentation	USACE-ERDC
Wayne Hodo	Geotechnical Centrifuge Modeling	USACE-ERDC
Wipawi Vanadit-Ellis	Geotechnical Centrifuge Modeling	USACE-ERDC
Tarek Abdoun, PhD	Geotechnical Centrifuge Modeling	Rensselaer Polytechnic Institute
Marcelo Gonzalez, MS	Geotechnical Centrifuge Modeling	Rensselaer Polytechnic Institute
Dominic Moffitt	Geotechnical Centrifuge Modeling	Rensselaer Polytechnic Institute
Hassan Radwan	Geotechnical Centrifuge Modeling	Rensselaer Polytechnic Institute
Alex Sankovich	Geotechnical Centrifuge Modeling	Rensselaer Polytechnic Institute
Inthuorn Sasankal, PhD	Geotechnical Centrifuge Modeling	Rensselaer Polytechnic Institute
Javier Ubilla, MS	Geotechnical Centrifuge Modeling	Rensselaer Polytechnic Institute
Thomas F. Zimmie, PhD, PE	Geotechnical Centrifuge Modeling	Rensselaer Polytechnic Institute
Frans Barends, PhD, Ir	Geotechnical Centrifuge Modeling	Geodelft, Netherlands
Paul Schaminee, MSc	Geotechnical Centrifuge Modeling	Geodelft, Netherlands
Adam Bezuijen, MSc	Geotechnical Centrifuge Modeling	Geodelft, Netherlands
Kevin Stone, PhD	External Expert Consultancy	Brighton University, UK

## **Floodwall and Levee Performance Analysis**

On Monday, 29 August 2005, Hurricane Katrina struck the U.S. gulf coast. The effects of the storm were being felt in the New Orleans area during the early morning hours. The storm produced a massive surge of water on the coastal regions that overtopped and eroded away levees and floodwalls along the lower Mississippi River in Plaquemines Parish, along the eastern side of St. Bernard Parish, along the eastern side of New Orleans East, and in locations along the Gulf Intracoastal Waterway (GIWW) and the Inner Harbor Navigation Canal (IHNC). Surge water elevated the level of Lake Pontchartrain, and shifting storm winds forced the lake water against the levees and floodwalls along its southern shores and New Orleans outfall canals, and resulted in high surge levels in the IHNC, the Mississippi River Gulf Outlet (MRGO), the GIWW, and the Mississippi River.

Information regarding the performance of the floodwalls and levees making up the hurricane protective system for the New Orleans area, including St. Bernard Parish and Plaquemines Parish during Hurricane Katrina, is presented in this volume. The focus of the effort was to assess the performance of floodwalls and levees throughout the system, to investigate the most likely causes of the damage and failure of the levees and floodwalls in the system, to compare the damaged components with similar sections or reaches where the performance was satisfactory, and to understand the mechanisms that led to the breaches in order to assess likely future performance of the unbreached reaches of the flood protection system, and to provide a basis for the design of improvements capable of providing protection against future storms of even greater destructive power than Katrina.

The performance of levees and floodwalls varied significantly throughout the New Orleans area. The investigation described here indicates that the two main causes of breaches in the floodwall and levee system were erosion due to overtopping and instability due to soil foundation failure. The investigation has looked at the most likely causes of the damage and failure of the levees and floodwalls in the system and compares them with similar sections or reaches where the performance was satisfactory. It is important to understand in detail the most likely mechanisms that led to the breaches along the reaches in order to evaluate the likely future performance of the unbreached reaches of the flood protection system.

The investigation described here involved (1) comprehensive assessment of the background information and examination of the entire levee system to identify reaches that performed satisfactorily and those that suffered damage; (2) characterization of the damaged reaches based on the breach mechanism, the surge height, and the wave action; (3) detailed analyses to ensure that site conditions and breach mechanisms are well understood; and (4) use of this information to evaluate future performance of the flood protection system.

Breaches due to instability of floodwalls occurred at one location on the 17th Street Canal, at two locations on the London Avenue Canal, and at one location on the IHNC. Breaches due to erosion as a result of overtopping occurred at three locations on the IHNC and at many locations on the MRGO, the GIWW, and the Mississippi River levees. Figure 1 shows in red the extent of the damage to the levees and floodwalls. Of the 284 miles of levees and floodwalls, 169 miles were damaged. Figure 2 shows the locations of the major breaches in Orleans Parish.

The performance of levees varied significantly. In some areas, the levees performed well in spite of the fact that they were overtopped. In other areas, the levees were completely washed away after being overtopped. The keys to the ability of some levee reaches to withstand overtopping without erosion were (1) the type of material of which the levees were constructed, and (2) the severity of the surge and wave action to which the levees were subjected.

This report describes the limit equilibrium stability analyses, the centrifuge model studies, and the finite element soil-structure interaction studies used to evaluate floodwall and levee performance at the 17th Street Canal, the London Avenue Canal, the IHNC, and the Orleans Canal, followed by the studies performed to assess performance at breaches caused by erosion.

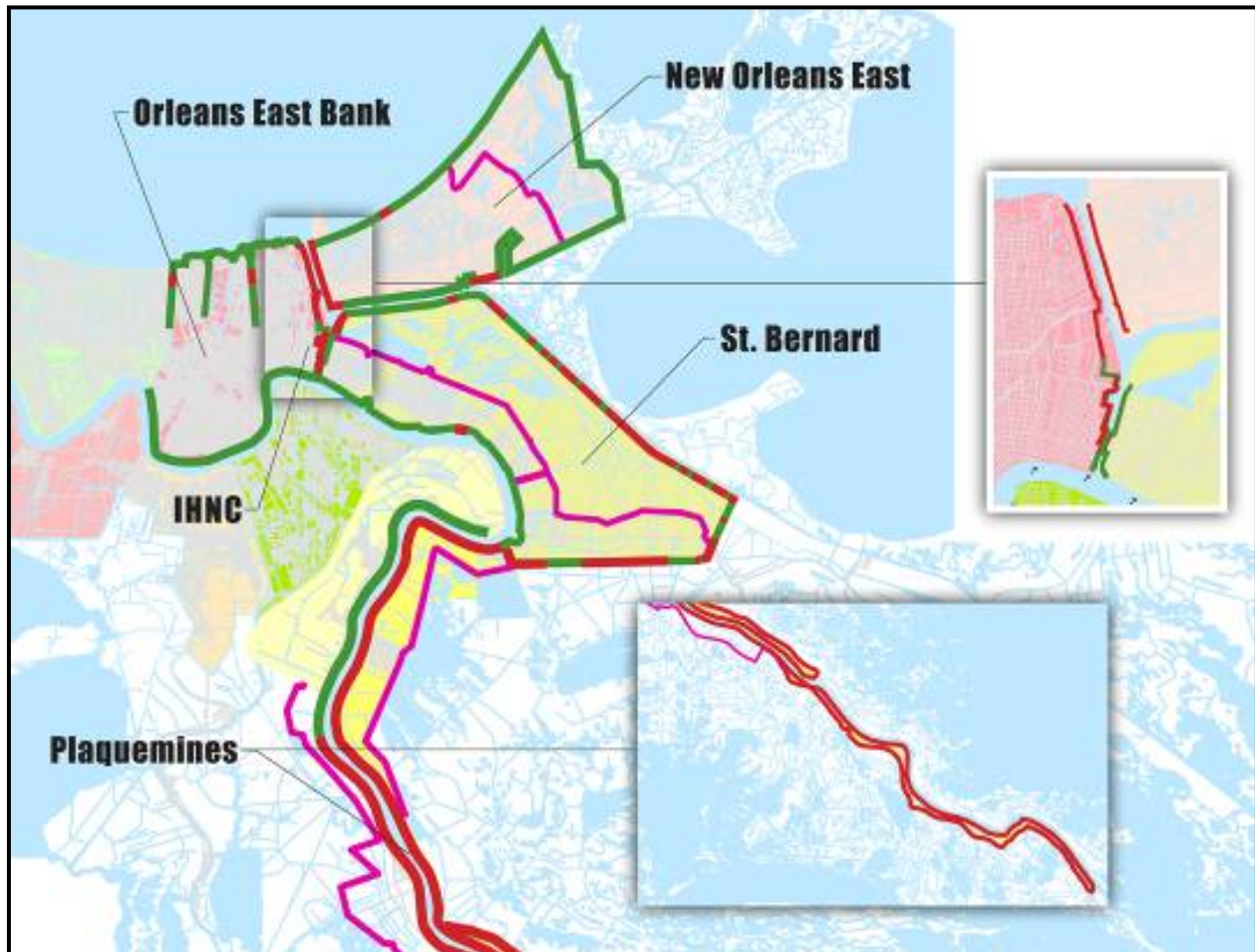


Figure 1. Damage to the New Orleans Hurricane Protection System.

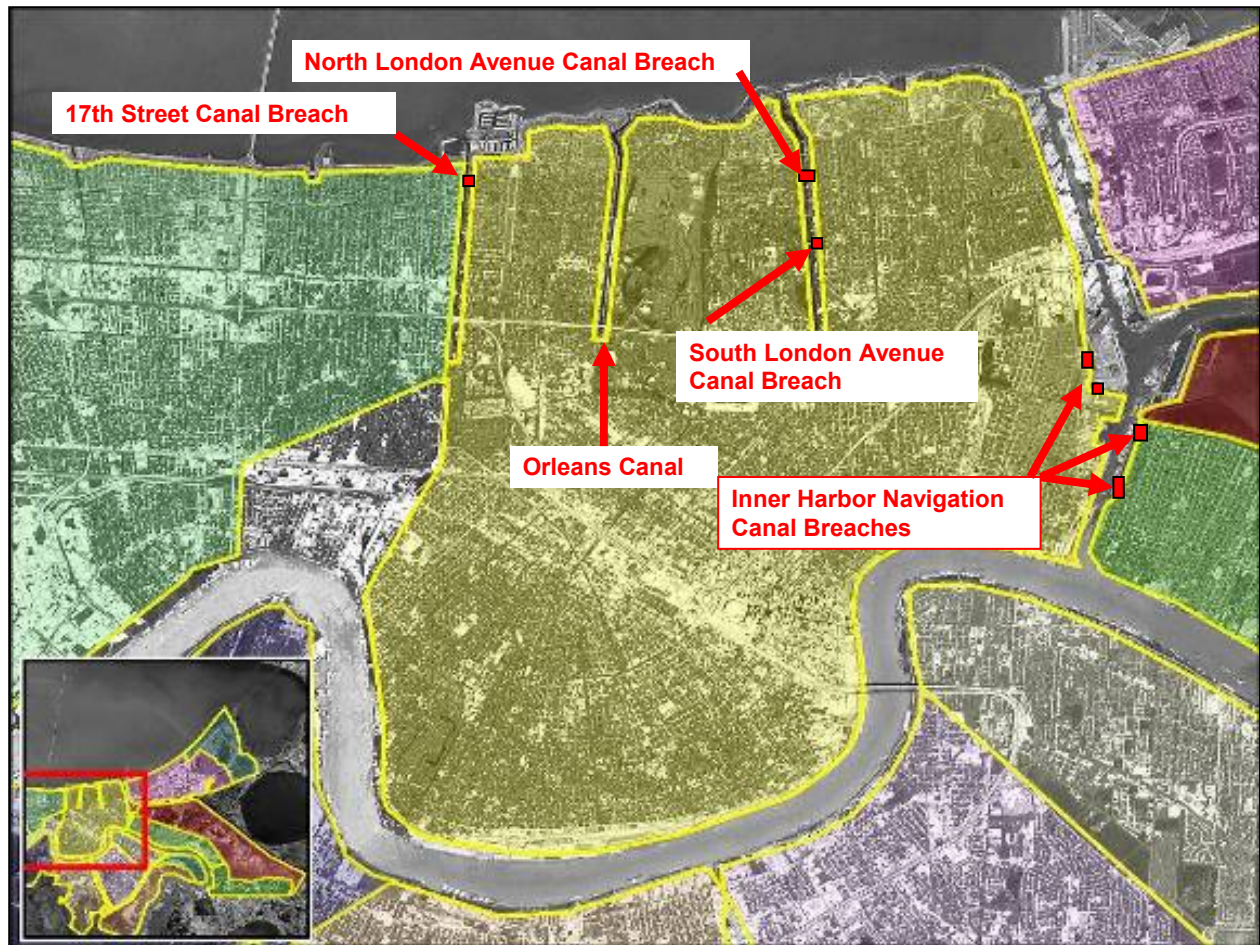


Figure 2. Location of breaches in Orleans Parish, East Bank.

## Hurricane Protection System

The hurricane protection system (HPS), outlined on the map in Figure 3, includes approximately 350 miles of protective structures, 56 miles of which are floodwalls. The majority of the floodwalls are I-walls with small sections of T-walls and a very small number of L-walls (basically similar to T-walls with a horizontal component on only one side at the base). Detailed maps showing the location of specific types of structures and their relationships to other features, such as pump stations and closures, are provided in Volume III and Volume VIII of this report. Figure 4 provides a schematic of the basic geometry of these structures.

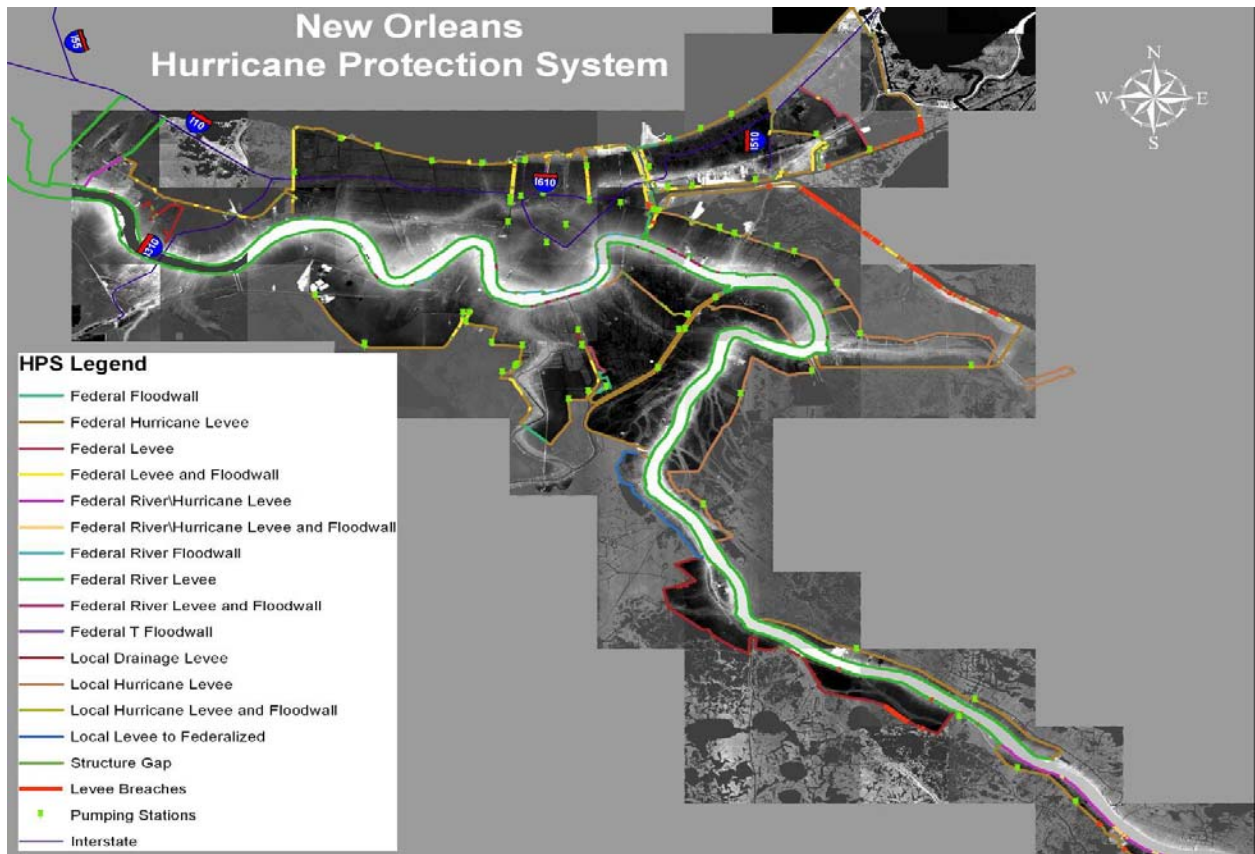


Figure 3. Outline of the New Orleans and Southeast Louisiana Hurricane Protection System.

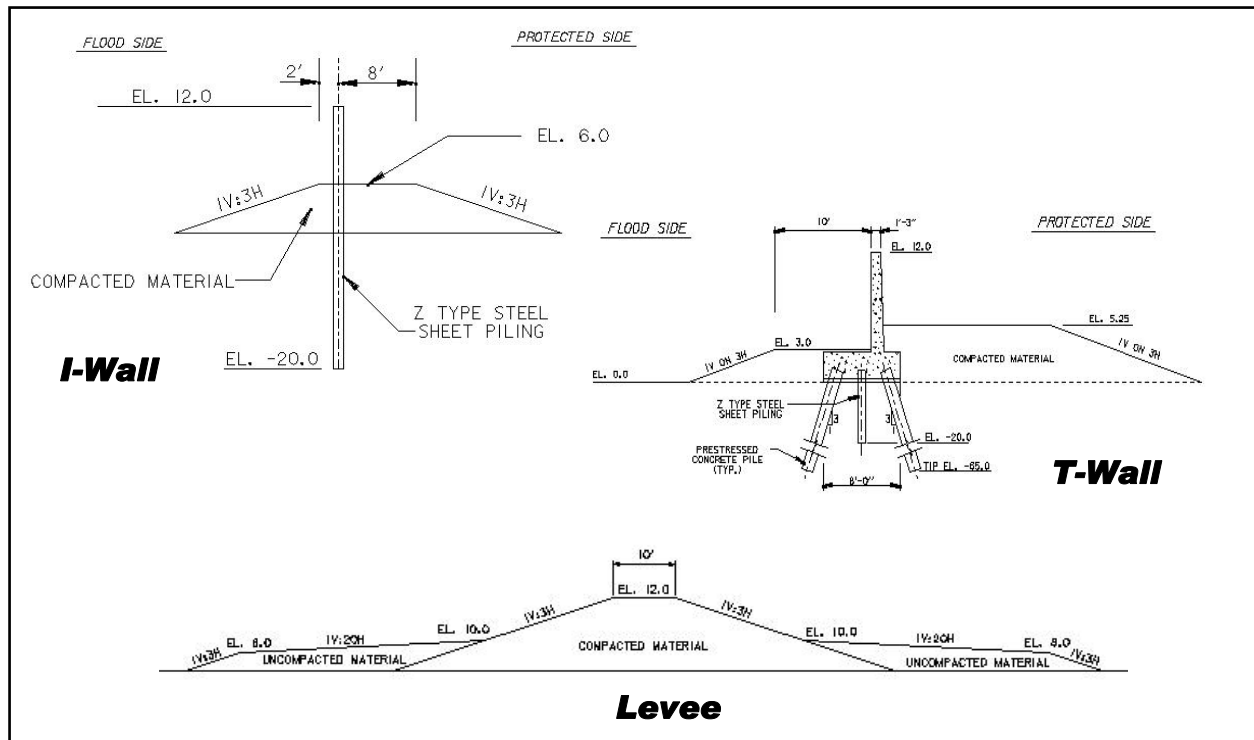


Figure 4. General schematic of major hurricane protection structures used in New Orleans and Vicinity.

## Geology of the New Orleans Area

The geologic history of the New Orleans area significantly influences the engineering properties of the foundation soils beneath the levees. Geologic and engineering data gathered from the different levee failures identifies a spatially complex geomorphic landscape, caused by Holocene sea level rise, development of different Mississippi River delta lobes, and the distributary channels associated with delta development. Overlying the Pleistocene surface beneath the New Orleans area are predominantly fine-grained, shallow-water depositional environments and related sediments associated with bay sound (or estuarine), nearshore-gulf, sandy beach, lacustrine, interdistributary, and paludal (marsh and swamp) environments. These environments define the New Orleans area history during the Holocene, and comprise the levee foundation for the different failure areas. A relict barrier beach ridge is present in the subsurface along the southern shore of Lake Pontchartrain. This relict beach blocked the filling of the lake with fluvial-deltaic sediments, impacted the supply and texture of sediment being deposited by advancing distributary channels, and influenced the engineering properties of these soils. Marsh and swamp soils beneath the failure area at the 17th Street Canal are much thicker in comparison to those beneath the London Avenue Canal because of the influence of the beach complex, and are thickest in the Industrial Canal area.

Additionally, anthropogenic activities in New Orleans during historic time contributed to the spatial complexity of this area and affected the engineering properties of the foundation soils. Anthropogenic activities included construction of drainage and navigation canals, pumping groundwater drainage, hydraulic filling of the Lake Pontchartrain lake front, and construction of

levees to prevent the river from flooding low-lying areas. Anthropogenic activities, combined with the geologic setting and subsidence in this region, are responsible for the unique landscape that created the New Orleans area. Historic settlement and subsidence in the New Orleans area have been most severe on the back barrier side of Pine Island Beach.

Subsidence did not contribute to the poor performance of the levee failures. However, subsidence has impacted the datum of many of the benchmarks in the city upon which engineering decisions and design were based and affected levee height and the level of flood protection.

A review of the geology and geologic history of coastal Louisiana is presented here to establish the general framework for the soils and stratigraphy beneath the New Orleans levee failures. Geologic processes active during the past 5,000 years directly relate to the development of the land mass upon which the New Orleans area is situated, and the resulting stratigraphy beneath the levee breaches at the 17th Street, London Avenue, and Inner Harbor Navigation Canals. Breaches of six I-wall reaches and one earthen levee occurred at these three canals. These canals were responsible for the extensive flooding in the New Orleans metropolitan area following Hurricane Katrina. Levees and floodwalls in the IHNC area were mainly overtopped by storm surge during Hurricane Katrina, while floodwalls at the 17th Street and London Avenue Canals were not overtopped, but failed at water levels below their design height. Geologists working in support of U.S. Army Corps of Engineers (USACE) flood control projects in the Lower Mississippi Valley (LMV) have typically classified the geology beneath structures and levees according to specific depositional environments. These lithostratigraphic units are associated with diagnostic fluvial and deltaic processes, and are classified according to soil texture, sedimentary structures, organic content, fossils, and associated engineering properties. USACE geologists have been involved with studies of the New Orleans area geology since the 1940s and have applied an engineering geology classification to the underlying stratigraphy. More information on the regional geology of the New Orleans area is provided in Appendices 2 and 21 of this volume.

## Physiography and Setting

The city of New Orleans is situated in Jefferson and Orleans Parishes along the eastern edge of the Mississippi River's deltaic plain. Broad natural levees associated with the Mississippi River, Bayou des Familles, and Bayou Metairie are the most prominent physiographic features in the area (Figure 5). Surface elevations are generally near sea level and range from approximately 15 ft above sea level along the crests of the Mississippi River levees to below sea level over much of the area north of the river. Increased urban reclamation of low-lying areas occurred after World War II by draining the cypress swamps that were present north of the city to meet the demands for expansion and population growth. A map of the greater New Orleans area from 1849 is presented in Figure 6, showing the extensive swamps and major physiographic features north of the river, before the advent of twentieth century urbanization. Continuous pumping of surface and ground water drainage to support residential development has contributed to the desiccation of these swamp and marsh soils, and has lowered the ground surface to below sea level for a significant portion of the city. Levees that encircle the city and continuous pumping of

surface water are required to keep the sea from reclaiming the “Crescent City.” Sea level rise of approximately 1 to 3 ft during the next century due to global warming will provide even greater challenges to local, state, and federal officials and engineers tasked with protecting this historic American city, and other cities along our nation’s coasts.

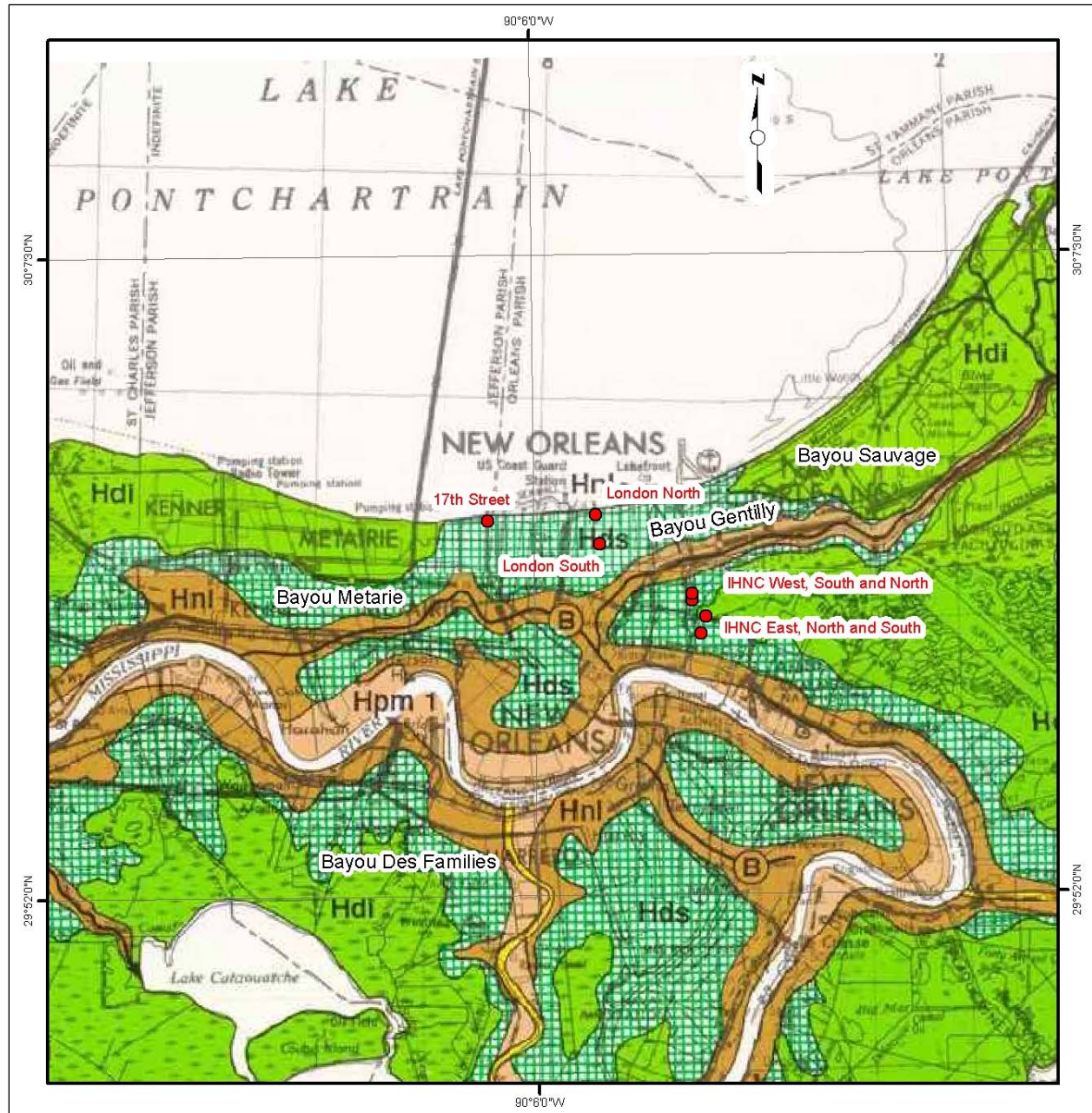


Figure 5. General map of the New Orleans area geology showing the limits of the different surface depositional environments (Saucier 1994). Map symbols are as follows: H = Holocene, d = deltaic, i = interdistributary, s = inland swamp, nl = natural levee, pm1 = point bar (most recent meander belt), and B=St. Bernard distributary channel. Bayous Metairie/Gentilly and Des Familles are abandoned St. Bernard distributary channel.



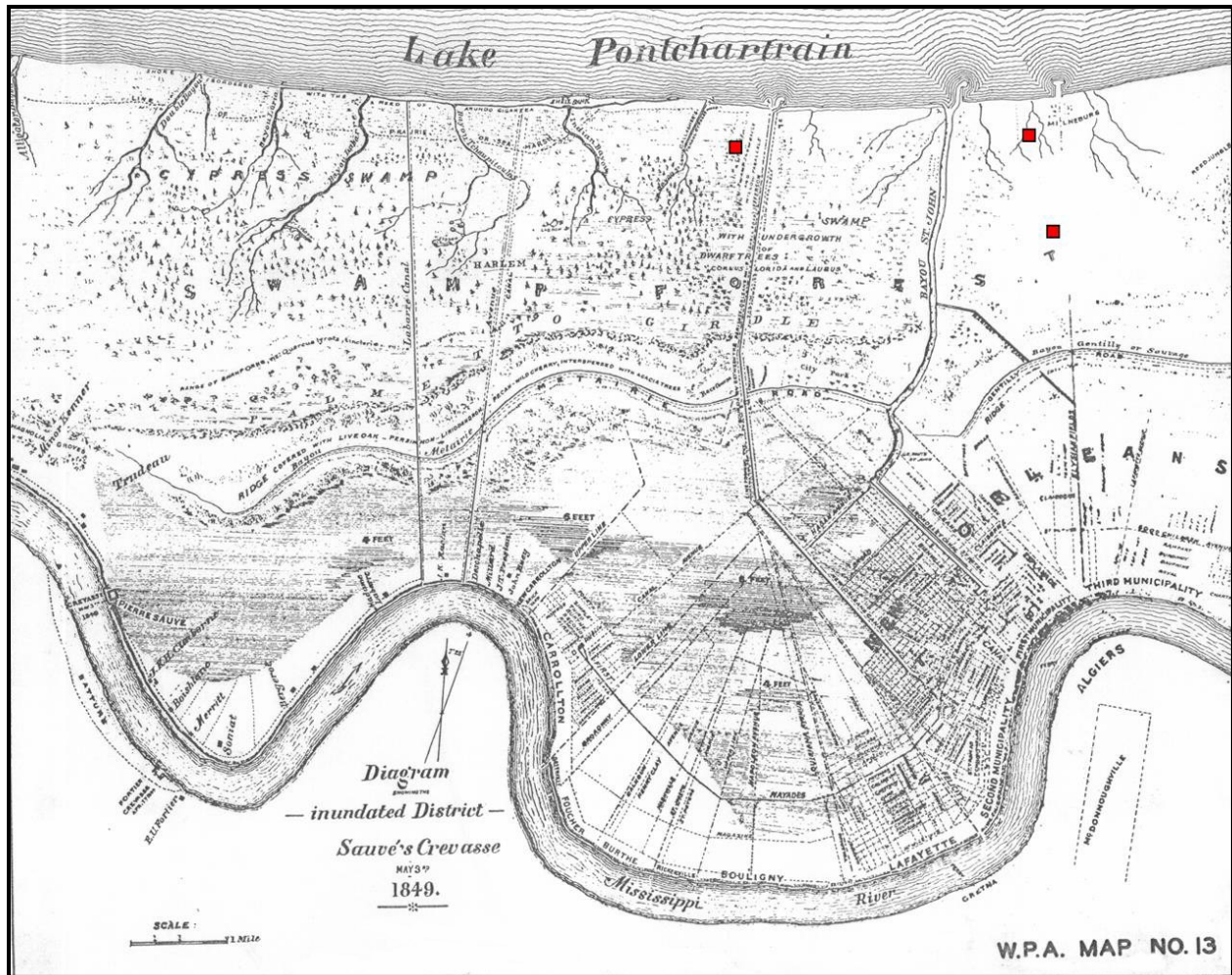


Figure 6. New Orleans area map from 1849 showing the locations of the Bayous Metairie and Gentilly distributary channel, the cypress swamps north of the city, and locations of 17th Street, London North, and South Canal breaches (marked by red squares, beginning from left to right and going clockwise). Bayous Metairie and Gentilly merge into the Bayou Sauvage distributary channel east of the New Orleans area. From Work Projects Administration (1937).

## Geologic History

A geologic history has been developed for the Mississippi River's deltaic plain based upon thousands of engineering borings drilled during the past 50 years, thousands of radiocarbon age dates from organic deltaic sediments, and numerous geologic studies conducted in this region. More than 10,000 borings have been drilled in the greater New Orleans area during the past 50 years in support of foundations for the many engineered structures. Boring data identify a complex geology that is related to the different course shifts by the Mississippi River and formation of its deltas during Holocene time (Figure 7). Continental glaciers covered much of North America 15,000 years before the present, with sea level approximately 350 ft below the present level and the Gulf shoreline significantly farther seaward than its present location. The ancestral Mississippi River and its tributaries were entrenched into the underlying Pleistocene

surface below Baton Rouge and had developed a broad drainage basin, approximately 25 miles wide, with the axis of this entrenchment in the vicinity of Houma, approximately 45 miles southwest of New Orleans. Global warming and glacial melting caused eustatic sea level rise, which stabilized between 4,000 and 6,000 years ago, and was 10 to 15 ft lower than the present level (Figure 8).

Holocene sea level rise drowned the drainage valley and tributary network of the ancestral Mississippi River and caused massive deposition of fluvial sediment within this broad alluvial valley. Creation of the present-day deltaic plain began with the sea level near its present stand. Coastal Louisiana is the product of numerous, but generally short-lived, delta systems that have built seaward by deposition of fluvial transported sediment. These deltas have been subsequently reworked and modified by coastal transgressive processes. Five major deltaic systems have built seaward during the past 7,000 years, as shown in Figure 7b.

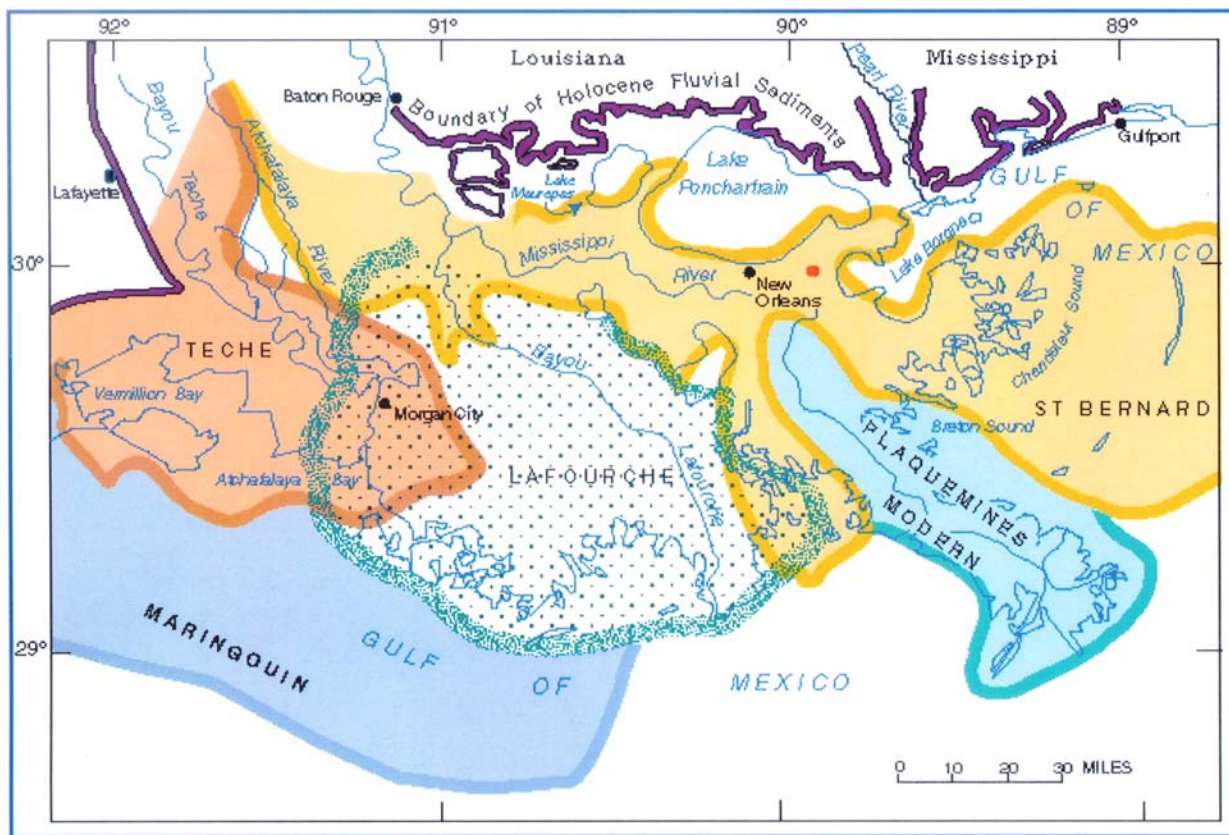


Figure 7a. Holocene deltas of the Mississippi River (after Fraizer 1967).

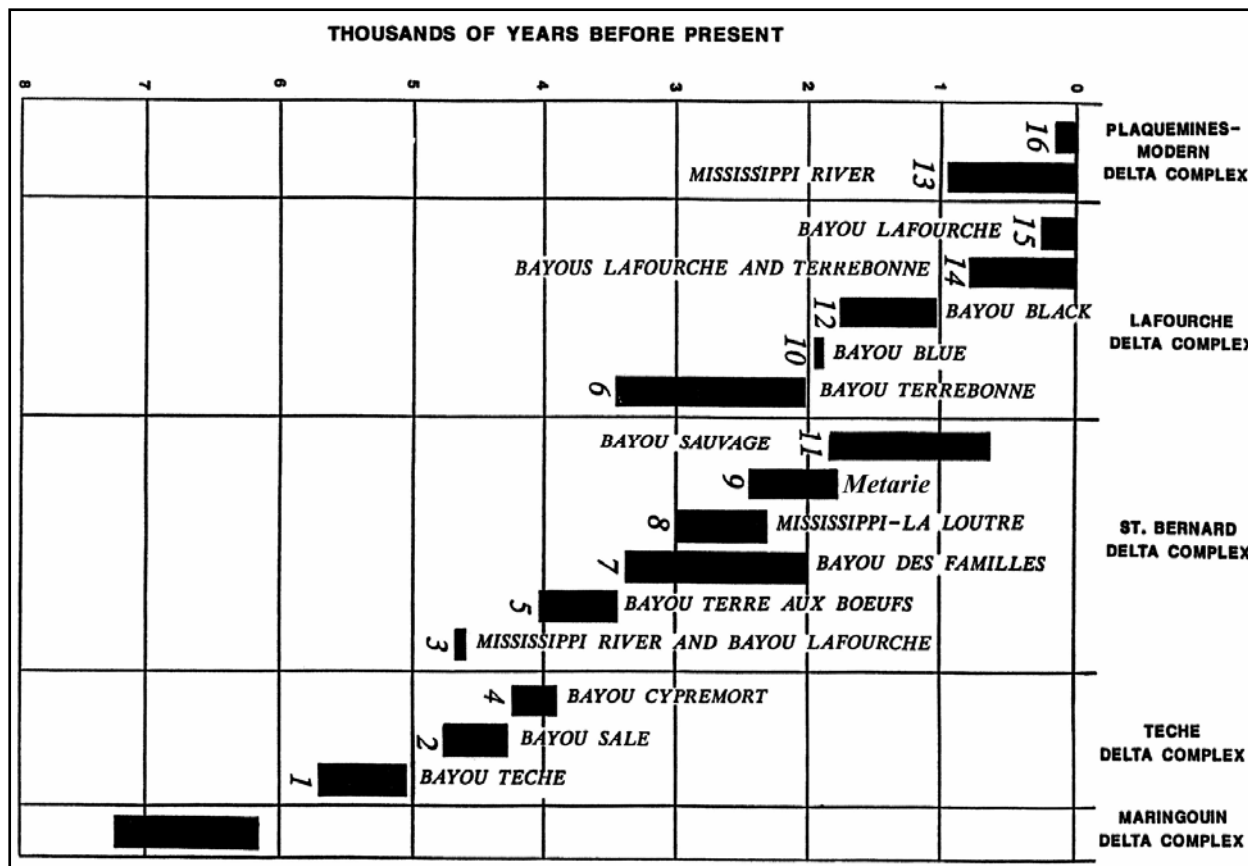


Figure 7b. Chronology of major Holocene distributary channels (after Fraizer 1967).

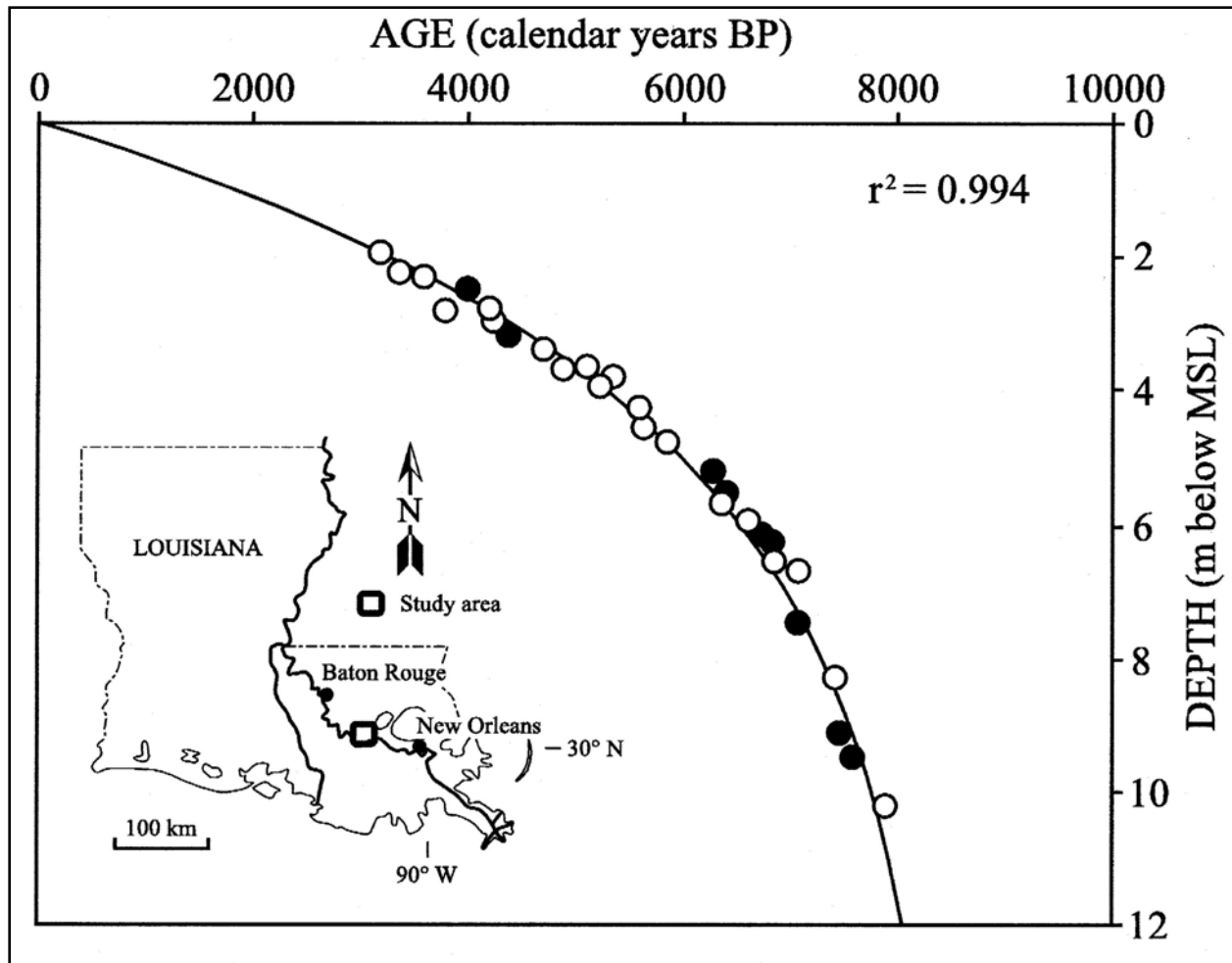


Figure 8. Holocene sea-level curve for the Eastern Mississippi River deltaic plain based on carbon-14 dating of basal peats from the transgressive contact at the Holocene and Pleistocene contact (Tornqvist et al. 2004).

Each delta system contains a network of several major distributary channels and numerous smaller channels that terminate at the sea's edge where they discharge transported sediment to the sea. Collectively, this network of seaward prograding and bifurcating distributary channels forms a short-lived delta lobe complex. Relative ages of these deltas and the major distributary channels (Figure 7b) are well established by radiocarbon dating of the sediments in these systems. The first major advance of a delta into the New Orleans area occurred by the St. Bernard system approximately 3,500 to 4,000 years ago via several major distributary channels (see Figures 5 and 7b). The land in the New Orleans area was established by this delta system. Partial Mississippi River flow continued to pass through the New Orleans reach following abandonment of this delta for the Lafourche delta complex south of Donaldsonville. After abandonment of the Lafourche system, approximately 500 years before the present, Mississippi River flow returned to the present course. Historic construction of levees has prevented the river from seeking a different and shorter route to the gulf. Active deltaic growth is occurring at the mouth of the Mississippi River and at the mouth of the Atchafalaya River.

## Geologic Structure and Faulting

Holocene sediments underlying New Orleans are part of the seaward thickening wedge of Quaternary sediments that dip gently to the south and fill the Gulf of Mexico basin. Geologic structures within this sedimentary prism are pier-cement salt domes and growth faults. No salt domes are present beneath the greater New Orleans area. Faulting has been identified in the subsurface throughout the deltaic plain and in the Pleistocene deposits exposed at the surface north of Lake Pontchartrain. These faults are generally not considered tectonically active. Instead, they are related to sedimentary loading, compaction, and consolidation of sediments in the Gulf of Mexico basin. A detailed study of the Pleistocene deposits did not identify faulting in the New Orleans area. The study identified only one nearby fault in Lake Pontchartrain. Recognition of this fault was based on closely spaced borings and geophysical data. Subsequent geologic mapping of the eastern deltaic plain did not identify any Holocene faults based solely on boring and engineering data. Surface faults occurring in Holocene sediments by movement in the underlying Pleistocene deposits are difficult to detect because unconsolidated sediments tend to warp rather than shear. A better resolution of Holocene and Pleistocene stratigraphy using seismic data, combined with closely spaced borings, and a dense network of elevation benchmarks, is needed to determine whether Holocene movement in deltaic sediments is associated with the underlying Pleistocene fault structure.

Geologists in the New Orleans District generally evaluate the presence of faulting in studies of the subsurface stratigraphy during boring programs to determine the geotechnical properties of the foundation for the proposed structures. Additionally, radiometric dating of organic sediments is routinely conducted as part of the site investigations to determine geologic-based subsidence histories for the area under study. Fault movements are generally factored into the subsidence history for the structure. Evidence of faulting would be reflected by subsidence, especially if the rates are abnormally high. Furthermore, land loss and engineering geology mapping studies by the New Orleans District have been evaluated for the presence of faults, as linear trends in land loss may define their presence. In the New Orleans area, no evidence of faulting was identified at the canal levee failures from the boring and stratigraphic evidence gathered and evaluated by the Interagency Performance Evaluation Task Force (IPET) team during focused studies at these areas. Stratigraphic evidence obtained and evaluated from these sites indicates that other mechanisms are responsible for the different canal failures.

## Holocene Environments of Deposition

The geology in the Lower Mississippi Valley and the New Orleans area has traditionally been defined by USACE geologists according to depositional environments. Surface environments include natural levee, point bar, inland swamp, fresh marsh, and abandoned distributary channels (see Figure 5). Distributary channels are associated with two major St. Bernard distributary systems, the Bayou des Familles-Barataria and the Bayou Metairie-Sauvage system (Figure 7b). The Bayou des Familles-Barataria extends due south from the Mississippi River and was active approximately 2,000 to 3,400 years before the present (Figure 4), while the Bayou Metairie-Sauvage-Gentilly course is located north of the Mississippi River and was active about 2,500 to 700 years before the present. These distributary systems

filled the shallow water in the New Orleans area with fluvial-deltaic sediments. Overbank deposition from these active distributary channels has formed well-developed natural levees that transition to inland swamps and low-lying marsh environments. Sediments within these different environments generally become finer-grained with increasing distance from the distributary channels, and have a corresponding increase in organic content.

USACE foundation and regional geologic studies show the Holocene fill ranges in thickness from 70 to 80 ft across much of the New Orleans area, and is composed of stacked depositional environments, related to shifting delta systems and their seaward advancement and growth. Where the Mississippi River has scoured in the bends of the river, the Holocene fill exceeds 150 ft in thickness. Major deltaic environments overlying the Pleistocene surface in the vicinity of the canal failures include nearshore gulf, bay sound-estuarine, intradelta, relict beach, lacustrine, and interdistributary environments. Regional geologic maps and cross sections from the Louisiana Coastal Plain and the greater New Orleans area are presented on a USACE geology website of the LMV and show the vertical and horizontal limits of these different environments of deposition in the subsurface (see [lmvmapping.erdc.usace.army.mil](http://lmvmapping.erdc.usace.army.mil)). Similarly, cross sections were developed from the boring information at the different failure sites where they define the vertical and horizontal limits of these environments in the subsurface, presented in discussions about each breach site in Appendices 2 and 21 of this volume.

Correlations between depositional environments and the engineering properties of the soils that form these lithostratigraphic units are summarized in Table 1. A detailed discussion and presentation of the physical and engineering properties characteristic of these different depositional environments is beyond the scope of this study. A comprehensive description of these environments is provided in several USACE studies, which are presented at the above LMV geology website.

**Table 1a. Selected engineering properties of deltaic depositional environments, soil texture, water content, and unit weight (Kolb 1962; Kolb and Van Lopik 1965).**

DEPOSITIONAL TYPES	LITHOLOGY PERCENT					REMARKS
	0	25	50	75	100	
NATURAL LEVEES						Disposed in narrow bands flanking the Mississippi River and its abandoned courses and distributaries. Elevation varies from 25 feet near Baton Rouge to sea level.
POINT BAR						Usually found flanking the more prominent bends of present and abandoned courses. Thickness in excess of 100 feet.
PRODELTA CLAYS						Fat clay in offshore areas and at depth beneath deltaic plain. Thickness ranges between 50 and 400 feet.
INTRA DELTA						Coarse portion of subaqueous delta. Intricately interfingered deposits. Disposed in broad wedges about abandoned courses and major distributaries.
INTERDIS-TRIBUTARY						Forms clay wedges between major distributaries. Minor amounts of silts and fine sands typically occur in very thin but distinct layers between clay strata.
ABANDONED DIS-TRIBUTARY						Form belts of clayey sediments from a few feet to more than 1000 feet in width and from less than 10 to more than 50 feet in depth.
ABANDONED COURSE						Form belts of fairly coarse sediment in abandoned Mississippi River courses. Lower portion filled with sands, upper portion with silts and clays. Coarsest fill near point of diversion.
SWAMP						Tree-covered organic deposits flanking the inner borders of the marsh and subject to fresh-water inundation. Deposits 3 to 10 feet thick.
MARSH						Forms 90 percent of land surface in the deltaic plain. Ranges from watery organic oozes to fairly firm organic silts and clays. Average thickness 15 feet.
ABANDONED TIDAL CHANNELS						Found principally in peripheral marsh areas. Average depths on the order of 25 feet. Widths average 200 feet. Filling varies from peat to organic clay.
SAND BEACH						Border the open gulf except in areas of active deltaic advance. May be a mile or more wide and more than 10 miles long. Sand may pile as high as 30 feet and subside to depths 30 feet below gulf level.
SHELL BEACH						Border landward shores of protected bays and sounds and marshland lakes. Vary from 25 to 200 feet in width and from 2 to 6 feet in height. Lengths usually less than a mile.
LACUSTRINE						Deposits vary in thickness from 2 to 25 feet. Stratification in clayey lacustrine deposits is poorly developed or lacking.
REEF						Active reefs found principally in bay-sound areas. Buried reefs 5 to 10 feet thick a common occurrence within deltaic plain. Reach dimensions of 1/2-mile wide and 10-miles long.
BAY-SOUND						Relatively coarse sediments on bottoms of bays and sounds. Thickness between 3 and 20 feet.
NEARSHORE GULF						Found at the borders of the open ocean seaward of the barrier beaches. Thickness normally increases with distance from shore.
SUB-STRATUM						Massive sand and gravel deposits filling entrenched valley and grading laterally into nearshore gulf deposits. Material becomes coarser with depth.
PLEIS-TOCENE						Ancient former deltaic plain of Mississippi River. Consists of environments of deposition and associated lithology similar to those found in Recent deltaic plain. Depth of this ancient, eroded surface increases in a southerly and westerly direction in south-eastern Louisiana.

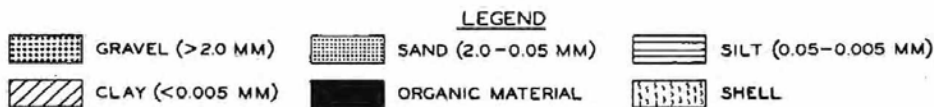


**Table 1b. Selected engineering properties of deltaic depositional environments (Kolb 1962, Kolb and Van Lopik 1965).**

DEPOSITIONAL TYPES	NATURAL WATER CONTENT PERCENT DRY WEIGHT	UNIT WEIGHT LB/CU FT	SHEAR STRENGTH <sup>(1)</sup> COHESIVE STRENGTH LB/SQ FT
	0 50 100 150 200 60	80 100 120 140	0 200 400 600 800
NATURAL LEVEES			
POINT BAR		INSUFFICIENT DATA	INSUFFICIENT DATA
PRODELTA CLAYS			
INTRADelta		INSUFFICIENT DATA	INSUFFICIENT DATA
INTERDISTRIBUTARY			
ABANDONED DISTRIBUTARY	INSUFFICIENT DATA	INSUFFICIENT DATA	INSUFFICIENT DATA
ABANDONED COURSE	INSUFFICIENT DATA	INSUFFICIENT DATA	INSUFFICIENT DATA
SWAMP			INSUFFICIENT DATA
MARSH	VALUES RANGE TO APPROXIMATELY 800 	INSUFFICIENT DATA	VERY LOW
ABANDONED TIDAL CHANNELS	INSUFFICIENT DATA	INSUFFICIENT DATA	VERY LOW
SAND BEACH	SATURATED	INSUFFICIENT DATA	0
SHELL BEACH	SATURATED	INSUFFICIENT DATA	0
LACUSTRINE			
REEF	SATURATED	INSUFFICIENT DATA	0
BAY-SOUND			
NEARSHORE GULF	SATURATED	INSUFFICIENT DATA	0
SUBSTRATUM	SATURATED	INSUFFICIENT DATA	0
PLEISTOCENE			

(1) SHEARING STRENGTH OF CLAYS BASED ON UNCONFINED COMPRESSION TESTS.

TYPICAL RANGE OF VALUES INDICATED BY LENGTH OF BAR. BAR WIDTH INDICATES RELATIVE DISTRIBUTION OF VALUES.



Classification of the subsurface stratigraphy beneath the failure sites by the IPET investigation team was made according to depositional environments from the available boring data. Geologic cross sections at each failure area were prepared from the available boring data to support the engineering analyses of the failure mechanisms. Interpretation of the underlying stratigraphy is based on the Corps classification of depositional environments gained from more than 50 years of corporate experience in geologic mapping and evaluation of fluvial deltaic deposits in the coastal plain in support of foundation studies for various flood control projects. Engineering properties of fluvial-deltaic soils are uniquely related to their origin, their age, local current and wave conditions, sedimentary structures, and subsequent geomorphic processes and anthropogenic changes that have occurred after their deposition. The greatest contrast in engineering properties occurs between the high- and low-energy depositional environments and sediment age, i.e., whether the sediments are Holocene or Pleistocene.

A prominent buried beach ridge lies between Lake Pontchartrain and the Mississippi River that has directly influenced levee foundation properties and contributed to the subsequent failures at the 17th Street and London Canals (Figure 5). A relatively stable, but lower (10 to 15 ft lower than present) sea level 4,000 to 5,000 years ago, permitted sediments from the Pearl River east of New Orleans area to be concentrated by longshore drift, forming a prominent sandy spit or barrier beach complex known as Pine Island Beach. The levee breach at the 17th Street Canal was located on the protected or back barrier side of this beach system, whereas both of the London Avenue Canal levee breaches were located on the main axis, where the maximum sand thickness occurs. Consequently, soft soils at the 17th Street break are much thicker and finer-grained than those beneath the London Canal. Foundation soils at the 17th Street Canal levee are dominated by clay, whereas those at the London Canal are composed mainly of sand. Levee failures in the IHNC area are located on the seaward side of the beach complex and south of the Bayou Metairie-Sauvage distributary system. The Pine Island Beach trend prevented this distributary system from completely filling Lake Pontchartrain with sediment. Because of the high sediment rates and close proximity to the Bayou Metairie-Sauvage distributary and the present course of Mississippi River, the IHNC area has thick deposits of fine-grained soils consisting of natural levee and inland swamp.

## **Subsidence and Settlement**

The loss of wetlands in coastal Louisiana is among the most severe in the United States. Historic rates have been as high as 42 square miles/year during the mid-1960s. During the period between 1983 and 1990, loss rates were about 25 square miles/year. Because of Hurricanes Katrina and Rita, rates are in excess of 200 square miles/year (*Times-Picayune*, 11 October 2006). Loss of wetlands in the Mississippi River deltaic plain is related to a combination of factors, including erosion by wave and storm surges, global sea-level rise, regional subsidence from sedimentary loading of the Gulf of Mexico Basin, local subsidence due to compaction and consolidation of the Holocene deltaic sediments, oil and ground water extraction, movement along Quaternary faults, movement of the underlying Jurassic salt layer, movement of salt domes, and impacts caused by anthropogenic activities.

Anthropogenic activities have included construction of levees, the building of flood control and diversion structures, dredging of navigation and petroleum canals, and the dewatering and pumping of low-lying coastal plain areas to support agricultural and urban development. Subsidence in the Louisiana coastal zone and the New Orleans area involves both sea level rise and the general lowering of the land surface because of the different natural and anthropogenic mechanisms listed above. Further contributing to the wetland loss has been the confinement of the Mississippi River to a fixed course by levee construction and bank stabilization, which has prevented fluvial transported sediments from reaching the distal parts of its former floodplain during the annual flooding, and the creation of new land areas by crevassing, channel avulsion, and formation of new deltas. In the New Orleans area, subsidence has been severe, due in large part to historic dewatering of swamp and marsh soils, and because of the lack of new sediment from reaching low-lying areas on the floodplain from levee confinement. Active land building by fluvial-deltaic processes in coastal Louisiana has been restricted to the Mississippi and Atchafalaya River deltas.

Subsidence rates are generally higher in the low-lying areas near the lakefront as compared to the natural levees flanking the active channel and its distributaries. Generally, the low-lying swamp areas (Figure 6) are more compressible due to their fine-grained texture and higher water contents, as compared to the natural levees' soils with lower water contents and coarser-grained textures. An underlying cause for the higher historic subsidence rates in the New Orleans area has been the construction of drainage canals during the twentieth century, and dewatering of the organic (swamp and marsh) soils shown in Figure 6 to accommodate the increased demands for land development and population growth. Lowering of ground water levels by construction of drainage canals and pumping of surface drainage has caused a corresponding net reduction in soil volume, oxidation of the dewatered organic sediments, and an overall decline in surface elevation throughout the city. More information is provided in Volume II and in Appendix 21 of this volume.

## **17th Street Canal Breach**

Observations made at the breach at the 17th Street Canal show that the most likely cause of breach is a soil foundation failure. Figure 9 shows an aerial photo of an approximately 450-ft breach in the floodwall along the east side of the 17th Street Outfall Canal south of the old Hammond Road Bridge. Figure 10 shows that a section of levee has moved more than 40 ft inward to the landside. It appears that the remaining levee section making up the breach was washed away by the water flowing through the breach. The top of the I-wall section of the floodwall in the breach can be seen adjacent to the levee section that moved into the landside.



Figure 9. Aerial photograph of the 17th Street Canal breach looking south from the Old Hammond Road Bridge.



Figure 10. Aerial photograph of the 17th Street Canal breach showing I-wall and embankment translation.

A transverse multi-beam sonar survey of the surface of the canal bottom and breach was conducted before construction of an emergency closure across the breach at the cross section shown in Figure 11. Topographic cross sections developed from the results of this survey are shown in Figures 12a and 12b. The survey showed that the crest of the levee on the canal side remained in place after the breach, as shown by the ground surface profile at Station 11+50 in Figure 13. It can be seen that the levee and floodwall moved about 40 ft laterally during the failure, and was tilted toward the landside at about 45 degrees after the failure.



Figure 11. Location of multi-beam sonar survey cross sections at the 17th Street Canal breach.

After the emergency closure was complete, and the water levels were drawn down, large blocks of the marsh were found strewn in neighborhoods surrounding the breach, as shown in Figure 14. A close examination of the marsh blocks reveals that an approximately 1-ft-thick clay layer is attached to the bottom of the marsh block (Figure 15). In order to inspect the failure plane or zone, a backhoe trench was excavated to expose a vertical surface through the slide block. A photograph of the side of this trench is shown in the upper left corner of Figure 16, and a closer view is shown in Figure 17. The photograph in Figure 17 shows a portion of the clay layer, which was initially located beneath the marsh layer, was displaced upward and over a portion of the marsh layer by the lateral displacement that occurred during the failure. The shearing mechanism that resulted in this condition is shown in Figure 18; the failure plane of the slide block was within the clay under the levee, and the failure plane came upward through the marsh layer further landward. A description of the geology and soil stratification in the area is discussed in the following section.

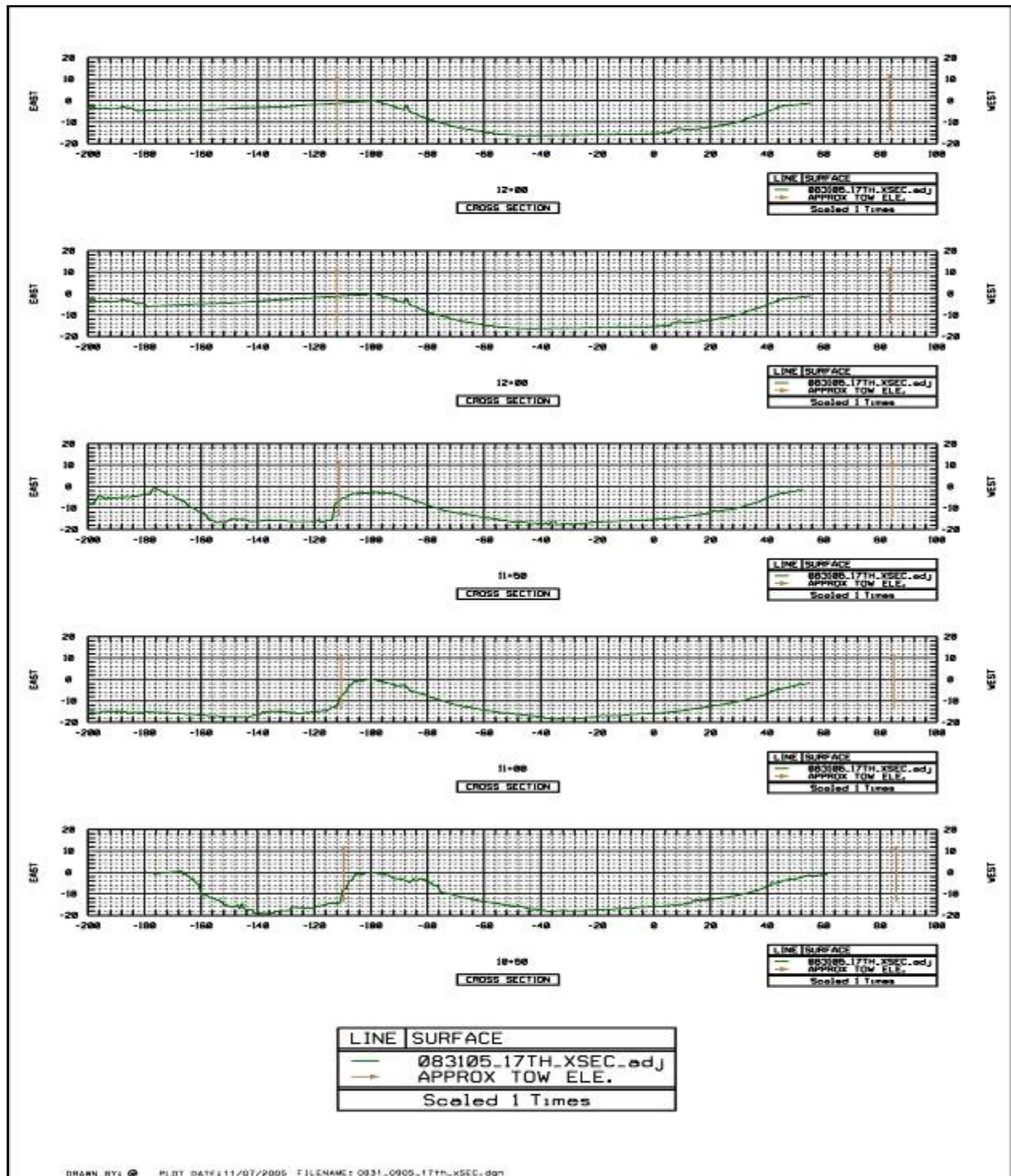


Figure 12a. Surface profiles at the 17th Street Canal breach.

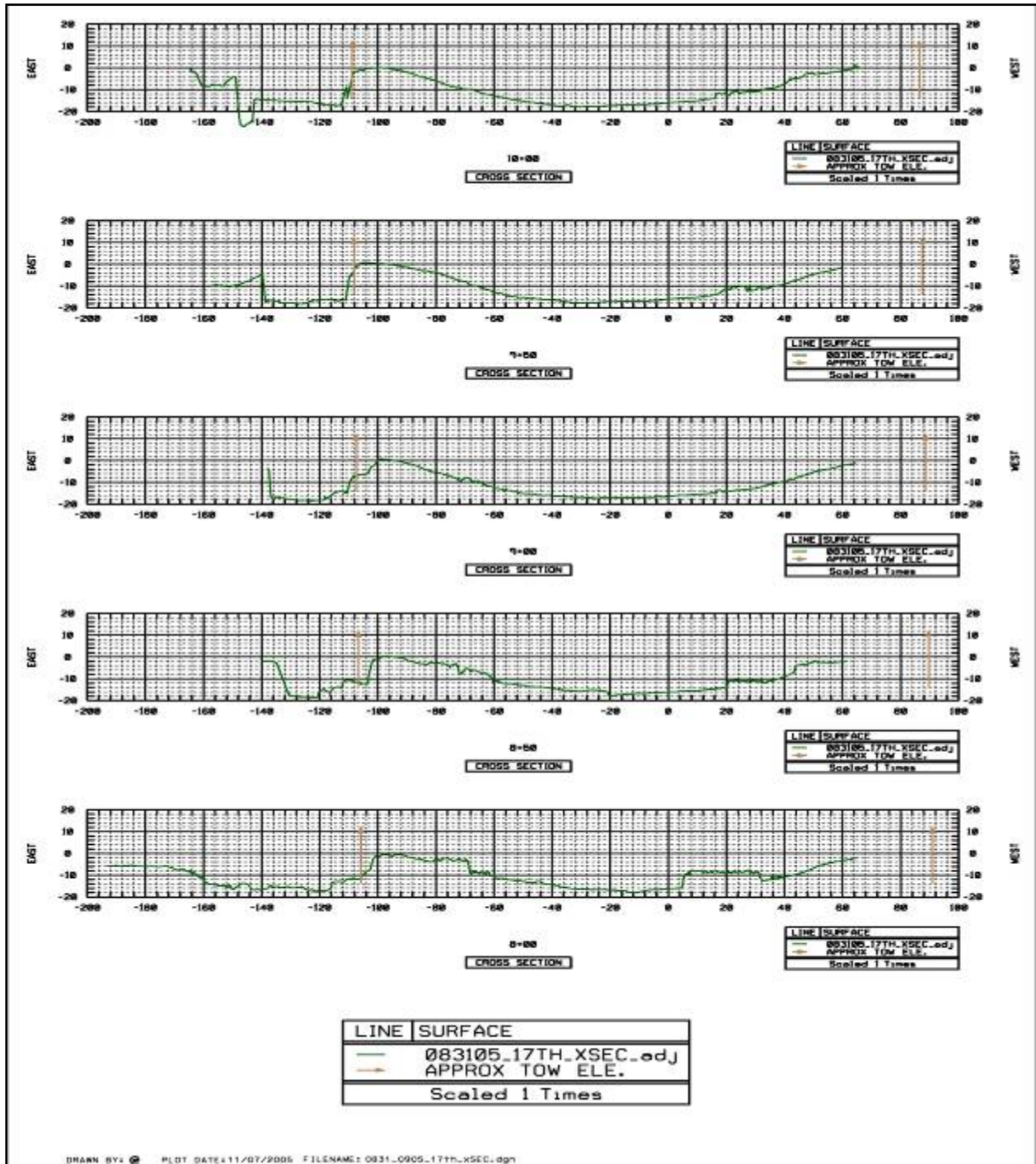


Figure 12b. Surface profiles at the 17th Street Canal breach.



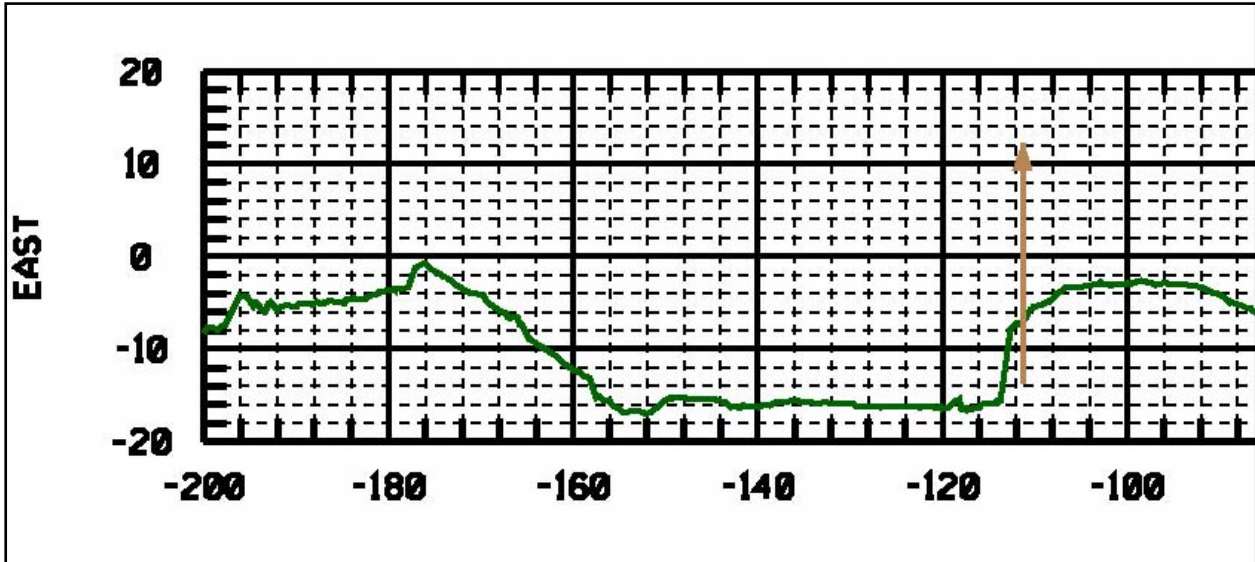
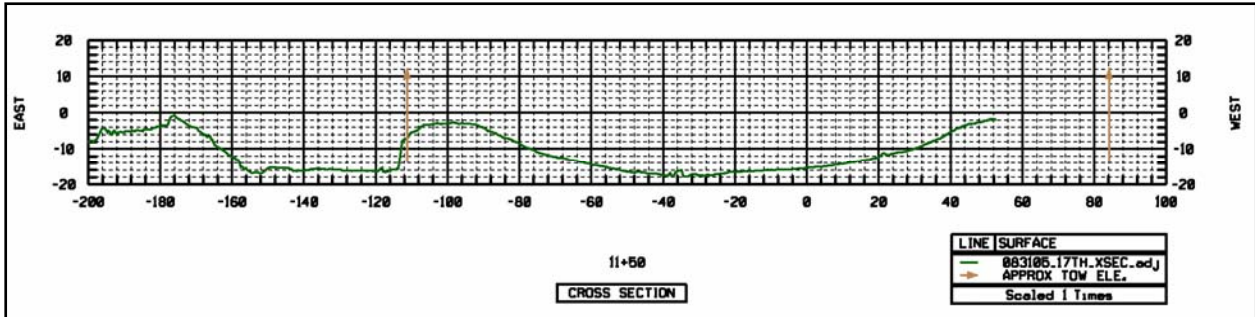


Figure 13. Profile for Station 11+50 through the 17th Street Canal breach.



Figure 14. Marsh blocks from the levee embankment at the 17th Street Canal breach.



Figure 15. Clay attached to marsh blocks at the 17th Street Canal breach.



Figure 16. Photographs taken at the 17th Street Canal breach after the failure.

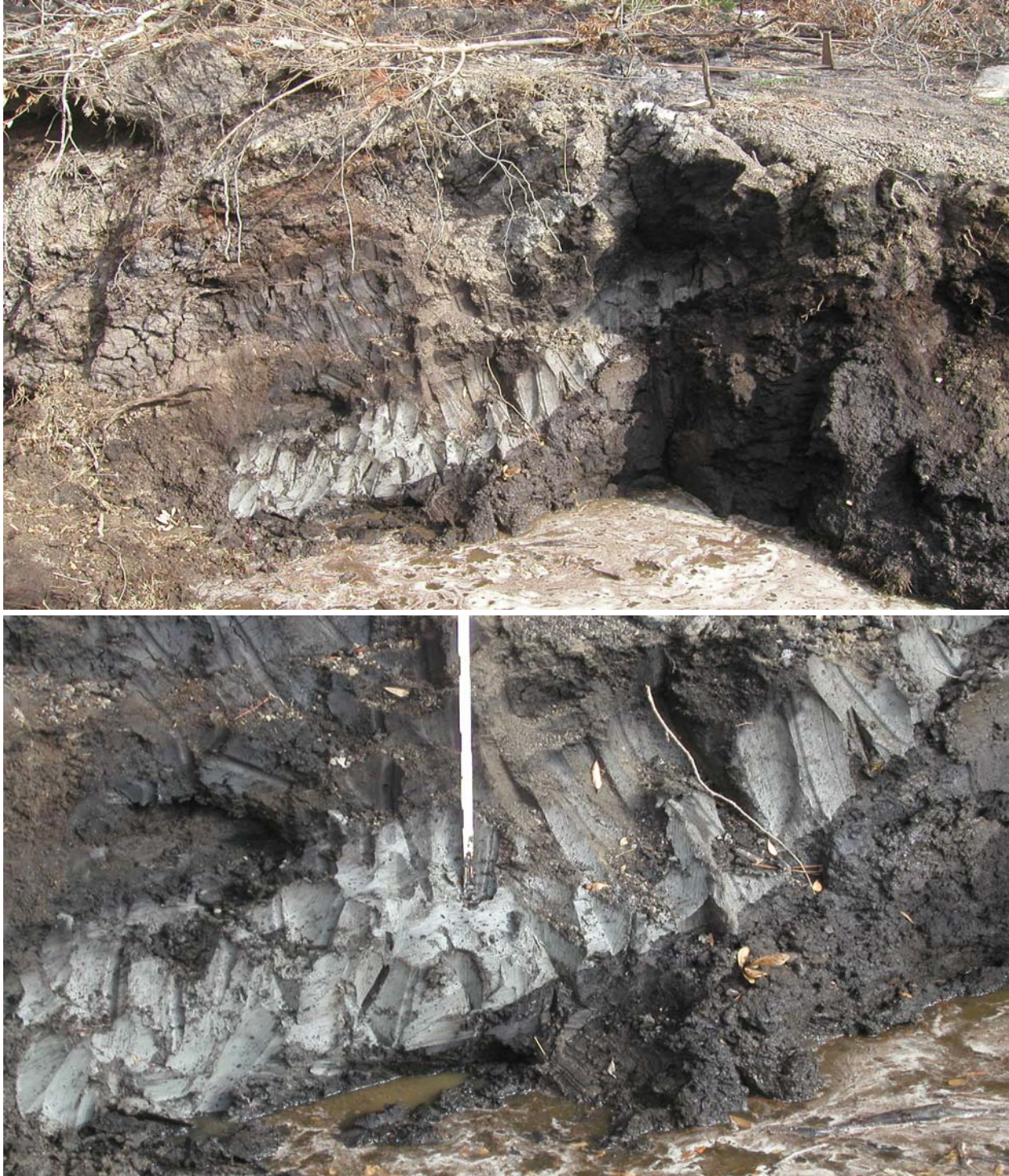


Figure 17. Exposed failure plane at the 17th Street Canal breach, showing clay that was initially below the marsh layer was displaced above some of the marsh material during the failure. The marsh material above and below the clay is the same layer, confirmed by age dating. The clay was moved into this position during the failure, as shown in Figure 18.

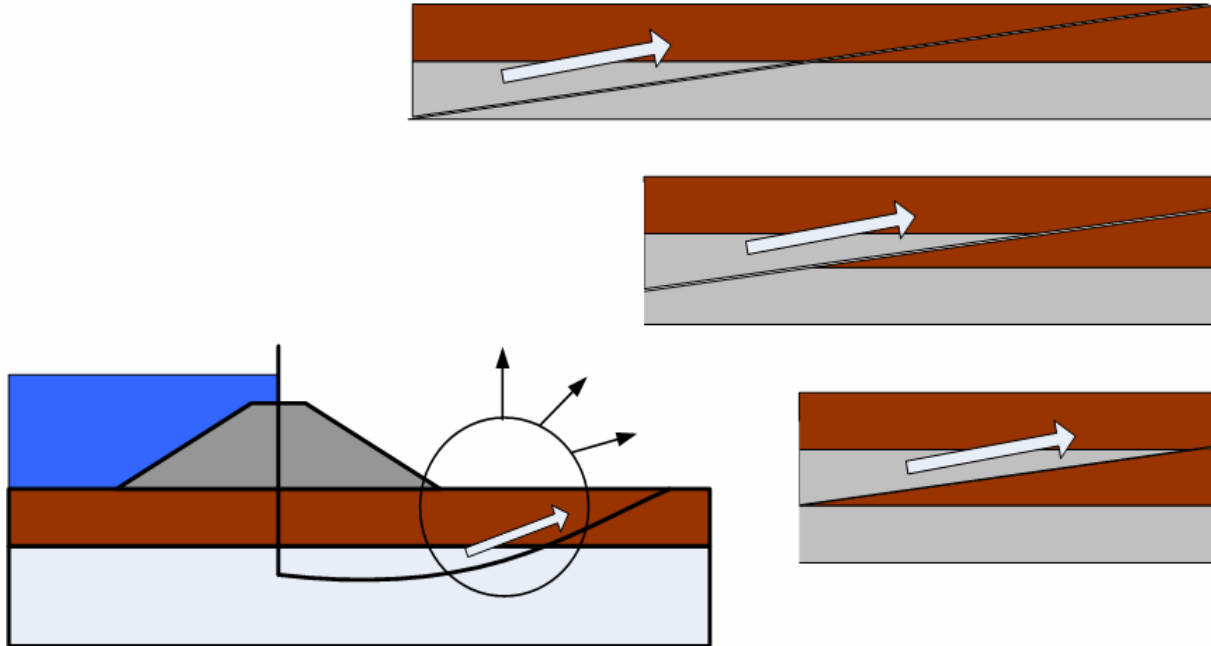


Figure 18. A portion of the clay layer, initially located beneath the marsh layer, was displaced upward and over a portion of the marsh layer as it was displaced laterally by the failure. A photograph of the displaced clay, with marsh material above it and below it, is shown in Figure 17.

## Soil Conditions and Soil Properties

The soil conditions in the area of the New Orleans outfall canals have been determined through evaluation of existing and recently drilled engineering borings, earlier geologic mapping studies of the area (See Appendix 2 - Dunbar et al. 1994, 1995; Dunbar, Torrey, and Wakeley 1999; Kolb, Smith, and Silva 1975; Kolb 1962; Kolb and Van Lopik 1958; and Saucier 1963, 1994), and new studies performed since August 2005.

Geologic mapping of the surface and subsurface in the vicinity of the canal failures identifies distinct depositional environments, related to Holocene (less than 10,000 years old) sea level rise and deposition of sediment by Mississippi River distributary channels during this period. Overlying the Pleistocene surface beneath the 17th Street Canal are approximately 50 to 60 ft of shallow water, fine-grained sediments consisting of bay sound or estuarine, beach, and lacustrine deposits as indicated in the cross section shown in Figure 19. Overlying this shallow water sequence are approximately 10 to 20 ft of marsh and swamp deposits that correspond to the late stages of deltaic sedimentation as these deltaic deposits became subaerial. A buried barrier beach ridge extends in a southwest to northeast direction in the subsurface, along the southern shore of Lake Pontchartrain, as shown by the geologic map in Figure 20. A stable sea level 10 to 15 ft lower than current levels permitted sandy sediments from the Pearl River to the east to be concentrated by longshore drift and formed a sandy spit or barrier beach complex in the New Orleans area (Saucier 1963, 1994). As shown by Figure 20, the site of the levee breach at the 17th Street Canal is located on the northern side of the beach ridge where the sand ridge is thinner and there is a layer of clay between the sand and the marsh layer, whereas both of the London Canal breaches are located over the thickest part of the barrier beach ridge complex, where the sand deposit lies directly beneath the marsh layer, as shown in Figure 19.

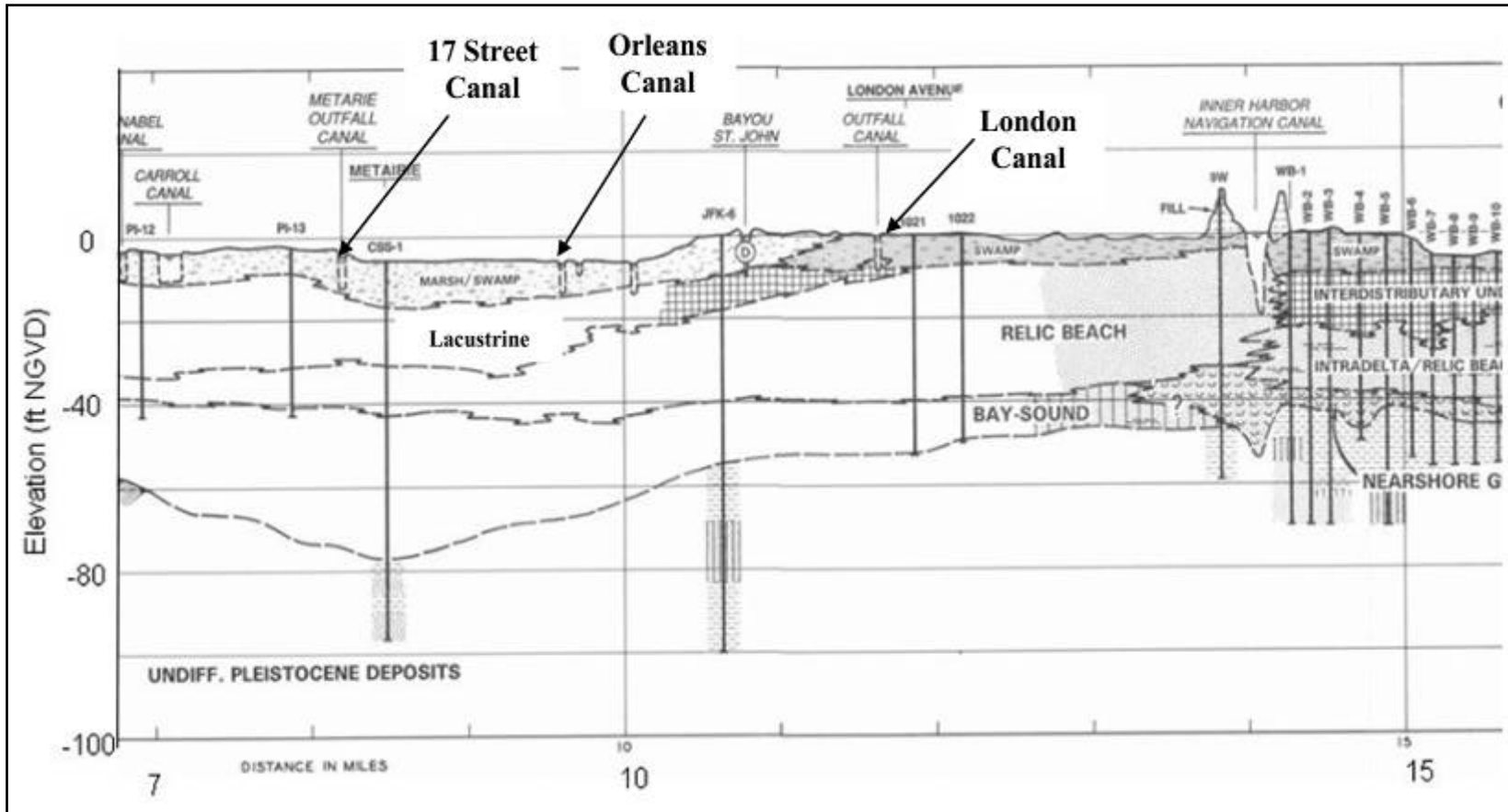


Figure 19. Geological cross section extending west to east across eastern Jefferson Parish and into western Orleans Parish. Section runs from near the 17th Street Canal to the Inner Harbor Navigation Canal. Major outfall canals in Orleans Parish are noted on the section. The cross section shows the different environments of deposition in the subsurface overlying the Pleistocene (10,000 to 2 million years old) surface. Holocene (less than 10,000 years old) shallow water fill composed of between 50 and 60 ft of bay-sound (and/or estuarine), relic beach (i.e., buried Pine Island Barrier beach complex) and lacustrine or interdistributary deposits. Shallow water environments are overlain by 10 to 20 ft of marsh and swamp deposits. Detailed explanation of environments with discussion of lithogology and engineering properties is presented in Appendix 1. Cross section modified from east half of section C –C', Spanish Fort Quadrangle (Dunbar et al. 1994). Maps and cross sections from the New Orleans area are available at [lvmapping.erd.c.usace.army.mil](http://lvmapping.erd.c.usace.army.mil).

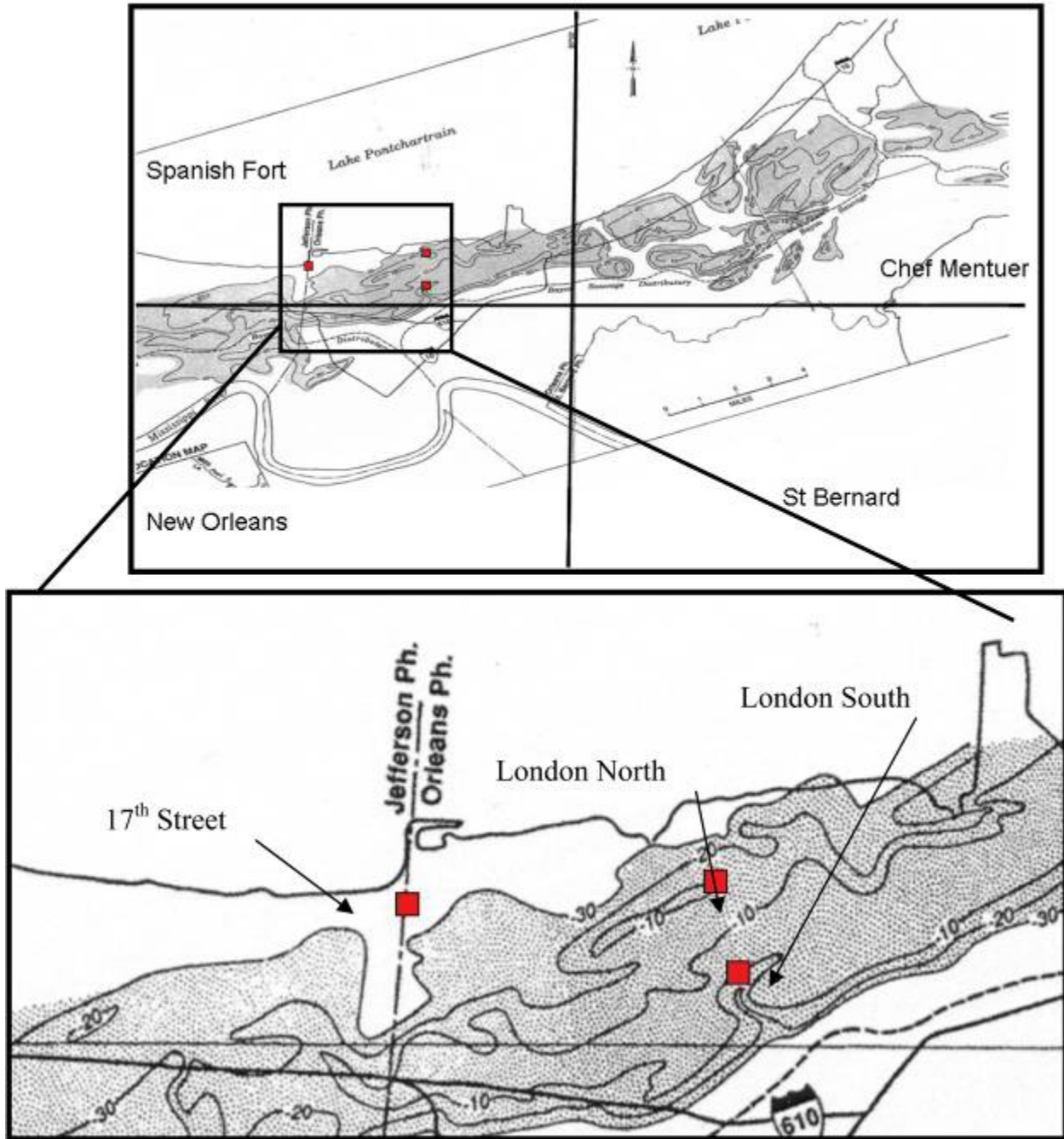


Figure 20. Generalized contour map showing Pine Island Beach contour values are in ft MSL (Saucier 1994). Upper figure shows general trend of the contours of the top of beach ridge in the New Orleans area, lower figure shows detailed view at the canals. London Canal levee failures are located along the axis of the beach. The 17th Street Canal levee break is located on the protected or back barrier side of the beach ridge and consequently is dominated by fine-grained deposits corresponding to low-energy depositional type settings. Extent of beach ridge shown extends across the Spanish Fort, Chef Mentuer, and New Orleans 15-min. USGS topographic quadrangles.

## Shear Strength Assessment for Analysis of the 17th Street Canal Breach

A considerable number of borings had been made in the breach area and in neighboring areas before the failure. Additional borings have been drilled, cone penetration tests have been performed, and test pits have been excavated since the failure. Figure 21 shows the locations of the available borings and Cone Penetration Test probes. Several hundred unconfined compression tests and unconsolidated-undrained (UU) tests have been conducted on the soils at the site. A summary of these is presented in Appendix 1, “Soil Data Report.”

A detailed representation of the soil stratification along the centerline of the levee in the breach area is shown in Figure 22. Figure 23 shows the cross section for Station 10+00, from the west bank to the east bank, where the breach occurred. The subsurface in the breach area was divided into six soil types over the depth of the investigation, as shown in Table 1.

<b>Layer</b>	<b>Approximate Elevation of Top of Layer, ft (NAVD88)</b>	<b>Approximate Elevation of Bottom of Layer, ft (NAVD88)</b>	<b>Soil Type</b>	<b>Consistency</b>
Embankment	5	-11.5	Clayey (CL's and CH)	Stiff
Marsh	-11.5	-16.5	Organic/Peat	Very Soft
Lacustrine	-16.5	-36.5	Clays (CH)	Very Soft
Beach Sand	-36.5	-45	Sand	
Bay Sound/Estuarine	-45	-75	Clayey (CH)	Stiff to Very Stiff
Pleistocene (Undifferentiated) Prairie Formation	-75		Clays – Generally CH with some sand	Stiff



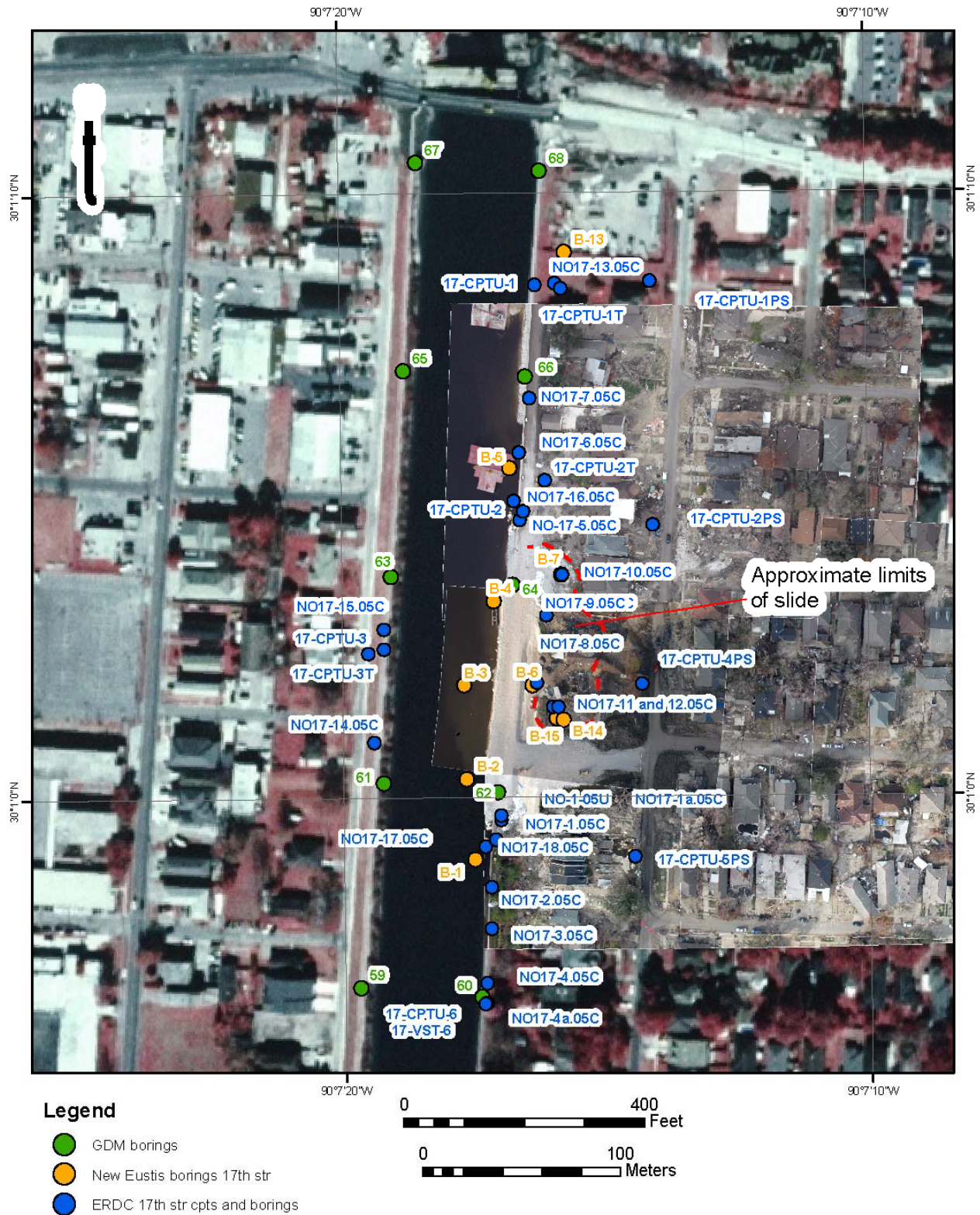


Figure 21. Boring and Cone Penetration Test location map – 17th Street Canal breach.

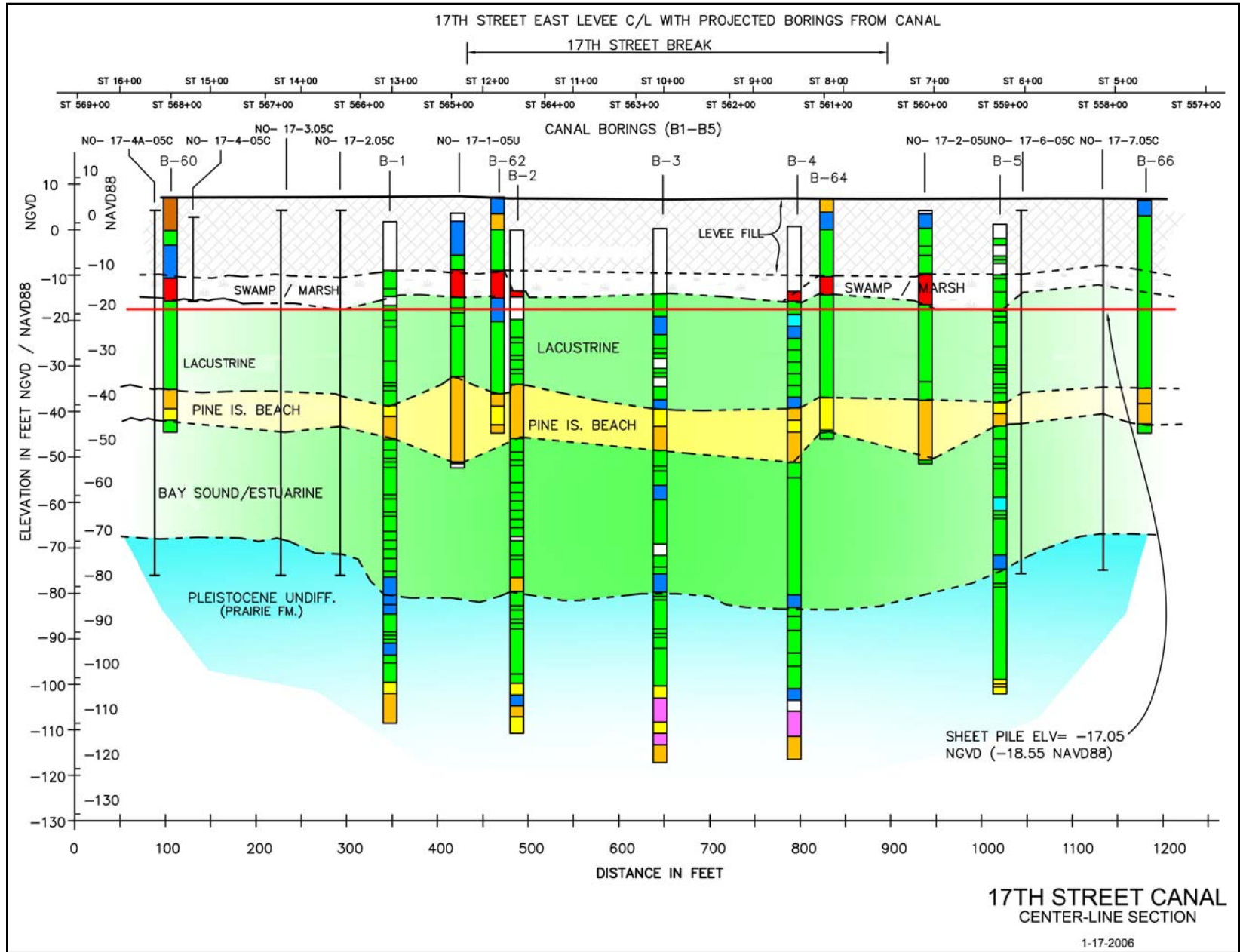


Figure 22. Centerline (CL) longitudinal section - 17th Street Canal breach.

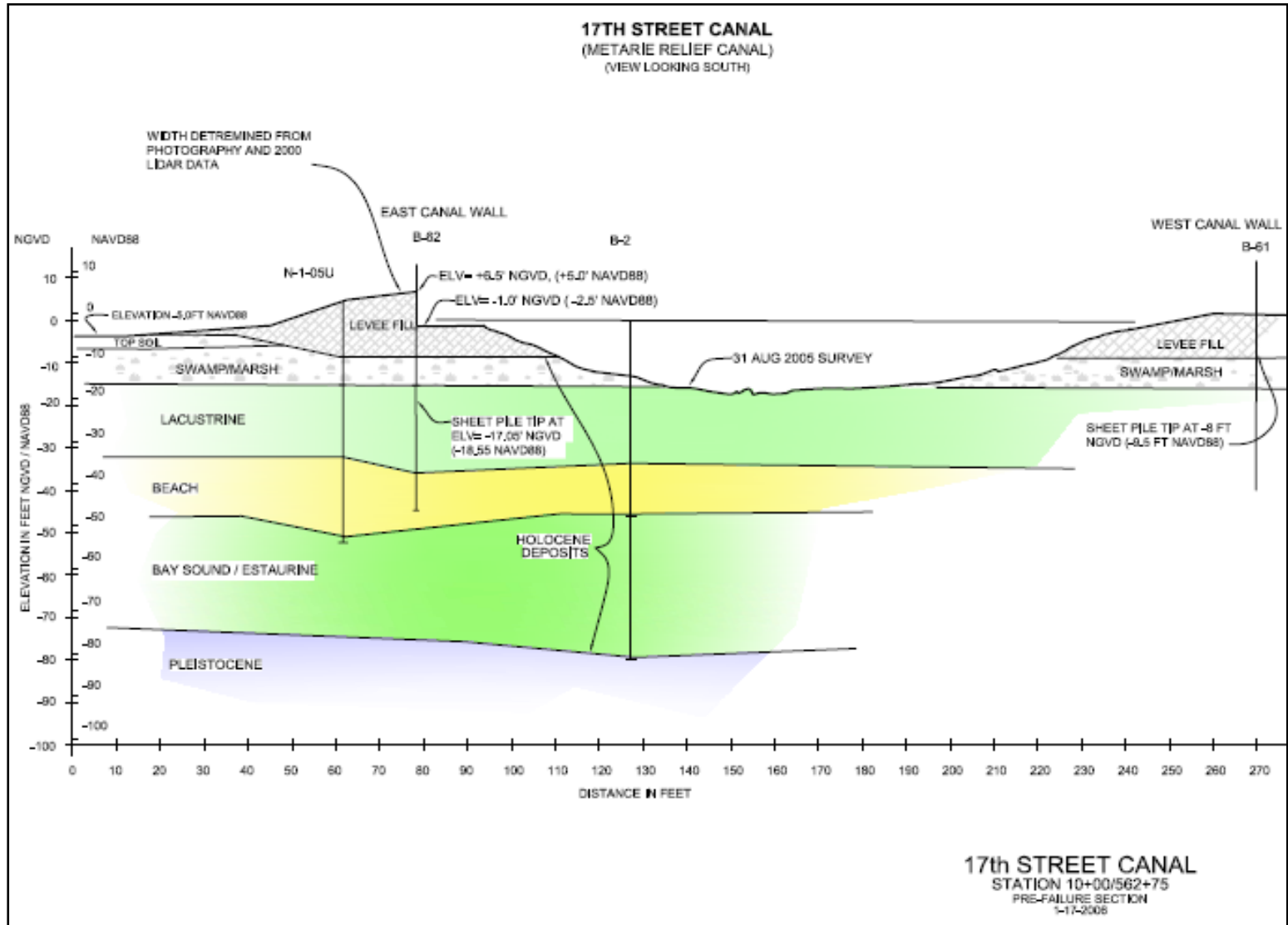


Figure 23. Prefailure cross section 17th Street Canal breach (New Stationing Sta 10+00) / (GDM Stationing Sta. 562+75).

The data available from previous and new studies in the 17th Street Canal area were used to develop a shear strength model, called here the IPET “strength model,” for use in analyzing the stability of the I-wall in the breach and adjacent areas. The strength model used for Station 10+00 of the 17th Street Canal analysis is shown in Figure 24.

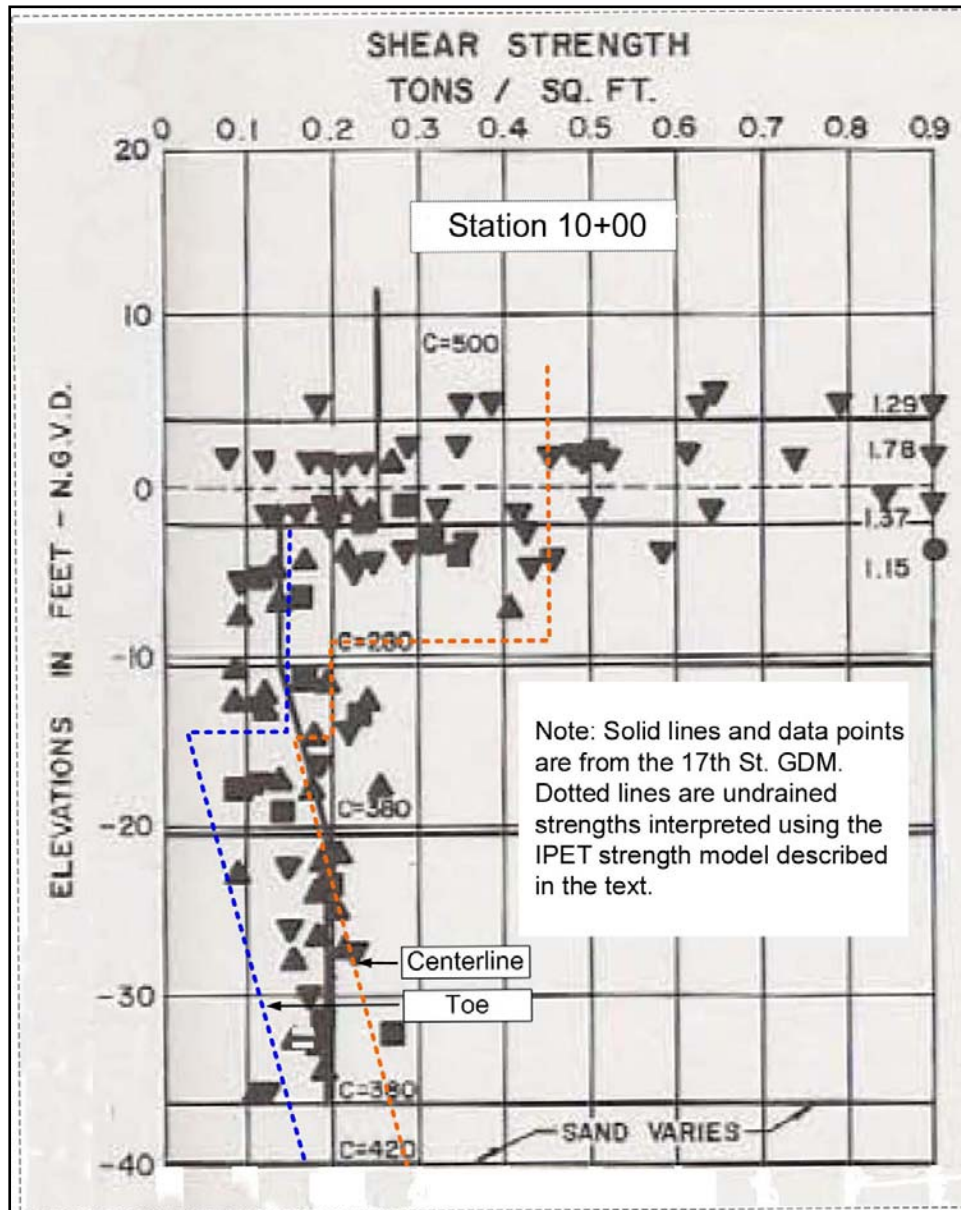


Figure 24. Comparison of undrained strength profiles used for the 17th Street I-wall design with strength profiles interpreted from the IPET strength model for Station 10+00.

The levee fill is compacted CL or CH material, with an average liquid limit of about 45%. Beneath the fill is a layer of marsh 5 ft to 10 ft thick. The marsh is composed of organic material from the cypress swamp that occupied the area, together with silt and clay deposited in the marsh. The average moist unit weight of the marsh is about 80 (pounds per cubic feet) pcf. Beneath the marsh is a lacustrine clay layer, with an average liquid limit of about 95%. The clay

is normally consolidated throughout its depth, having been covered and kept wet by the overlying layer of marsh.

The measured shear strengths of the levee fill scatter very widely, from about 120 psf to more than 5,000 psf, and cannot be interpreted without applying judgment. The values used are based on the combined judgment of the IPET team to make the most reasonable interpretation of the scattered data. Placing the greatest emphasis on data from UU tests on 5-in.-diameter samples, which appear to be the best quality data available,  $s_u = 900$  psf is a reasonable value to represent the levee fill. This strength can be compared to a value of 500 psf for the levee fill used in the design analyses. The marsh (or peat) deposit is stronger beneath the levee crest where it was consolidated under the weight of the levee, and weaker at the toe of the levee and beyond, where it less compressed. The measured shear strengths of the marsh scatter very widely, from about 50 psf to about 920 psf. Values of  $s_u = 400$  psf beneath the levee crest and  $s_u = 300$  psf beneath the levee toe appear to be representative of the measured values. These strengths can be compared to a value of 280 psf at all locations that was used in the design analyses.

The clay (which has been found to be the most important material with respect to stability of the I-wall and levee) is normally consolidated. Its undrained shear strength increases with depth at a rate of 11 psf per foot of depth. This rate of increase of strength with depth corresponds to a value of  $s_u / p' = 0.24$ . There is very little scatter in the results of the Cone Penetration Test with pore water pressure measurements – piezocone test (CPTU), and these values provide a good basis for establishing undrained strength profiles in the clay. The undrained strength at the top of the clay is equal to 0.24 times the effective overburden pressure at the top of the clay. With this model, the undrained shear strength of the clay varies with lateral position, being greatest beneath the levee crest where the effective overburden pressure is greatest and least at the levee toe and beyond where the pressure is lowest, and varying with depth, increasing at a rate of 11 psf per foot at all locations.

The design analyses used undrained strengths for the levee fill, the marsh, and the clay, and a drained friction angle to characterize the strength of the sand layer beneath the clay, as does the strength model described above. Thus, the strengths are directly comparable. Strengths from the IPET strength model are compared to the design strengths in Table 2.

<b>Table 2 Comparison of Strengths of the Levee and Marsh Used in the Design with the IPET Strength Model.</b>		
<b>Material</b>	<b>Strength Uses for Design</b>	<b>Strength Model Based on all Data Available in February 2006</b>
Levee fill	$s_u = 500$ psf, $\phi = 0$	$s_u = 900$ psf, $\phi = 0$
Marsh	$s_u = 280$ psf, $\phi = 0$	$s_u = 400$ psf, $\phi = 0$ beneath levee crest $s_u = 300$ psf, $\phi = 0$ beneath levee toe

It can be seen that the strengths for the levee fill and the marsh used in the design are consistently lower than those for the IPET strength model, which were estimated using all of the data available in February 2006.

The values of strength for the clay vary with depth and laterally, as discussed above. The rate of increase of strength with depth (11 psf per foot in the IPET strength model) is practically the same in the IPET strength model as for the design strengths. Beneath the levee crest, the design strengths are very close to the IPET strength model. At the toe of the levee, however, the strengths used in the design are considerably higher than the strengths from the IPET strength model.

Field observations and preliminary analyses show that the most important shear strength is the undrained strength of the clay. Critical slip surfaces intersect only small sections within the marsh and the levee fill, and do not intersect the sand layer beneath the clay at all. Therefore, the strengths of these materials have small influence on stability, and minor variations in these strengths from section to section would not control the location of the failure. For this reason, the comparison of strengths in the breach area with strengths elsewhere has been focused on the undrained strength of the clay.

Although the data are sparse, they are fairly consistent, and it appears that the clay strengths in the areas north and south of the breach are higher than those in the breach. Based on data available for comparison, the undrained strengths of the clay in the areas adjacent to the breach are 20% to 30% higher than those in the breach area. Strength differences of this magnitude are significant. They indicate that the reason the failure occurred where it did is very likely that the clay strengths in that area were lower than in adjacent areas to the north and south.

A more complete description of the IPET strength model and the tests that support it is contained in Appendix 3, “17th Street Shear Strength Evaluation.”

## **Limit Equilibrium Stability Assessment**

Limit equilibrium analyses were used to examine stability of the levee and I-wall. The results of these analyses are interpreted in terms of factors of safety and probabilities of failure.

Stability analyses were performed for three cross sections within the breach area using the IPET shear strength model. The results of these analyses were compared with the results of the analyses on which the design of the I-wall was based, and additional analyses were performed for the design cross-section geometry and shear strengths, using Spencer’s method and the computer program, SLIDE<sup>1</sup>. The SLIDE analysis results were checked using UTEXAS4<sup>2</sup>.

It was found that:

- The calculated factors of safety decreased as the elevation of the water level on the canal side of the wall increased, and

---

<sup>1</sup> Available from Rocscience Inc., 31 Balsam Avenue, Toronto, Ontario, Canada M4E 3B5.

<sup>2</sup> Available from Shinoak Software, 3406 Shinoak Drive, Austin, TX 78731.

- Smaller factors of safety were calculated when it was assumed that a gap existed between the wall and the soil on the canal side of the wall, with hydrostatic water pressures acting within this gap, increasing the load on the wall.

It seems likely that, as the water level in the canal rose, the I-wall deflected towards the landside, causing it to pull away from the levee fill. When the resulting gap between the fill and the wall filled with water, the increased hydrostatic pressure became a significant factor in decreasing the wall stability.

The results of the analyses are consistent with the performance of the I-wall in the breach area. Calculated water levels for factors of safety equal to 1.0 for the condition with a gap behind the wall range from 9.8 ft to 10.6 ft, which is approximately the water level in the canal when the breach in the levee fully opened. This is compared with a water level of 7 to 8 ft at the time when the I-wall began to lean based on an eyewitness report. In addition, it was found that using non-circular slip surfaces reduced the calculated factors of safety by about 5% as compared with those calculated using circular slip surfaces. Thus, considering the influence of waves increasing the effective average water level, and non-circular slip surfaces resulting in lower factors of safety, it is apparent that the results of the stability analyses are in close agreement with the observed performance.

The calculated factors of safety are about 25% lower when it is assumed that a separation or gap develops between the wall and the levee fill on the canal side of the wall. The results calculated, assuming that a gap formed and full hydrostatic water pressure acted in the gap, are consistent with field observations, indicating that it is highly likely that a gap did form in the areas where the wall failed. It seems likely that when a gap formed and the portion of the wall below the levee crest was loaded by water pressures, the factor of safety would have dropped quickly by about 25%. Soil-structure interaction analyses and centrifuge model tests have confirmed this mode of behavior.

The New Orleans District Method of Planes<sup>3</sup> used for the design analyses is a conservative method of slope stability analysis. All other things being equal, the factor of safety calculated using the Method of Planes was about 10% lower than the factor of safety calculated using Spencer's method<sup>4</sup>, which satisfies all conditions of equilibrium.

The factors of safety calculated in the design analyses were higher than the factors of safety calculated for the conditions that are believed to best represent the actual shear strengths, geometrical conditions, and loading at the time of failure. The principal differences between the design analyses and the conditions described in this report relate to (1) the assumption that a gap formed between the wall and the levee soil on the canal side of the wall, and (2) the fact that the design analyses used the same strength for the clay beneath the levee slopes, and for the area

---

<sup>3</sup> A study of the Method of Planes, undertaken by IPET at the request of the New Orleans District Task Force Guardian, indicates that the Method of Planes gives lower factors of safety than more accurate methods of analysis, such as Spencer's method. The magnitude of the difference between the two varies from case to case.

<sup>4</sup> Spencer, E. (1967). A method of analysis of the stability of embankments assuming parallel inter-slice forces. *Geotechnique*, Institution of Civil Engineers, Great Britain, Vol. 17, No. 1, March, pp. 11-26.

beyond the levee toe, as for the zone beneath the crest of the levee. The IPET strength model has lower strengths beneath the levee slopes and beyond the toe.

Factors of safety for areas adjacent to the breach, where clay strengths are higher, were about 15% higher than those calculated for the breach area. These differences in calculated factors of safety are not large; and it thus appears that the margin of safety was small in areas that did not fail. It is possible that gaps did not form in those areas, and the wall was, therefore, less severely loaded.

Estimates of probability of failure for a water level of 7.0 ft NAVD88 are about 12% in the breach area, and 1% in adjacent areas with clay strengths 20% higher. For a water level of 10.0 ft, the estimated probability of failure is 58% in the breach area and 16% in adjacent areas.

A more complete description of the stability analyses and results is contained in Appendix 4, “17th Street Slope Stability Analyses.”

### **Centrifuge Modeling Results for the 17th Street Canal Breach**

The physical (centrifuge) models of the levees on 17th Street, London Avenue, and Orleans Canals have provided detailed insights into the mechanisms that led to the breach. A more complete description of the centrifuge modeling effort is contained in the Appendix 5, “IPET Centrifuge Model Test Report.” The centrifuge modeling has contributed to the overall understanding of the performance of the outfall canal levees.

The centrifuge model results revealed that the gap formation had a major contribution to all of the beaches on the outfall canals. In all of the scale models where the toe of the sheet-pile wall terminated in the clay layer, such as the 17th Street Canal breach location, a translational failure occurred through the clay when the gap opened and filled with water. This is clearly seen in the instruments recording movement of the wall and in the video imagery (Figure 25).

The sliding surface developed near the top of the clay layer and progressed landwards until it was outside the levee, then turned upward to exit through the marsh layer. This mechanism is similar to the observations in the field from 17th Street. The movement of the model wall was arrested before larger displacements took place to capture the final state of the 17th Street model (Model 1) (Figure 25). Despite the fairly significant lateral movement, there is minimal heave of the swampy marsh layer on the landward side at the stage shown in Figure 26.



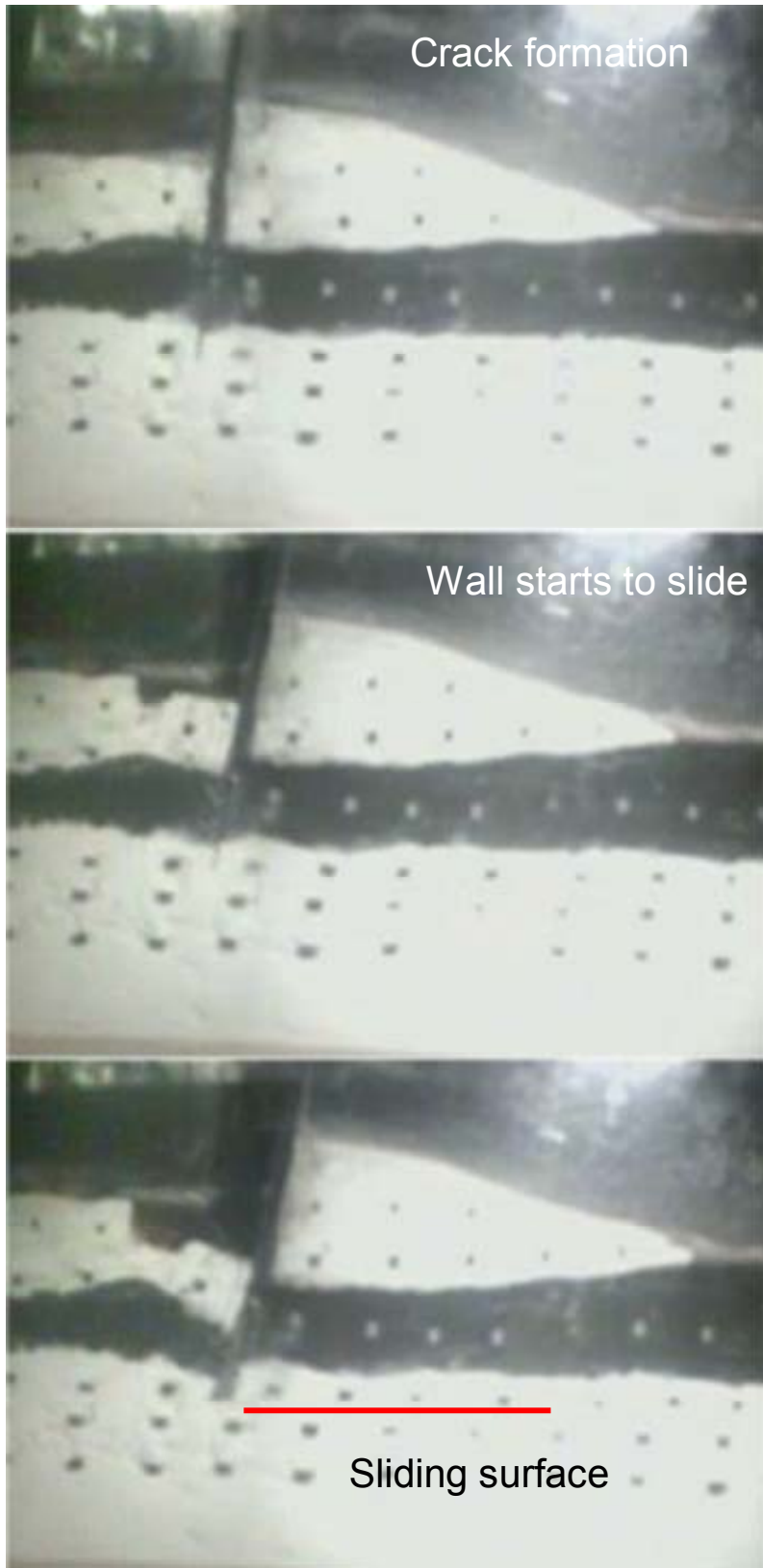


Figure 25. Sliding surface forms at top of clay layer in 17th Street Canal Model 1.

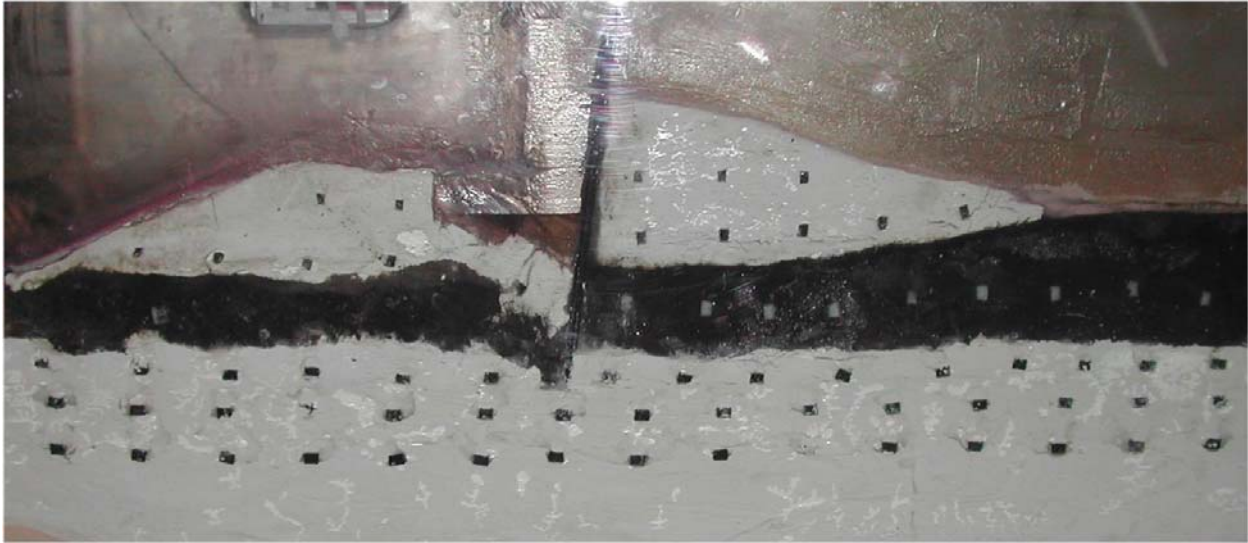


Figure 26. Final state of 17th Street Model 1 showing lateral translation on sliding surface starting at the toe of the wall and progressing landward.

All of the clay foundation models failed with a similar mechanism under the flood loading, commencing with a small rotation and formation of a gap behind the wall, followed by further rotation and large translation associated with a shear plane that formed from the toe of the sheet pile wall and progressed landwards through the upper part of the clay layer. This was consistent with the field observations.

Other observations relevant to the site conditions on the 17th Street Canal were also noted from the centrifuge model tests. The very soft, normally consolidated clay beneath the levee experienced significant settlements as the weight of the levee was increased to its full value. The marsh layer also tended to be compressed below the levee, but predominantly through elastic compression.

In the 17th Street Canal models, the formation of the gap behind the wall was followed by the immediate development of a slip movement at the toe of the wall, and an increasing rate of landward movement. As the initial slip surface extended toward the toe of the levee, the weaker clay farther from the centerline of the levee was less able to resist the driving forces acting on the levee block.

A more complete description of the centrifuge modeling effort is contained in Appendix 5, “IPET Centrifuge Model Test Report.”

### **Finite Element Soil-Structure Interaction Results for the 17th Street Canal Breach**

Two dimensional finite element soil-structure interaction analyses with PLAXIS and FLAC using a nonlinear hyperbolic soil stress-strain model were conducted to provide a third approach to the development of a complete understanding of the 17th Street Canal breach mechanism. A two-dimensional (2-D) cross section at Station 10+00 of the east side of the 17th Street Canal at

the breach location was modeled, as shown in Figures 27 and 28. A detailed description of the nonlinear finite element soil-structure interaction analyses and results is contained in Appendix 6, "Soil-Structure Interaction Analysis of the Floodwalls at 17th Street."

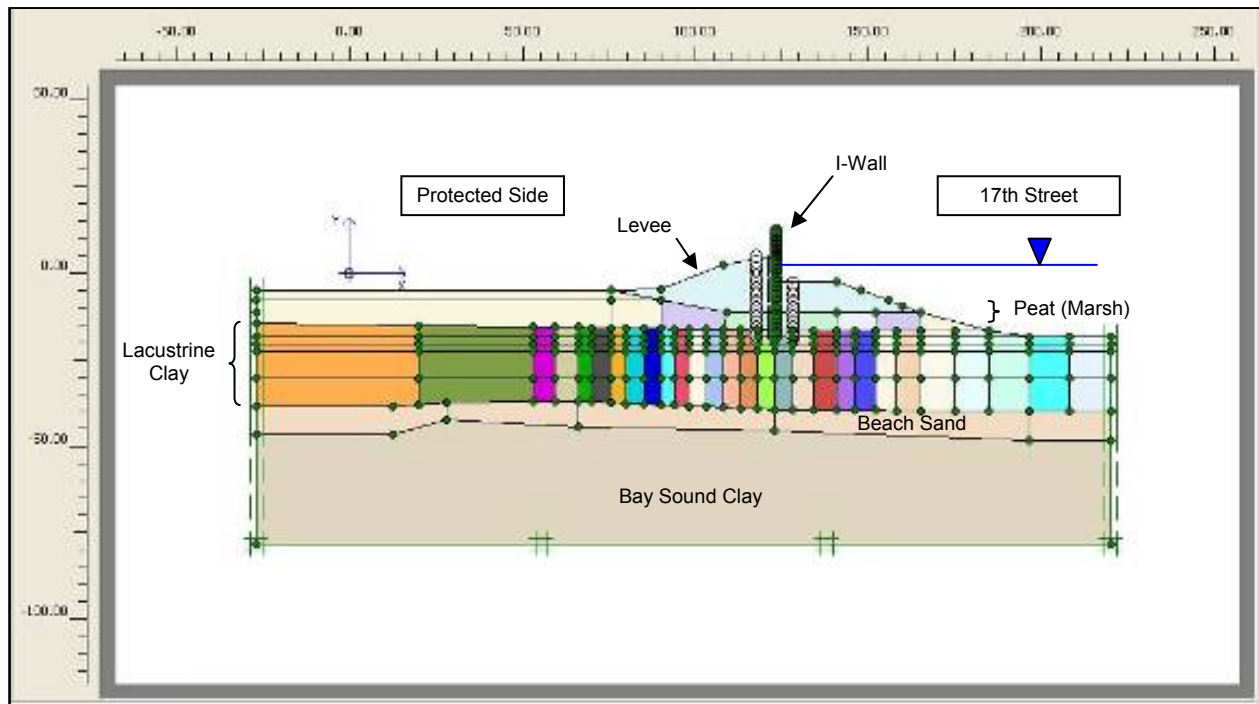


Figure 27. Two-dimensional cross-section model used in soil-structure interaction analysis of Station 10+00 on the 17th Street Canal east side breach.

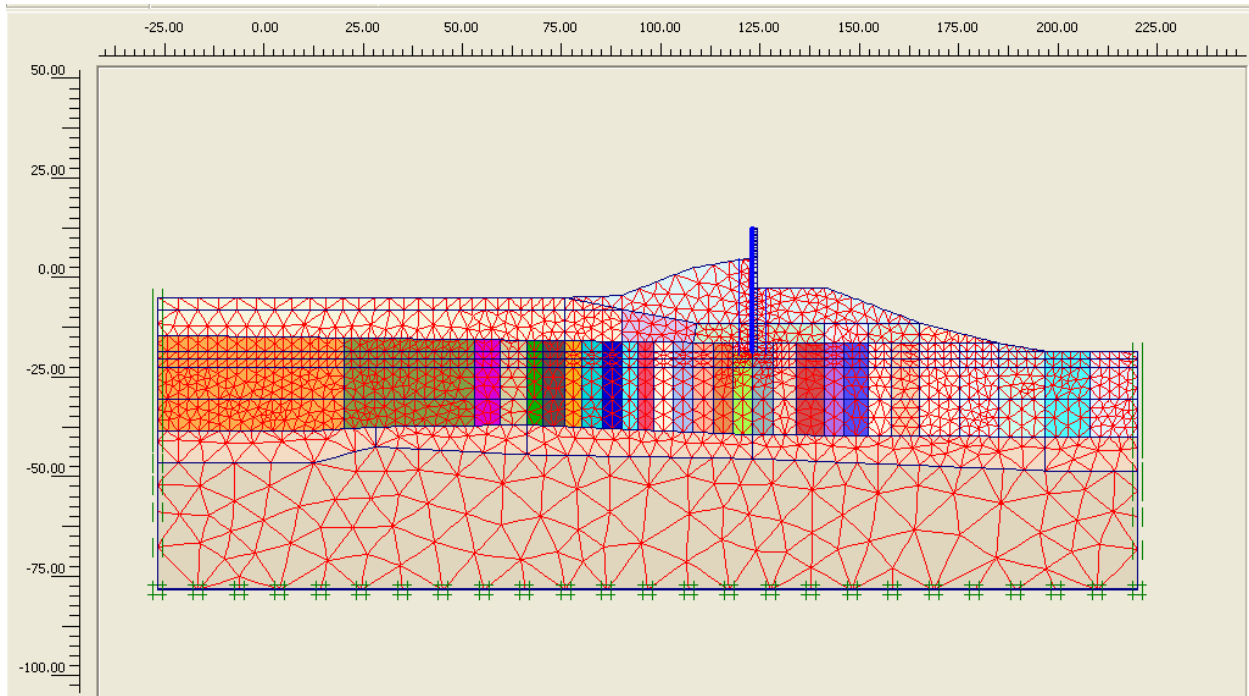


Figure 28. Finite element mesh used in soil-structure interaction analysis of Station 10+00 on the 17th Street Canal east side breach.

The finite element analyses show that gap formed as the water rose on the canal side of the wall. The criterion for gap formation was earth pressure against the wall less than the hydrostatic water pressure at that depth. When that condition was reached, the finite element mesh was adjusted to separate the soil elements from the wall elements with a gap. The gap began to open when the water in the canal rose to elevation 6.5 ft. Eventually, the gap extended to the tip of the sheet pile, which was at the lacustrine clay-marsh interface. Factors of safety were computed using the strength-reduction method. The strength-reduction method involves performing a series of finite element analyses using values of the strength parameters  $c$  and  $\phi$  (or  $c'$  and  $\phi'$ ) that are reduced by dividing them by assumed values of factor of safety. The correct factor of safety, as determined by this method, is the smallest value that results in unstable conditions in the analysis. When the gap developed and filled with water, the factor of safety decreased suddenly by about 25%, from 1.45 to 1.16, as shown in Figure 29.



Figure 29. Factor of safety versus canal water elevation computed in the soil-structure interaction analysis of Station 10+00 on the 17th Street Canal east side breach.

The development of a gap, which immediately filled with water, resulted in a marked increase in calculated displacements, as shown in Figure 30. As the water in the canal rises from 6.5 to 9.0 ft NGVD, the maximum lateral deformation increases from 1.6 ft, the condition shown in Figure 31, to 5.3 ft, the conditions shown in Figure 32; and the factor of safety decreases from 1.16 to 0.98. Figure 33 shows that the contours of maximum shear strains form a shear surface that compares well with the critical failure surface found in the limit equilibrium stability analysis, Figure 34.

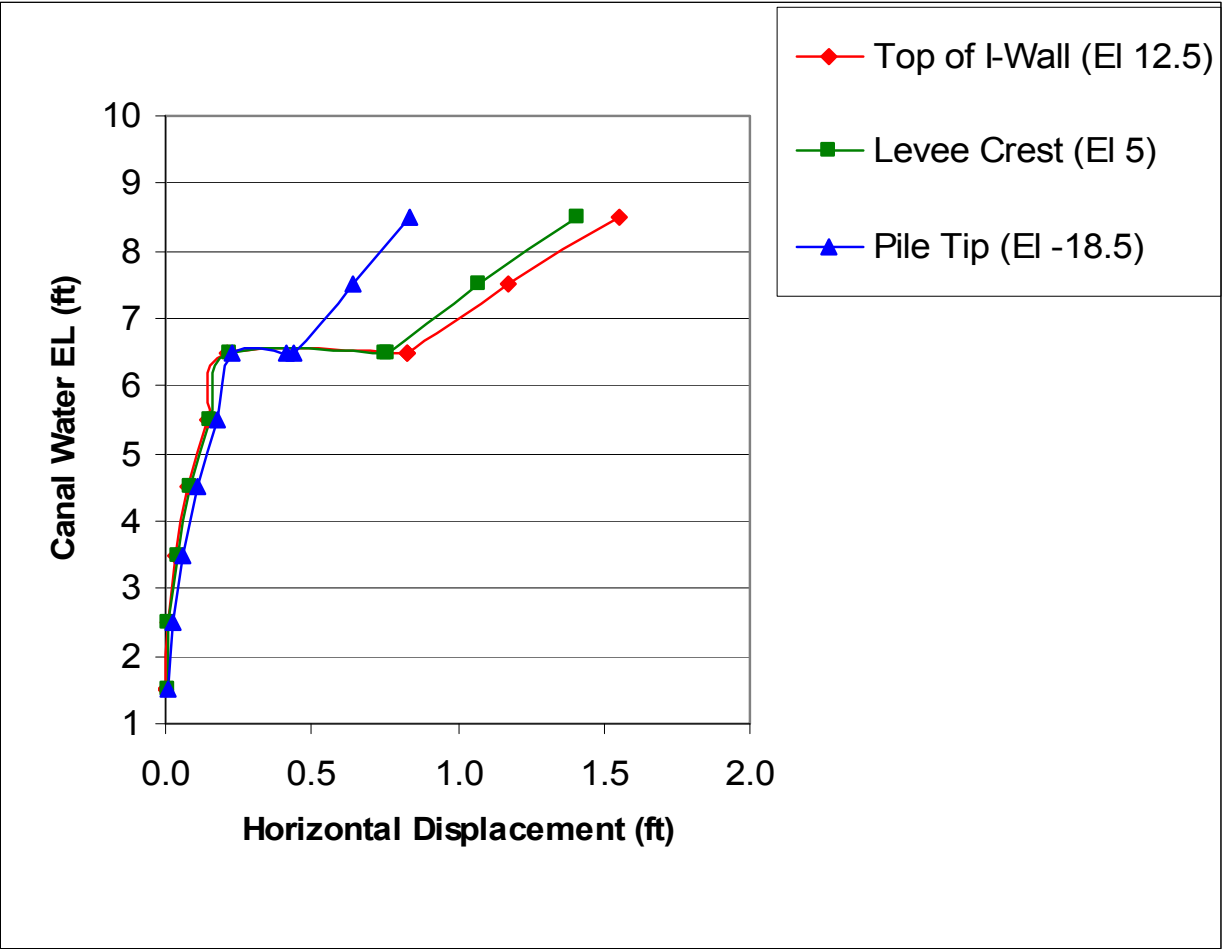


Figure 30. Horizontal sheet pile deflections versus canal water elevation computed in the soil-structure interaction analysis of Station 10+00 on the 17th Street Canal east side breach.

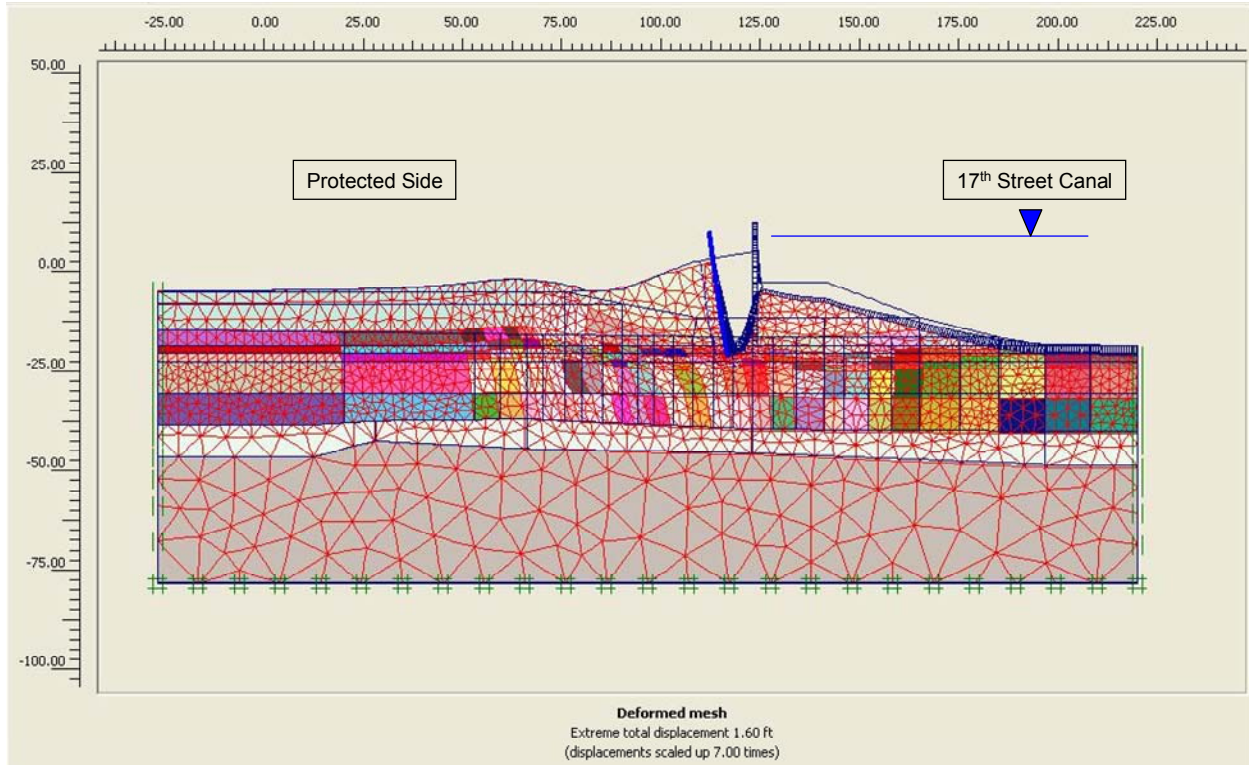


Figure 31. Deformed mesh for canal elevation 6.5 ft and gap to elevation -18.5 ft computed in the soil-structure interaction analysis of Station 10+00 on the 17th Street Canal east side breach (Note: Canal elevation not to scale in figure).

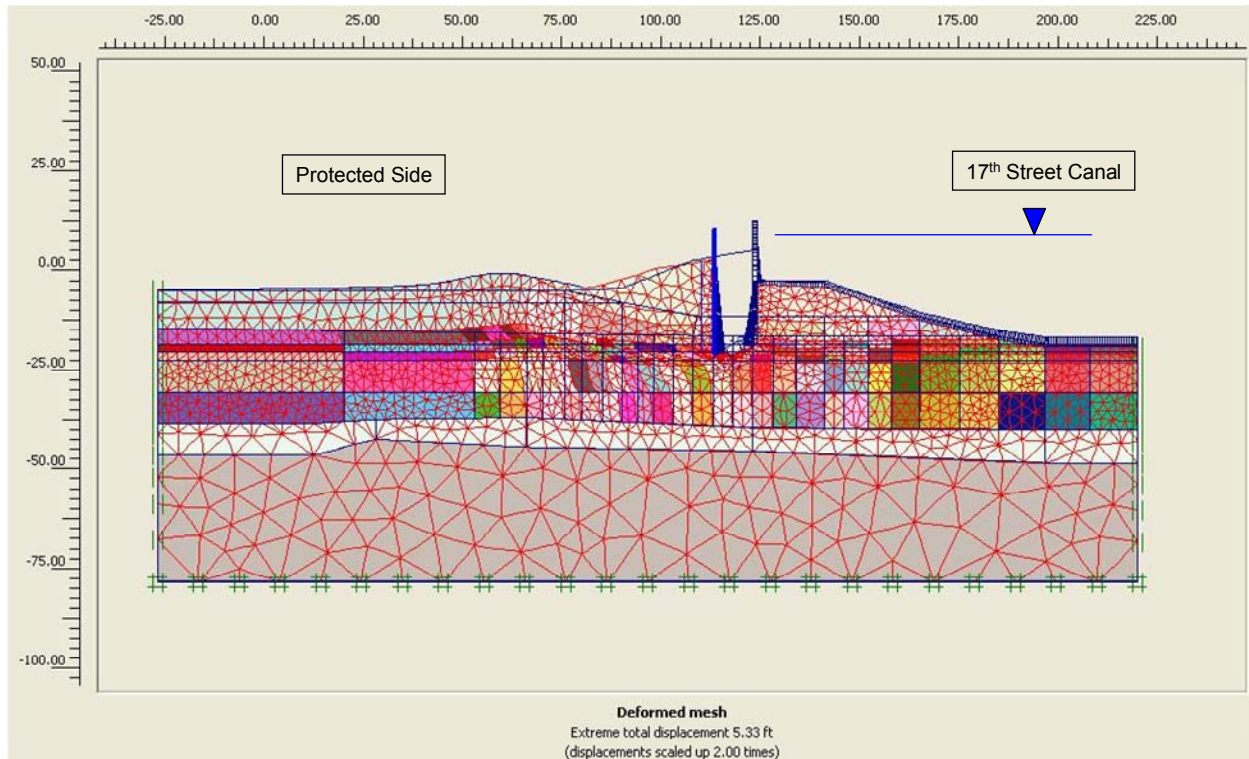


Figure 32. Deformed mesh for canal elevation 9.0 ft and gap to elevation -18.5 ft computed in the soil-structure interaction analysis of Station 10+00 on the 17th Street Canal east side breach (Note: Canal elevation not to scale in figure).



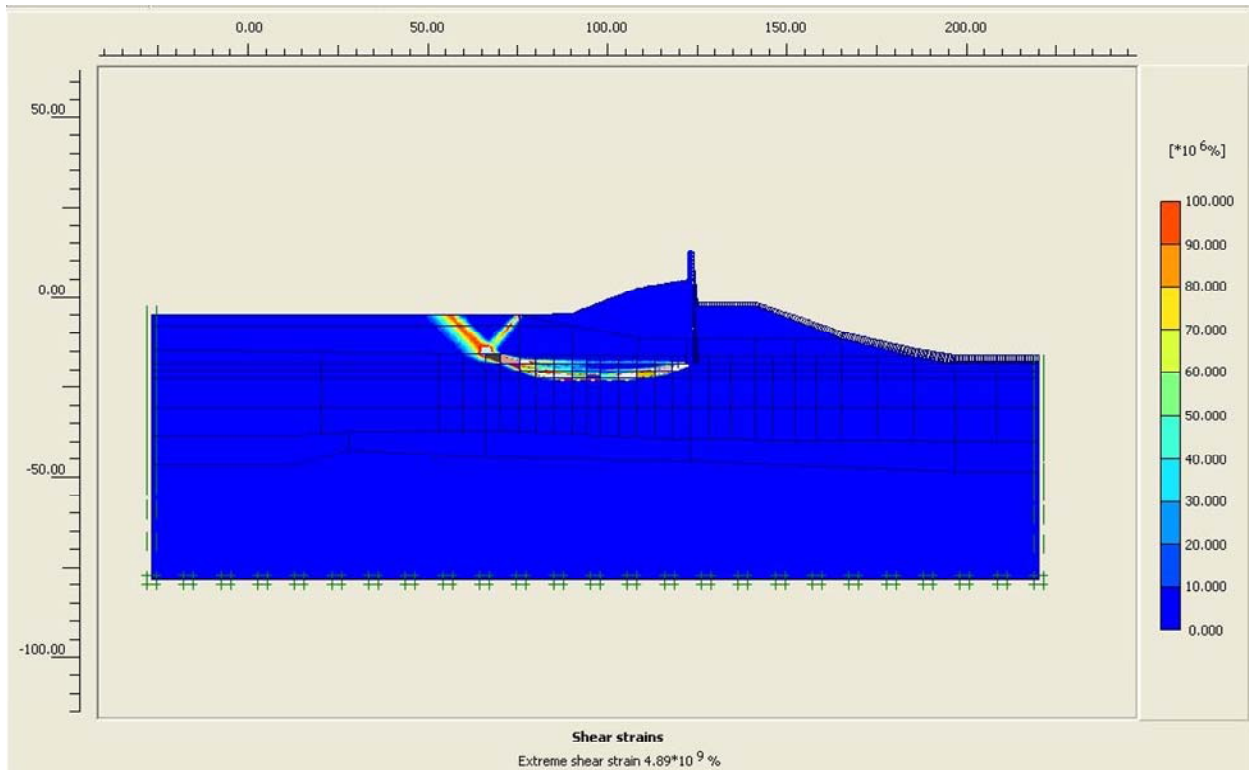


Figure 33. Reaches of large shear strains from strength reduction for canal elevation 9.0 ft and gap to elevation -18.5 ft computed in the soil-structure interaction analysis of Station 10+00 on the 17th Street Canal east side breach.

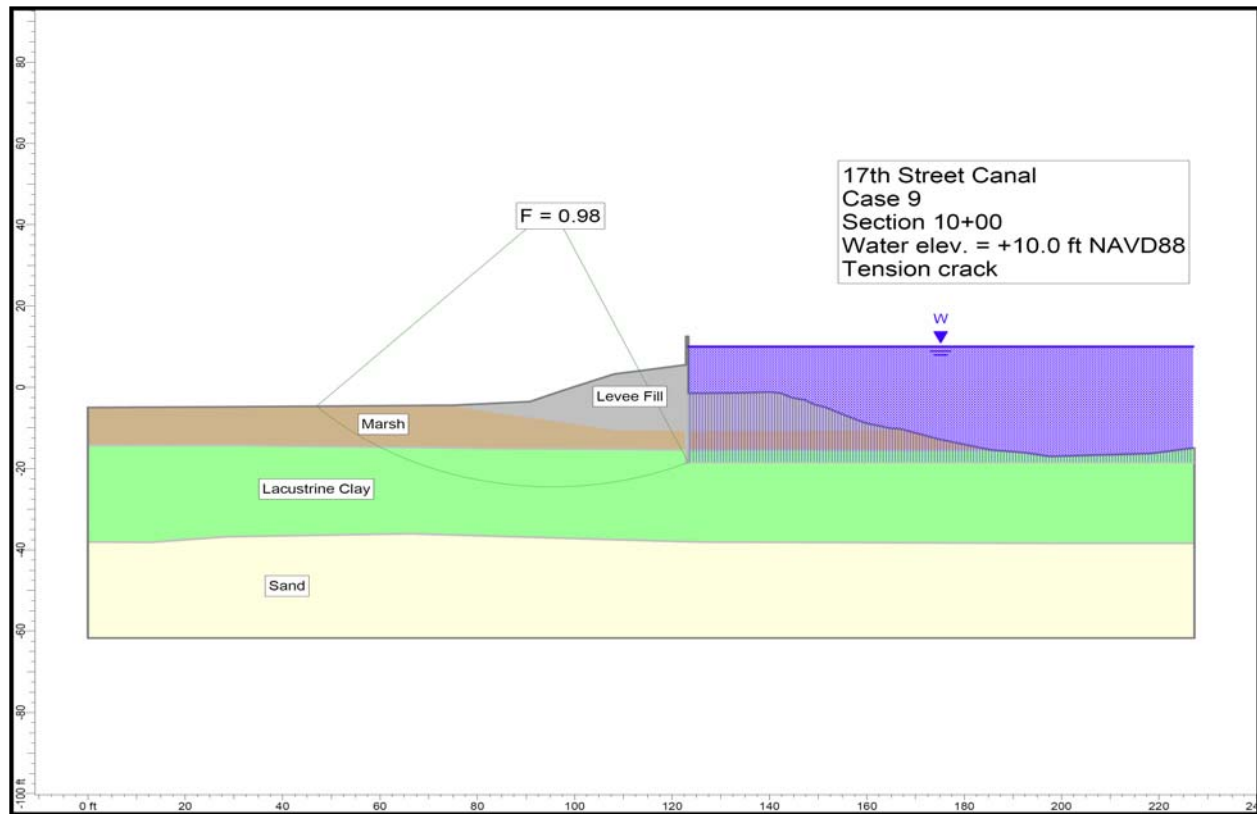


Figure 34. Critical circle for 17th Street Canal Station 10+00 – water elevation 10 ft, with a water-filled gap behind the wall.

A more complete description of the finite element soil-structure interaction is contained in Appendix 6, “Soil-Structure Interaction Analysis of the Floodwalls at 17th Street.”

### Summary of 17th Street Canal Breach Assessment

Eye-witness reports indicate that the breach began to develop about 6:00 a.m. on Monday, 29 August 2005, and was fully developed before 9:00 a.m. Field evidence, analyses, and physical model tests show that the breach was due to instability caused by shear failure within the clay in the foundation beneath the levee and the I-wall, with a rupture surface that extended laterally beneath the levee, and exited upward through the marsh layer. A key factor in the failure was the formation of a gap between the wall and the levee fill on the canal side of the wall, allowing water pressure to act on the wall below the surface of the levee. Another important factor was the low shear strength of the foundation clay beneath the outer parts of the levee and beyond the toe of the levee.

These two important factors in the mechanism of failure have significant system-wide implications because gap formation and lateral variation of shear strength beneath the levee must be considered for other locations throughout the system when geologic conditions are similar to those at the 17th Street Canal.

## Assessment of London Avenue Canal Breaches

Two I-wall failures resulting in breaches occurred at the London Avenue Canal during Hurricane Katrina, one on the east side of the canal at Mirabeau Avenue (the south breach), and the other on the west side of the canal at Robert E. Lee Boulevard (the north breach). At both locations, the levees and I-walls were founded on a layer of marsh material overlying sand. In addition, the I-wall on the east side, across the canal from the north breach, moved and tilted, but did not breach.

The south breach, shown in Figure 35, occurred about 7:00 a.m. to 8:00 a.m. on 29 August 2005, when the water level in the canal was 8.2 ft to 9.5 ft NAVD88. The breach was narrower than the breach at the 17th Street and the London Avenue north breach. A deep scour hole formed due to the inrush of water, and a large amount of eroded sand was deposited in the neighborhood inland of the breach. It appears that the breach was quite narrow when it formed, and subsequently widened to about 60 ft as wall panels adjacent to the initial breach were undermined by scour, and tilted into the scour hole.



Figure 35. South breach, London Avenue Canal.

The north breach, shown in Figure 36, occurred about 7:00 a.m. to 7:30 a.m. on 29 August, about an hour after the south breach, when the canal water level was 8.2 ft to 8.9 ft NAVD88. The breach was about 410 ft wide, approximately the same width as the breach at 17th Street. As the breach occurred, the ground surface on the protected side of the levee heaved upward, taking with it the playhouse shown in Figure 37. The upward movement of the playhouse can be discerned by comparing the before and after photos in Figure 37. The I-wall opposite the north breach (on the east side of the canal) moved and tilted significantly, presumably at about the same time as the breach occurred on the west side, but the east I-wall did not breach; this tilted but intact I-wall is shown in Figure 38. A line of sinkholes was observed at the inland side of the distressed east I-wall, and a sand boil at the inboard embankment toe indicates that erosive seepage and piping had occurred beneath the levee.



Figure 36. North breach, London Avenue Canal.



Figure 37. Playhouse at the London Avenue Canal north breach before the failure (top photo) and after (bottom photo).



Figure 38. Tilted I-wall opposite the north breach on the London Avenue Canal.

At both the south and north breach locations, it seems likely that underseepage and internal erosion caused or contributed to the failures.

It is not possible to establish the cause of the south breach with certainty based on the field observations made after the failure. The failed sections of the I-wall have not yet been found, and large volumes of sand were moved by the inflow of water through the breach, covering the landscape. The failure might have resulted from underseepage erosion and piping, or from sliding instability aggravated by underseepage and uplift pressures. Analyses have been performed to examine both of these possibilities.

As shown in Figure 36, a long section of the floodwall at the north breach was displaced laterally, and it seems likely that sliding instability was likely the primary mode of failure, with seepage and high pore pressures in the sand as a significant contributing factor. It seems likely that the failure and breach were the result of insufficient passive resistance to counteract the water pressure forces to which the wall was subjected. The passive resistance was likely reduced by the effects of water seeping through the foundation soils beneath the levee and the marsh layer inland, inducing uplift pressures and reducing shear strengths. Analyses have been performed to examine the likelihood of erosion and piping, and instability due to uplift and reduced shear resistance.

## Seepage and Stability Analyses of the London Avenue Canal Breaches

Seepage and stability analyses were performed to investigate if the erosion and piping and/or sliding instability caused the foundation failure at these breach locations. Finite element analyses of seepage beneath the I-wall were performed to determine the pore pressures in the sand beneath the marsh layer. The characteristics of the cross sections for the south and north breach are shown in Figure 39 and Figure 40. The relevant materials are the sand at the base of the section, the overlying marsh layer, and the clayey levee fill. Thorough analyses of transient and steady seepage indicated that (a) steady seepage through the sand was established quickly, and (b) the pore pressures within the sand and the uplift pressures on the base of the marsh layer are not affected by the permeability values assigned to the marsh layer and the levee fill, provided that those materials are at least two orders of magnitude less permeable than the sand. The values of permeability of the marsh layer and the levee fill used in the seepage analyses were selected in accordance with these findings, and were considered to be reasonable estimates of the permeabilities of these materials. A more complete description of the seepage analysis is contained in Appendix 8, "Analysis of London Avenue Canal I-Wall Breaches."

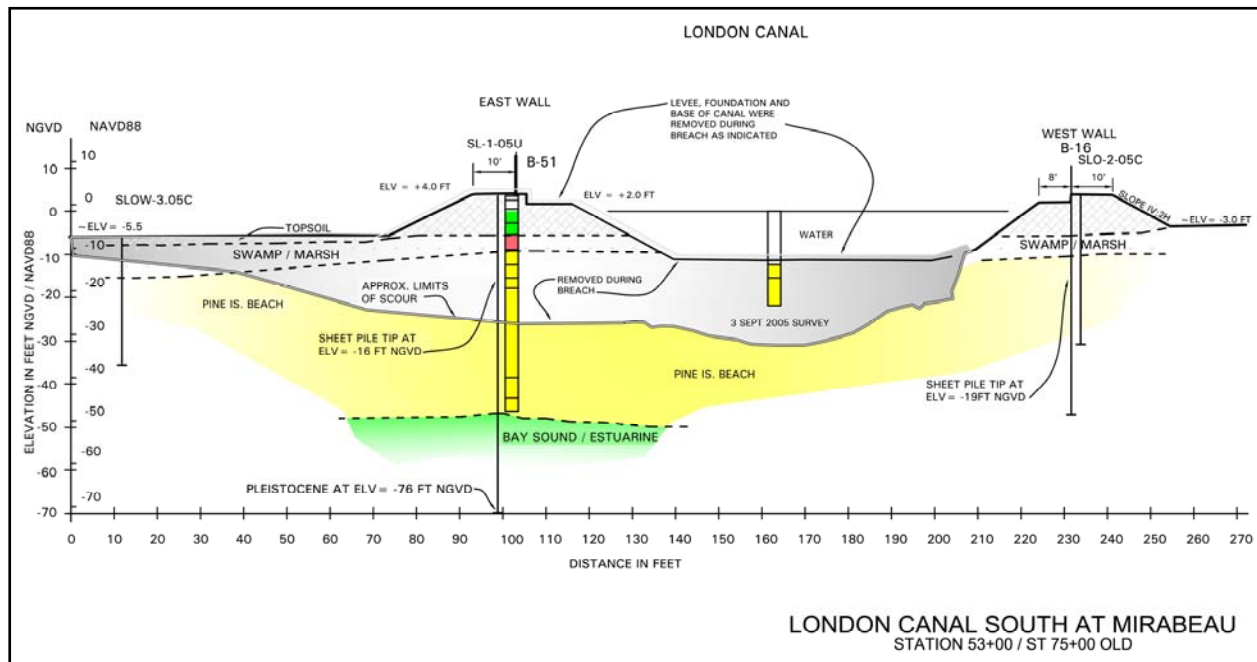


Figure 39. London Avenue Canal south breach cross section.

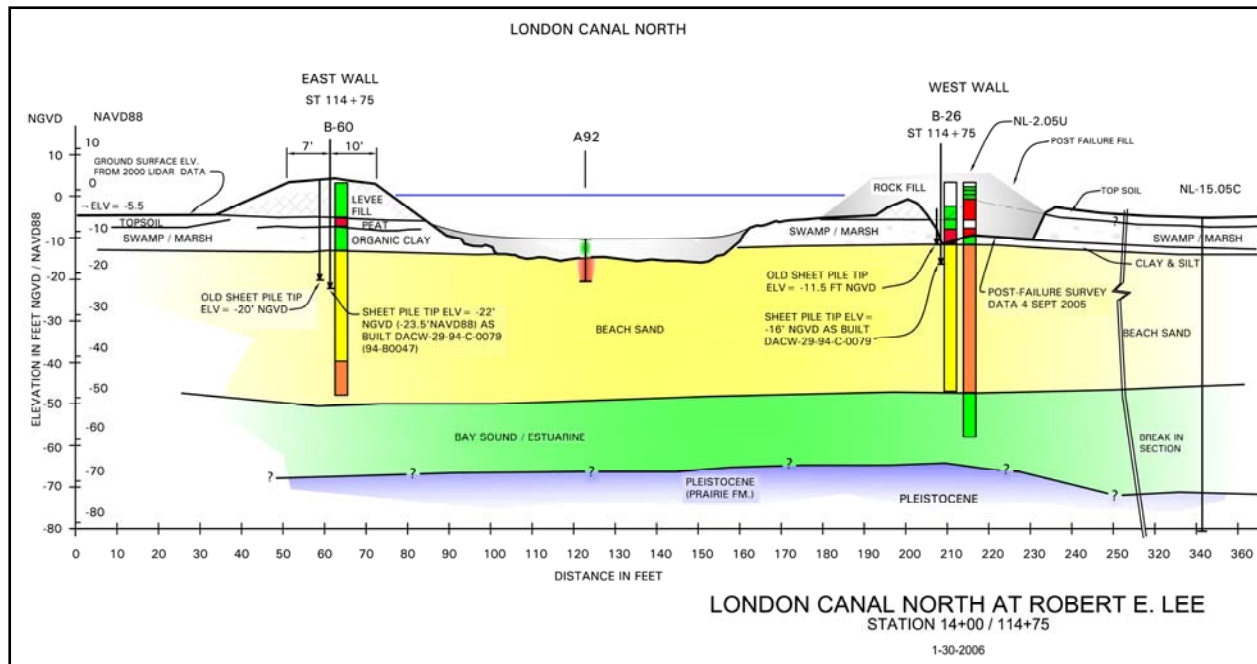


Figure 40. London Avenue Canal north breach cross section.

In conditions such as those at London Avenue, with the I-walls penetrating down to the cohesionless sand layer in the foundation, a crack or gap extending to the tip of the sheet pile is not possible because the sand is incapable of sustaining a crack. These cases were analyzed using what was termed a “half-cracked” condition, with the crack extending only to the top of the sand. Below the top of the sand, the sheet pile is loaded by water pressures that are lower than hydrostatic and active earth pressures.

The analyses described in Appendix 8, “Analysis of London Avenue Canal I-Wall Breaches,” indicate a strong likelihood that high uplift pressure on the base of the levee and the marsh layer was a key factor in the failures at both the south and the north breaches. At both locations, these high uplift pressures probably resulted in the development of a rupture through the marsh layer, and hydraulic gradients large enough to cause erosion of the sand upward through the rupture.

At the south breach area, this erosion may have been the principal mode of failure, with gross instability occurring after considerable volumes of sand, marsh, and levee fill had been removed by erosion and piping. Without alteration of the south breach cross section by erosion and piping, the calculated factors of safety with respect to instability are greater than 1.0, indicating that alteration of the profile by erosion and piping probably played a principal role in the failure at this location where the sand was dense, and the sand friction angle would have been high. The conclusion that the failure probably started in a small zone of intense seepage is consistent with the narrow breach that eventually developed.



At the north breach area, the probability of erosion and piping is slightly less than at the south breach, although still very high. The probability of instability at the north breach is higher than at the south breach, due to the fact that the sand at the north breach was loose and would have had a low friction angle. High uplift pressures likely resulted in a rupture through the marsh layer and the underlying thin layer of lacustrine clay. At this location, however, the high pore pressures within the sand would have been sufficient to cause instability without significant alteration of the cross section by erosion. The failure at the north affected a much wider zone than the failure at the south, indicating that intense localized erosion and piping probably did not play a key role in the failure at the north breach. It appears that high uplift pressures and lower friction angle of the less dense sand were key elements in the failure at the north breach.

### **Centrifuge Modeling Results for the London Avenue Canal Breaches**

In the London Avenue Canal model tests, where the toe of the sheet pile wall penetrated into the sand and was restrained from lateral movement by the sand, the opening of the gap on the canal side of the floodwall was followed by rotation of the top of the wall landward. With the opening of the gap, the model tests for the London south breach and the London north breach both showed gross movements indicative of wall failure, as may be seen in Figure 41. Rotation of the wall was accompanied by a translational sliding of the landward part of the levee and marsh layer, on top of the underlying sand. Rotation of the wall is linked to reduction in effective stress on the sand layer beneath the landward side of the levee. Once the gap was fully opened, pore pressure transducers in the foundation sand layer showed that the pore pressure in the sand rose very significantly. The increasing water pressure in the sand layer reduced the effective stress at the base of the marsh layer. The reduction in vertical effective stress has two effects: the first is to increase the likelihood of uplift of the swampy marsh (as the increasing water pressure in the foundation balances or exceeds the weight of the levee and marsh layer above), and the second is to reduce the stiffness of the sand surrounding the toe of the sheet pile wall, reducing the passive resistance that the sand provides.



Figure 41. Superposition of video images of the rotational failure of the London south model wall, Model 1.

The high pore water pressures under the toe of the levee on the landward side and under the swampy marsh led to water being ejected from the ground at the toe of the levee. This may be deduced from the piezometric heads near the toe of the levee, and can be seen clearly in the video images of the landward toe. Figure 42 shows a view of the levee and floodwall as seen from the backyard of houses behind the levee, showing black water emerging from the toe of the levee as the floodwall rotates landward. This supports the earlier assessment based on seepage analyses that a rupture through the marsh layer overlying the sand at the south breach led to a failure initiated by erosion and piping.

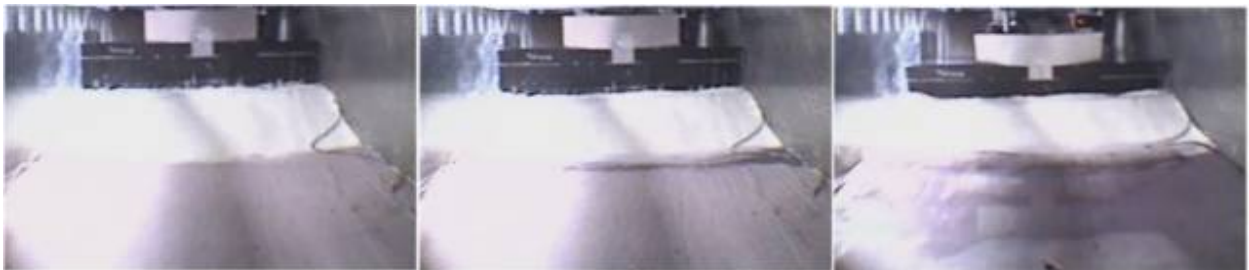


Figure 42. Water emerging from toe of levee as failure progresses, London south Model 2.

A more complete description of the centrifuge modeling effort is contained in Appendix 5, "IPET Centrifuge Model Test Report."

### Finite Element Soil-Structure Interaction Results for London Avenue Canal Breaches

Finite element soil-structure interaction analyses were conducted to provide a third approach to the development of a complete understanding of the London Avenue Canal breach mechanisms. A two-dimensional cross section through the north breach is shown in Figures 43 and 44. The older sheet-pile wall shown in the figures, which was left in place when the newer one was constructed, does not influence the results of the analysis in any significant way. A detailed description of the nonlinear finite element soil-structure interaction analyses is contained in Appendix 9, "Soil-Structure Interaction Analysis of the Floodwalls at London Canal."

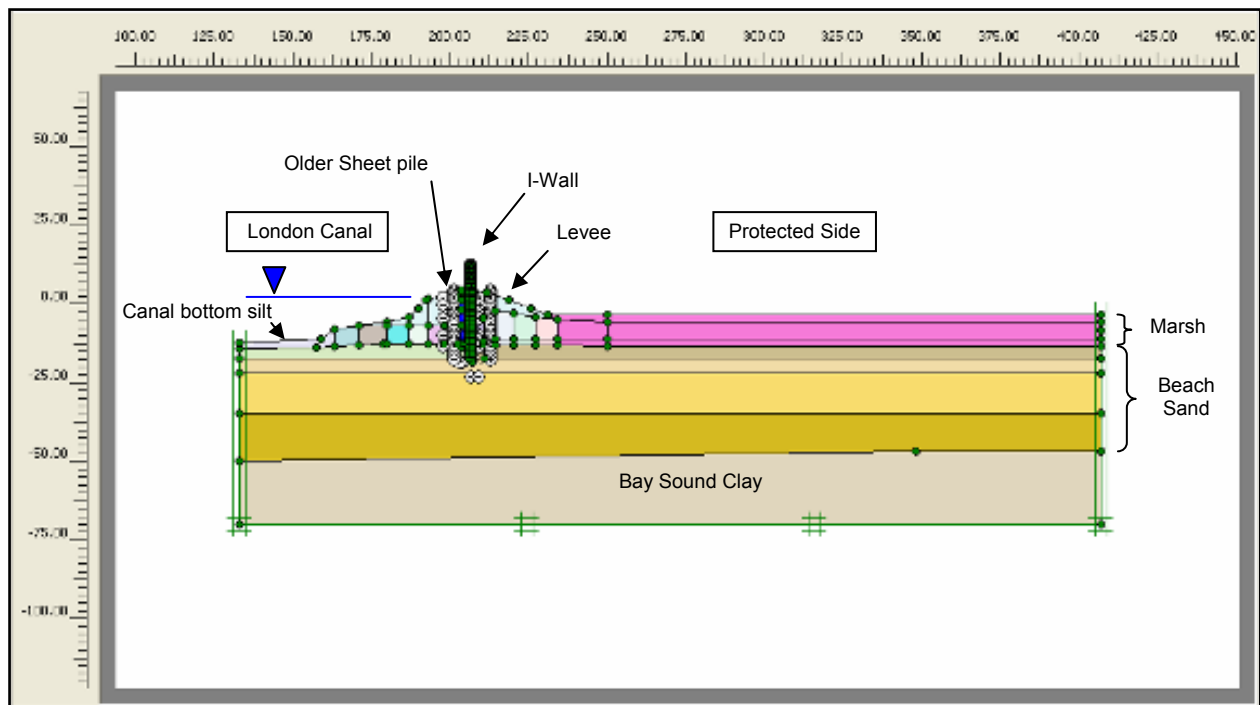


Figure 43. Two-dimensional cross-section model used in the SSI analysis of the London Avenue Canal north breach.

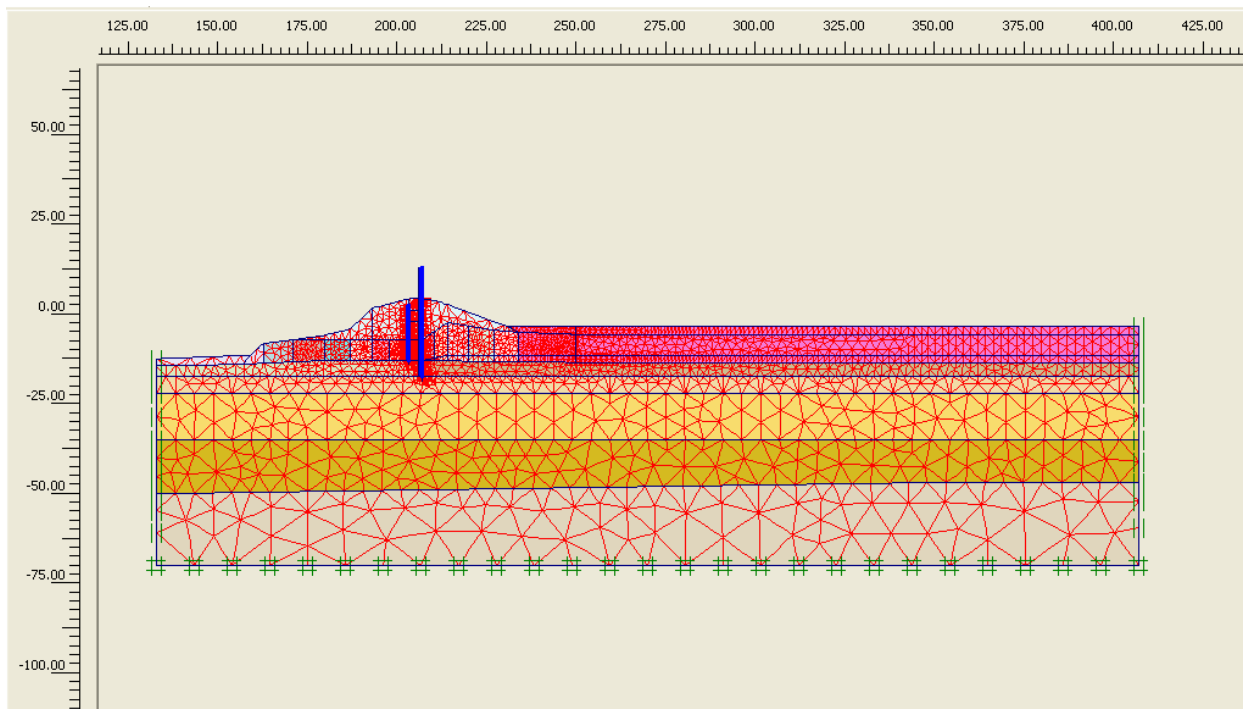


Figure 44. Finite element mesh used in the SSI analysis of the London Avenue Canal north breach.

Like the limit equilibrium stability analysis and centrifuge tests, the finite element analyses showed that the formation of a gap down to the sand layer leads quickly to failure because the sand layer below the marsh layer is fully saturated, see seepage analyses in Appendix 17. Some of the details regarding formation of the gap were found to be dependent on the stiffness assigned to the levee fill and the marsh layer. The lower and upper limits of the possible stiffness values for the levee fill and the marsh layer were used to investigate the effect of stiffness on the formation of the gap. Figure 45 shows how the gap increased in depth as the canal water elevation increased. The gap began to form once the canal water elevation reached the crest of the levee, and progressed down the wall as the canal water elevation continued to rise. The rate of progression of the gap down the wall was found to depend on the soil stiffness, with the stiffer soil allowing the canal water elevation to reach a higher level before the gap extends to the top of the sand layer.

Once the gap extended full depth, the water pressure in the sand rose rapidly, and the elevated water pressure in the sand layer reduced the vertical effective stress at the base of the marsh layer (Figure 46). The reduction in vertical effective stress has two effects: the first is to increase the uplift pressure on the bottom of the marsh layer, as shown in Figure 46; and the second is to reduce the stiffness of the sand surrounding the tip of the sheet-pile wall, reducing the passive resistance provided by the sand.

The finite element soil-structure interaction analyses are consistent with the behavior observed in the centrifuge tests, where the opening of the gap on the canal side of the floodwall was followed by rotation of the wall landward, as shown in Figure 47. Figure 48 shows the horizontal displacement of the top and tip of the wall as the canal water rises. It shows that the

tip did not translate horizontally; instead, the wall rotated about the tip. Figure 48 also shows the significant increase in rotation of the wall once the gap reached the sand layer.

The factor of safety decreased substantially when the gap opened fully, as may be seen in Figures 48 and 49. When the crack (or gap) opened, the factor of safety decreased with no change in water level, as shown by the horizontal line segments in Figures 48 and 49. For the low-stiffness soil, the gap opened fully at a canal water elevation of 6.0 ft, and the factor of safety decreased from 2.5 to 1.8. For the stiff soil, the gap opened fully at a canal water elevation of 8.0 ft, and the factor of safety decreased immediately from 2.1 to below 1.0. If the canal bottom was covered with silt, and the sand layer was therefore not connected to the canal, the opening of the gap would be the means for connecting the sand layer to the canal.

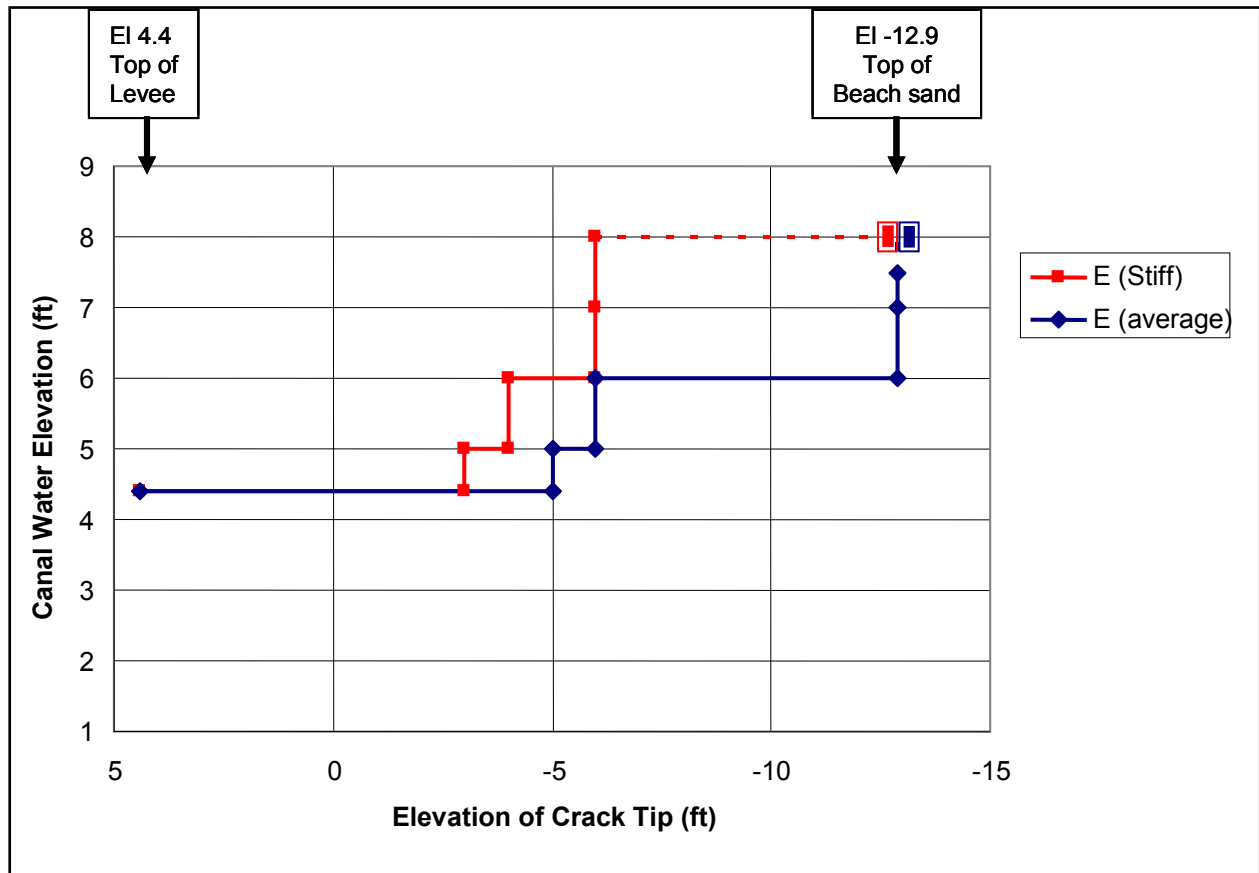


Figure 45. Elevation of gap tip versus canal water elevation.

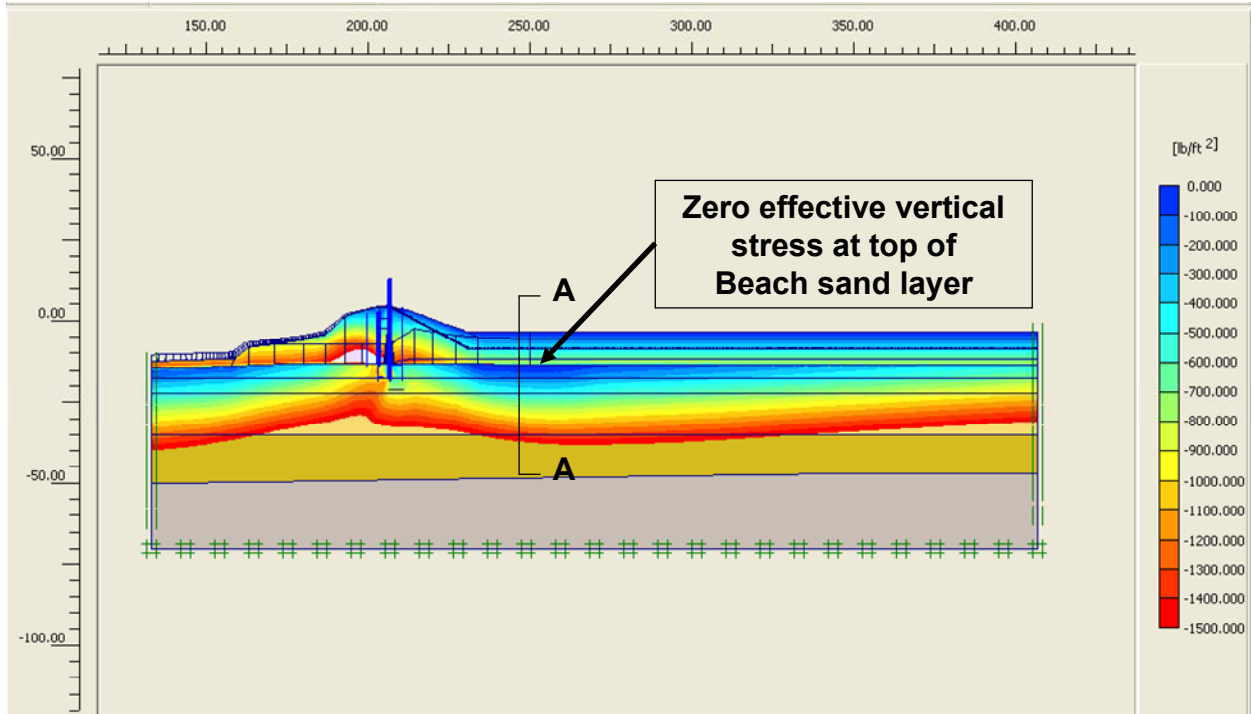


Figure 46. Effective vertical stress in the beach sand for the analysis using average stiffness values with canal elevation 6.0 ft and gap to elevation -12.9 for the London Avenue north breach.

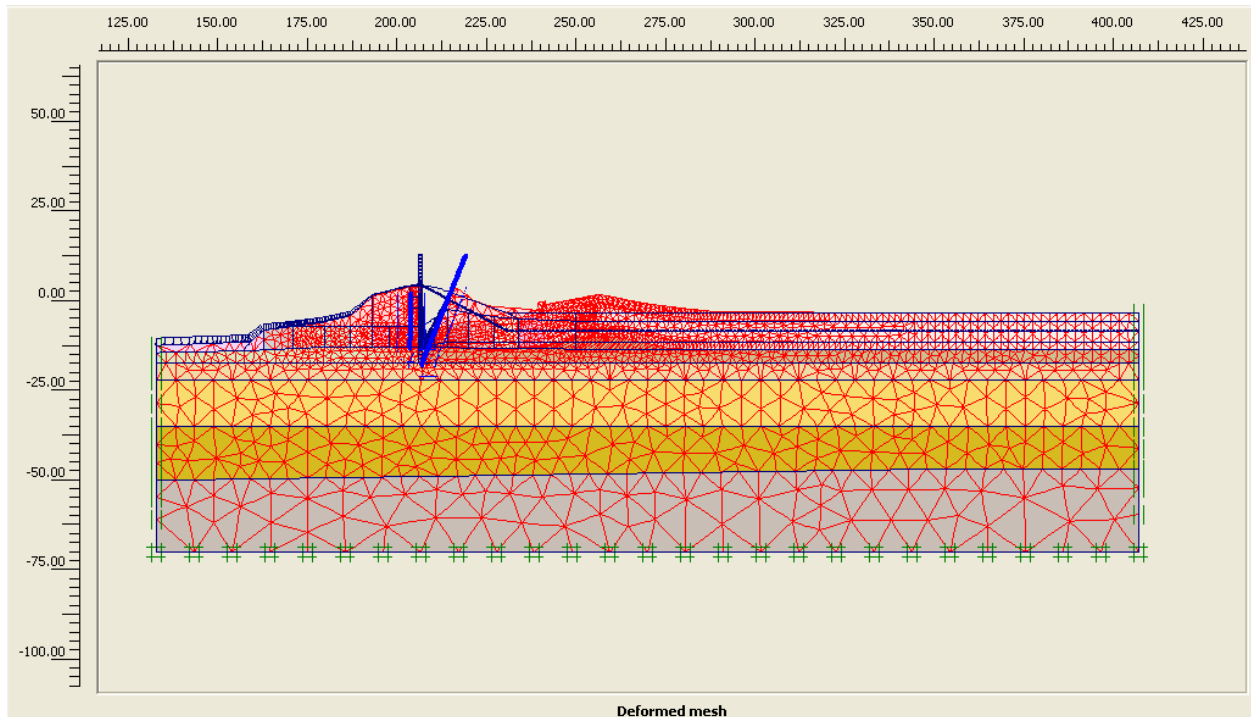


Figure 47. Ultimate mechanism from strength reduction analysis using average stiffness values with canal elevation 6.0 ft and gap to elevation -12.9 ft, London Avenue north breach (displacements are exaggerated).

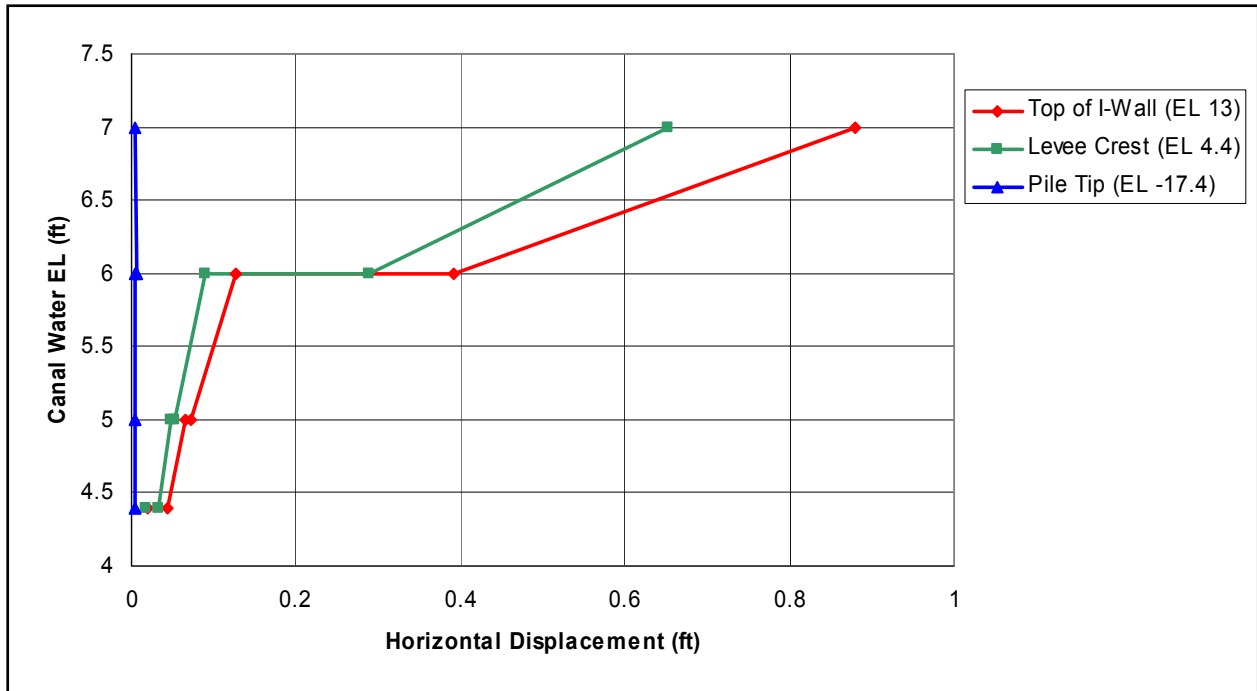


Figure 48. Horizontal sheet pile deformations versus canal water elevation computed using average stiffness values for the London Avenue Canal north breach.

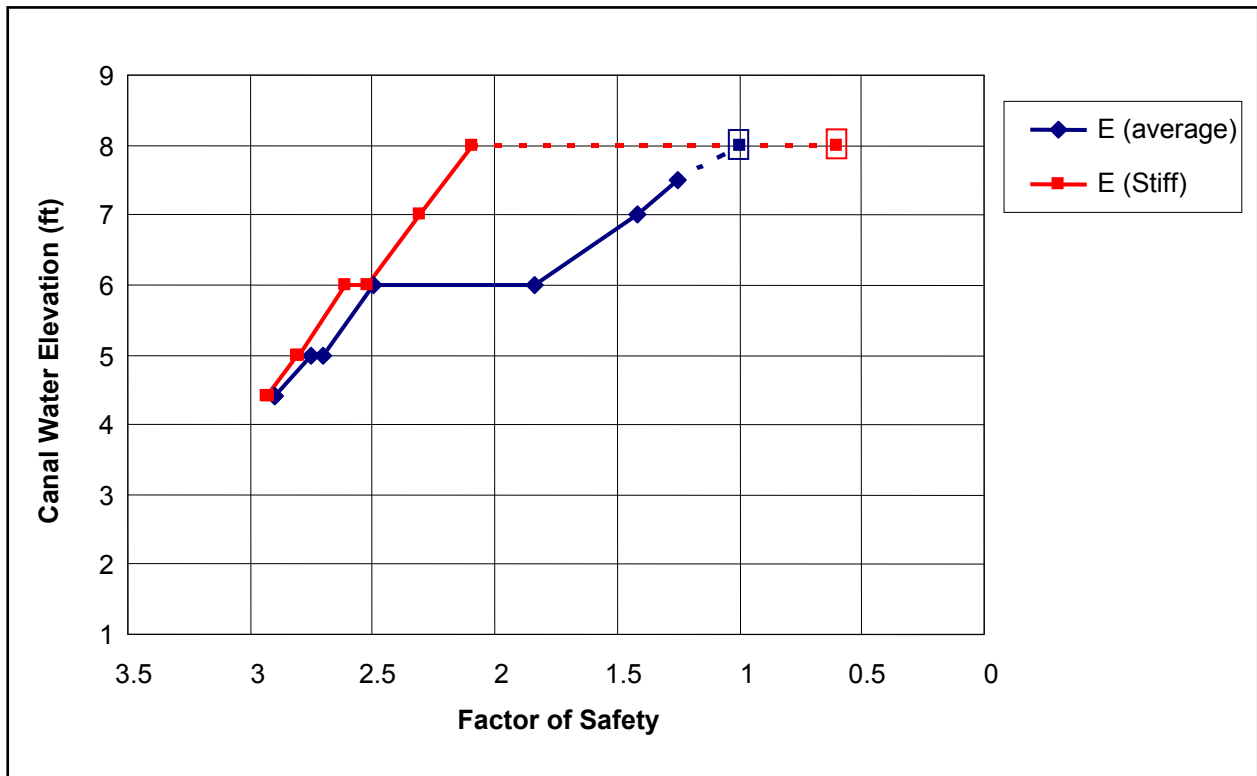


Figure 49. Factor of safety versus canal water elevation calculated using the strength reduction method for the London Avenue Canal north breach.

## **Summary of Assessment of the London Avenue Canal Breaches**

The breach on the London Avenue Canal near Mirabeau Avenue (the south breach) occurred at 7:00 a.m. to 8:00 a.m. on Monday, 29 August 2005. The breach on the London Avenue Canal near Robert E. Lee Boulevard (the north breach) occurred by 7:30 a.m. Field evidence, analyses, and physical model tests show that the breaches were due to the effects of high water pressures within the sand layer beneath the levee and I-wall, and high water loads on the walls. The London Avenue Canal breaches had a key factor in common with the 17th Street Canal breach – formation of a gap between the wall and the levee fill on the canal side of the wall. At both the 17th Street Canal and the London Avenue Canal, formation of a gap allowed high water pressures to act on the wall below the surface of the levee, severely loading the wall. At the London Avenue Canal, an additional effect of the gap was that water flowed down through the gap into the underlying sand. High water pressures in the sand uplifted the marsh layer on the landside of the levee, resulting in concentrated flow and erosion, removing material and reducing support for the floodwall.

Analyses of the south breach showed that erosion is most likely the principal mode of failure, with sliding instability occurring after significant volumes of sand and marsh had been removed by erosion and piping. Without alteration of the south breach cross section by erosion and piping on the landside of the levee, the calculated factors of safety with respect to sliding instability are greater than 1.0, indicating that alteration of the cross section by erosion and piping probably played a principal role in the failure at this location.

Field observations at the north breach indicate that the canal-side levee crest remained intact after the breach, and a playhouse on the property adjacent to the breach was heaved upward as the ground beneath it heaved upward during the failure. The analyses described in this report show that conditions for erosion and piping were present at the north breach, but the more likely cause of the failure was sliding instability. High uplift pressures likely resulted in a rupture through the marsh layer and the underlying thin layer of clay. At this location, however, the high pore pressures within the sand would reduce passive resistance sufficiently to result in sliding instability without significant alteration of the cross section.

It seems reasonable to assume that the wall on the opposite side of the canal from the north breach, which moved and tilted, must have been close to failure, but this location has not been analyzed in detail.

## **Assessment of Inner Harbor Navigation Canal Breaches**

Four breaches occurred on the IHNC during Hurricane Katrina on the morning of 29 August. Two of the breaches occurred on the east bank between the Florida Avenue Bridge and the North Claiborne Avenue Bridge adjacent to the 9th Ward, and two on the west bank, just north of the intersection of France Road and Florida Avenue. The locations of these breaches are shown in Figure 50. Three of the breaches involved failures of floodwalls on levees, and one involved failure of a levee due to overtopping erosion.



All of the IHNC floodwalls and levees were overtopped on 29 August. The peak storm surge elevation in the IHNC was 14.2 ft at 9:00 a.m., as can be seen in Figure 51. This peak water level is about 1.7 ft above the tops of the floodwalls and levees. The reaches where the floodwalls and levees did not collapse have, therefore, survived water loading considerably higher than the design loading.

Initial observations after the hurricane revealed that overtopping had eroded at least one section of levee (without floodwall) along the west bank and had eroded the soil adjacent to the wall at three other locations along the east and west bank (Figure 50). It appeared that water flowing over the floodwall scoured and eroded the levee on the protected side of the I-wall, exposing the supporting sheet piles and reducing the passive resistance, as can be seen in Figure 52. The erosion appeared to be so severe at the breach locations that the sheet piles may have lost all foundation support, resulting in failures of the type shown in Figure 53. Perhaps the best evidence of this scour can be seen along the unbreached reaches of the east bank I-walls, where U-shaped scour trenches were found adjacent to the I-walls. As the scour increased, the I-wall may have moved laterally and leaned toward the protected side, causing the scour trench to grow as the water cascaded farther down the slope until sufficient soil resistance was lost and complete failure occurred.

Although it is clear that the walls were overtopped, and that their stability was compromised by the erosion that occurred, it is also clear that one of the east side breaches occurred before the wall was overtopped. Eyewitness reports indicate that the water level in the 9th Ward near Florida Avenue was rising as early as 5:00 a.m., when the water level in the IHNC was still below the top of the floodwall, as shown by the hydrograph in Figure 54. Stability analyses indicate that foundation instability would occur before overtopping at the north breach on the east side of the IHNC. This breach location is, thus, the likely source of the early flooding in the Lower 9th Ward. Stability analyses indicate that the other three breach locations would not have failed before they were overtopped.

The soil immediately beneath the levees and floodwalls at all four breach locations included marsh, beneath which was clay, and beneath the clay, sand. Through most of their lengths, the critical circles passed through the marsh and clay. The critical circles did not extend to the sand layer beneath the clay.

Formation of a gap on the canal side of the wall, allowing hydrostatic water pressure acting through the full depth of the gap, causes a very significant reduction in the value of the calculated factor of safety. Evidence that a gap did form behind the wall near the breaches can be seen in Figures 55 and 56.

Stability analyses of the north breach on the east side resulted in a computed factor of safety equal to 1.0, with a gap on the canal side of the wall and water in the IHNC at elevation 11.2 ft. This is about 1.0 ft higher than the average IHNC water level at the time floodwater was observed in the Lower 9th Ward. Considering that the effective water level could have been 1.0 ft higher due to wave effects, this result is consistent with the observed IHNC water level when floodwater was first reported in the Lower 9th Ward. Thus, it appears that the north breach

occurred before overtopping, and that this breach was the source of the first influx of water into the 9th Ward.

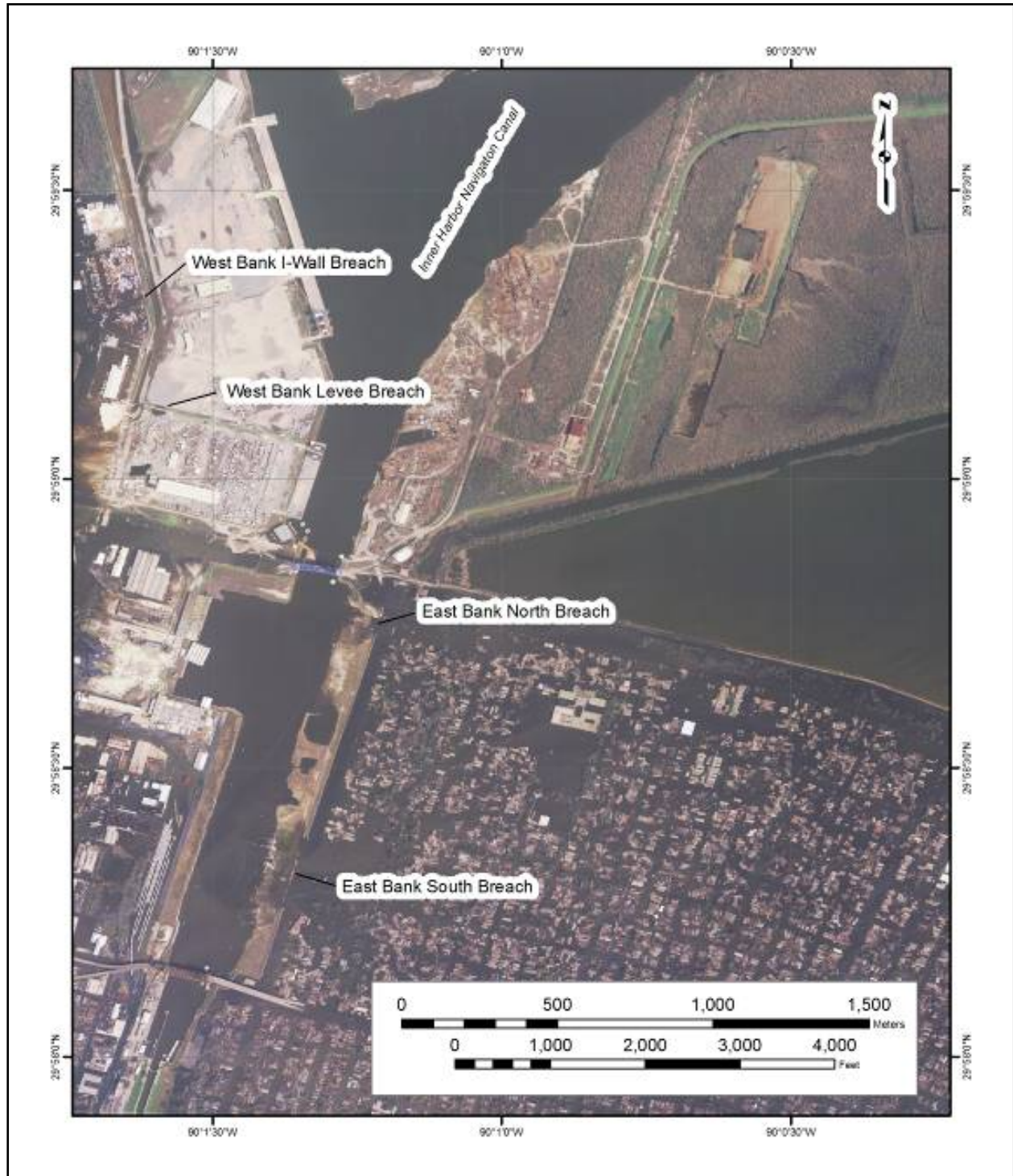


Figure 50. Four breach locations on the Inner Harbor Navigation Canal.

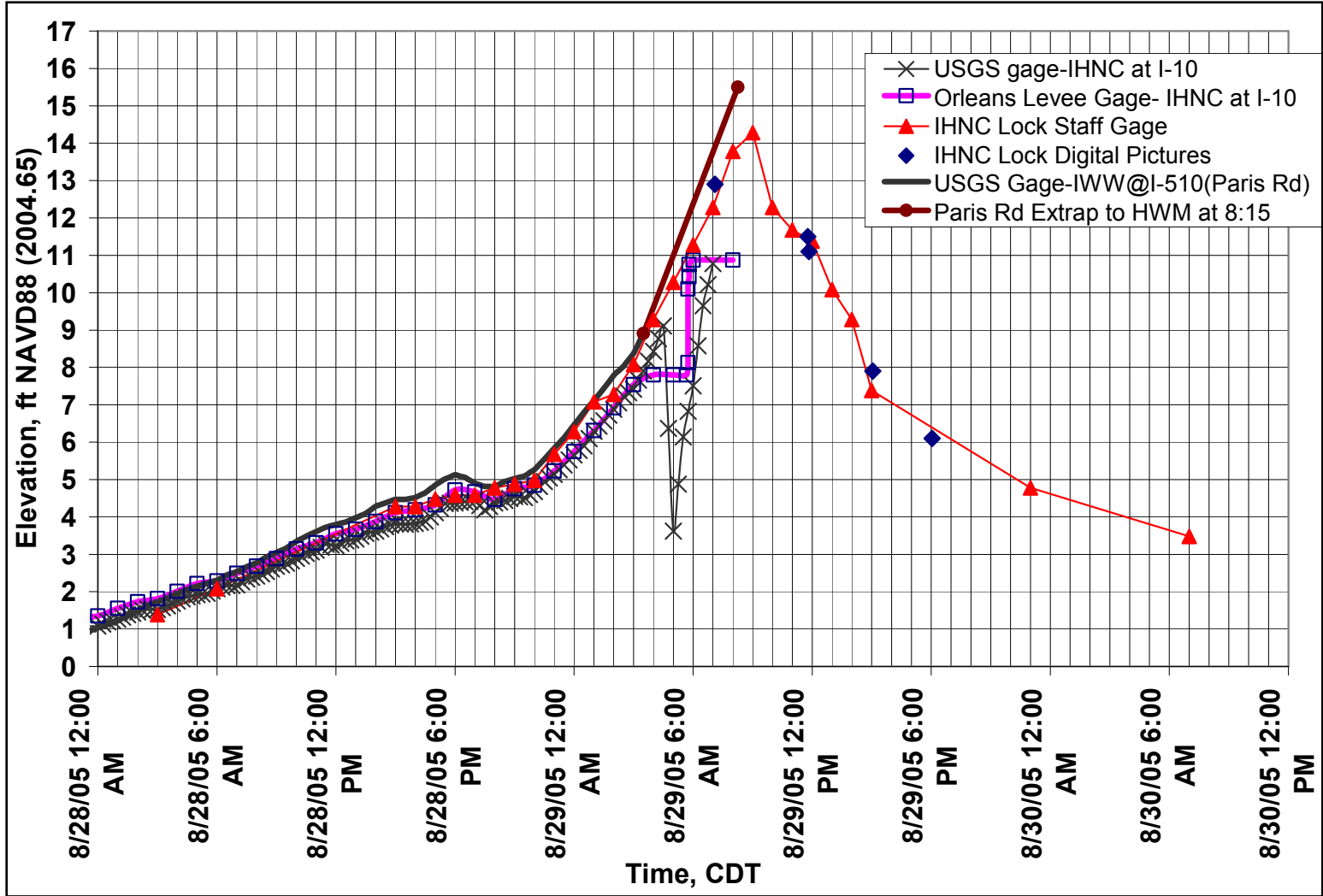


Figure 51. Hydrograph for IHNC.



Figure 52. Scour and Erosion on the Protected Side of the IHNC adjacent to the 9th Ward in the vicinity of the south breach.



Figure 53. Scour and erosion leading to the failure of the I-wall on the IHNC adjacent the south breach (9th Ward).

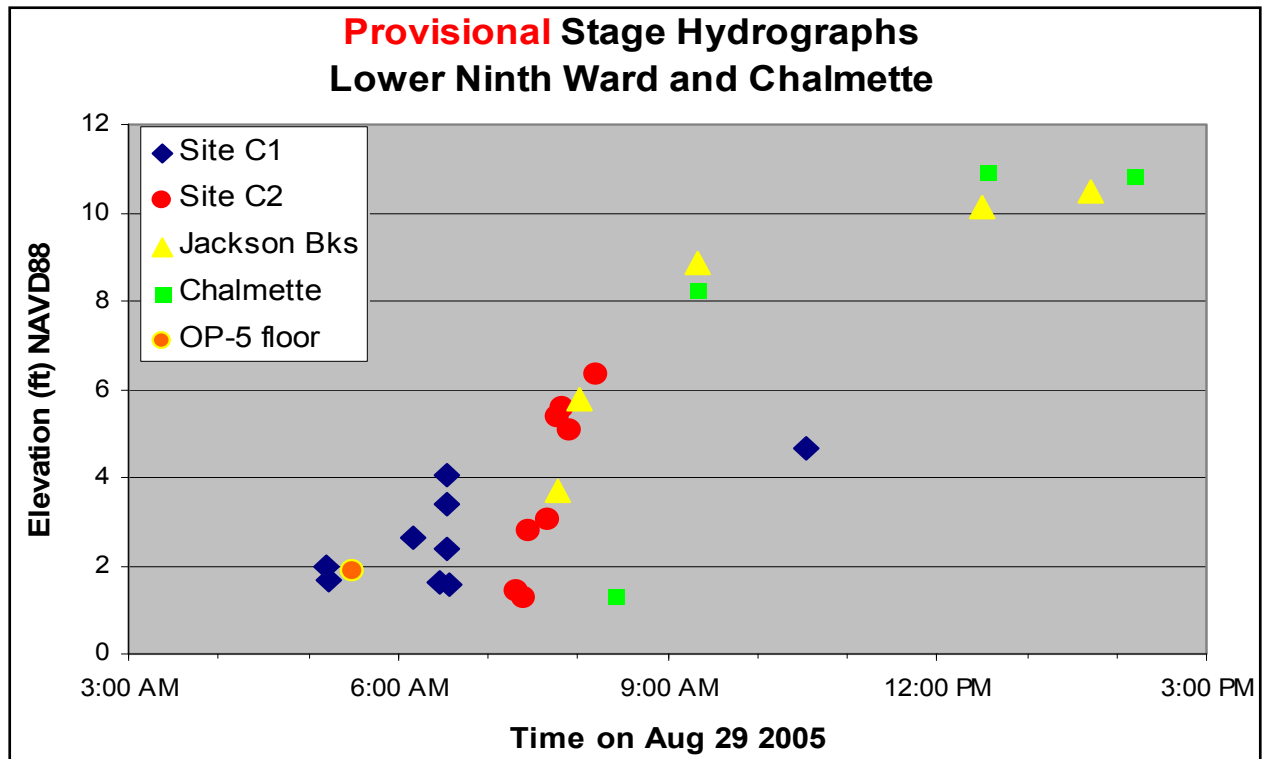


Figure 54. Hydrograph for the 9th Ward inundation.



Figure 55. IHNC East Bank – south breach – wall movement.



Figure 56. IHNC East Bank – north breach – wall movement.

Stability analyses of the south breach on the east side and the north breach on the west side resulted in computed factors of safety larger than 1.0 with the water level at the top of the wall and a gap behind the wall, indicating that the walls at those locations would have remained stable if none of the soil supporting the wall had been removed by erosion. Stability analysis of the south breach on the west side, where there was no I-wall, showed that the factor of safety there was also high, and the breach was due to overtopping erosion.

The lower computed factor of safety at the north breach on the east side is attributable to the fact that the ground elevation on the protected side is lower at that location and there was less soil on the protected side of the wall that was able to provide support for the wall.

The IPET strength model used for the north breach on the east bank, which is based on all of the data available in May 2006, agrees fairly closely with the design strengths reported in General Design Memorandum (GDM) No. 3 under the center of the levee. Both the GDM and the IPET strength model assign lower strengths beneath the embankment toe and beyond than beneath the crest of the embankment, but the GDM strengths at this location are higher than the IPET strengths. The GDM strengths are, thus, reasonably consistent with the currently available data.

The design analyses were performed using the Method of Planes, without a gap between the wall and the levee fill on the canal side of the wall. For the canal water level at 10.5 ft (the design water level), the factor of safety computed using the Method of Planes was 1.25. The minimum factor of safety calculated for the same conditions using Spencer's method was 1.45, indicating that the Method of Planes is conservative by about 14% in this case.

In summary, the foundation failure at the north breach on the east side of the IHNC was a result of differences between the actual conditions and assumptions used as the basis for the design. Those differences are (1) the ground surface beyond the toe of the levee at the north breach location was lower than the landside ground surface in the design cross section, and (2) the design analyses did not consider the possibility of a gap forming behind the wall, allowing water to run into the gap and increase the load on the wall. The other three breaches on the IHNC were due to overtopping and erosion.

## **Assessment of Orleans Canal and Michoud Canal I-Walls**

The I-walls at the Orleans Canal and Michoud Canal did not fail, even though they were severely loaded during Hurricane Katrina. The purpose of studying them was to be able to make detailed comparisons between their successful performance and that of the I-walls at 17th Street Canal, London Avenue Canal, and IHNC, which breached. It is important to determine if the analysis and physical modeling methods that indicated unstable conditions for the 17th Street Canal, London Avenue Canal, and IHNC I-walls, which did fail, would indicate stable conditions for the Orleans Canal and Michoud Canal I-walls, which did not fail. These assessments of stable I-walls provide insight into the performance of other I-walls in the HPS.

### **Analysis of the Performance of the Orleans Canal I-Walls**

At the Orleans Canal south area (Station 8+61), the marsh layer beneath the levee is underlain by sand, as shown in Figure 57. At the Orleans Canal north area (Station 64+27), the marsh layer beneath the levee is underlain by clay, as shown in Figure 58. The geologic conditions at these two locations on the Orleans Canal are, thus, directly comparable to the locations at the 17th Street Canal and the London Avenue Canal where breaches occurred.



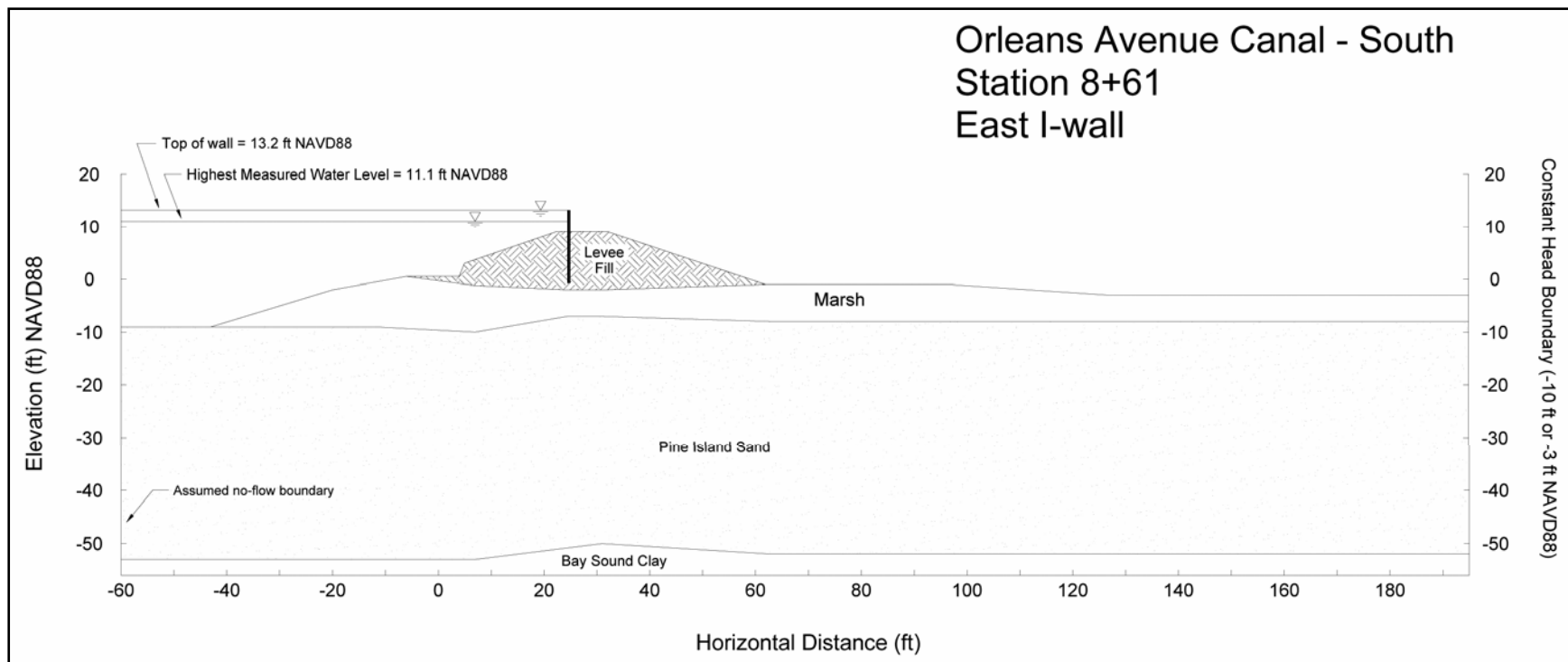


Figure 57. Schematic cross section at Orleans south, with seepage boundary conditions.

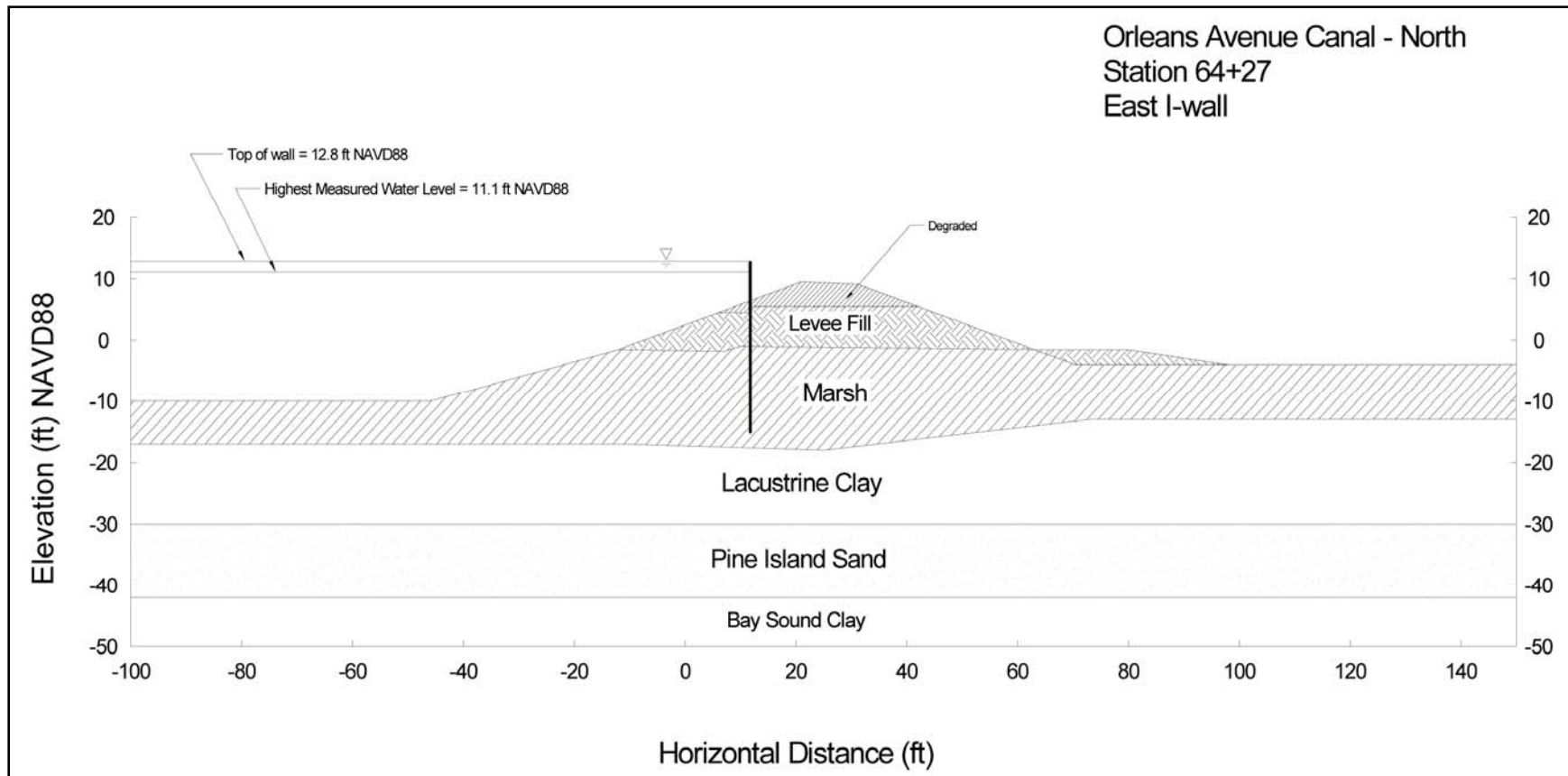


Figure 58. Schematic cross section of Orleans north.

For purposes of evaluating stability of the walls, it was assumed that a gap would form as it had at the other I-wall locations. There are two possible conditions regarding formation of a gap behind the wall. The first involves a gap extending to the bottom of the wall, as considered at the 17th Street Canal. The second involves continuation of this gap below the bottom of the wall, by hydraulic fracturing of the levee fill and marsh material below the wall. Hydraulic fracturing is possible in any location where (1) water pressures exceed the total stress on a potential fracture plane, as would be the case for a vertical plane extending below the bottom of the wall, and (2) the soil has sufficient strength for the gap to remain open, supported by the water pressure. For the conditions at Orleans south, the levee fill and marsh are strong enough to maintain a water-filled gap extending down to the marsh-sand interface. Water would fill this gap, loading the wall and the fracture plane below the wall, and introducing the canal head at the top of the sand.

Formation of a hydraulic fracture below the bottom of the wall would result in very severe loading on the wall for two reasons: (1) the gap would allow water to flow directly into the sand layer, increasing pore pressures and uplift pressures, and (2) the gap beneath the wall would extend the vertical face on which water pressures would act, thereby greatly increasing the water load acting on the plane of the wall. Although formation of a deeper gap by hydraulic fracturing has not been confirmed by field observation, it does appear to be feasible in soils as strong as the levee fill and marsh at Orleans south. Although occurrence of hydraulic fracturing is a scenario not often encountered, it is believed to be a condition that should be evaluated in this study of the performance of the Orleans south I-wall.

The same type of seepage analysis and interpretation of results that showed high hydraulic gradients, factors of safety less than 1.0, and probability of erosion greater than 99% at the London Avenue south breach showed moderate hydraulic gradients, factors of safety larger than 1.0, and probabilities of erosion of 3% and 28% for the highest water level experienced on the Orleans Canal, with an assumed gap extending below the tip of the wall to the top of the sand layer. The fact that no signs of erosion due to underseepage were observed in the Orleans south area after the flood neither confirms nor refutes these calculated probabilities. The analyses indicate a possibility of erosion, but this would not necessarily result in failure of the I-wall. Erosion, if it did occur beneath the marsh layer, might not result in visible manifestations at the ground surface, and might not move a sufficient quantity of sand to alter the cross section significantly.

The same type of stability analyses and interpretation of results that showed factors of safety less than 1.0, and probabilities of instability ranging from 70% to 97% at the London Avenue north breach, showed factors of safety ranging from 1.9 to 2.7 for the highest water level observed at the Orleans Canal, and probabilities of instability lower than one in one million.

The same type of stability analyses and interpretation of results that showed factors of safety ranging from 1.0 to 1.2 for a range of water levels, and probabilities of instability ranging from 12% to 60% for the 17th Street Canal breach, showed factors of safety ranging from 1.5 to 1.6 for the highest water level observed at the Orleans Canal, and probabilities of instability ranging from 1% to 3%.

These results show that the methods of stability analysis applied to conditions with clay beneath the levee and marsh layer are capable of modeling instability where it occurs, and stable conditions where they occur.

A more complete description of the stability analyses and results is contained in Appendix 10, “Analysis of the Performance of the Orleans Canal I-Walls.”

### Centrifuge Modeling Results for the Orleans Canal I-Wall

Similar to the cases for slope stability and seepage analyses, scale models of the Orleans Canal sections were tested in the geotechnical centrifuge to confirm that a failure would not occur for these sections. The cross section chosen to represent the southern portion of the Orleans Avenue levees is similar to the cross section at London Avenue, except that the levee is wider and higher, and the penetration of the floodwall is less (the toe of the wall is at the base of the levee/top of the swampy marsh layer).

As with the other levee sections, the instruments beneath the model levee responded to the rising water in the canal by increased water pressures in the sand, reducing nearly linearly from a maximum near the canal to a minimum to the landward side of the levee, as shown in Figure 59. As the water level rose in the Orleans Avenue Canal, the floodwall did not show any movement to indicate the opening of a gap. A cross section through the centrifuge model at the maximum water level reached during Hurricane Katrina is shown in Figure 60.

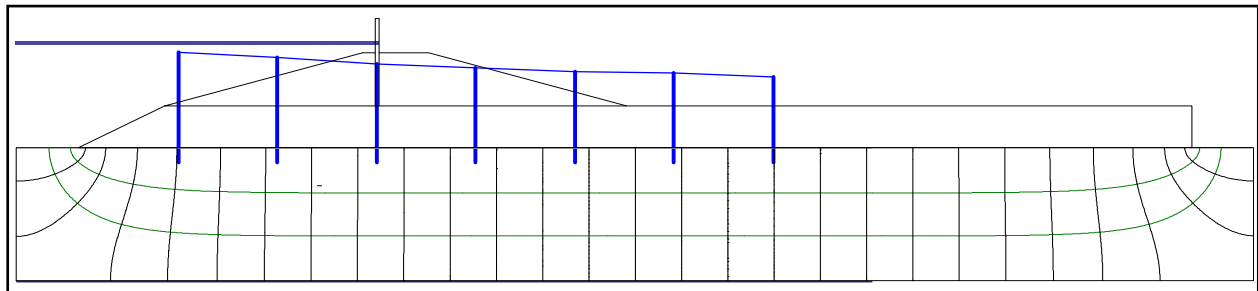


Figure 59. Seepage flow net for Orleans Avenue south with piezometric levels under the swampy marsh at Katrina flood level.



Figure 60. Orleans south model at Katrina flood level

The piezometric levels below the swampy marsh in the Orleans south model showed a declining level from the canal side to the protected side of the levee, as may be seen in Figure 61. The additional height and width of the Orleans south levee, seen superimposed in the figure for both Orleans south and London south, significantly increase its capacity to resist the flood levels, and no evidence was seen of a gap opening through the swampy marsh to provide a hydraulic connection to the sand below. The London Avenue Canal south breach piezometric levels and cross section, shown in Figure 55 for comparison, show a more critical condition in terms of uplift under the landward side of the levee. Both models, however, show high piezometric levels near the toe of the levee on the landward side, sufficient to lead to uplift of the marsh layer.

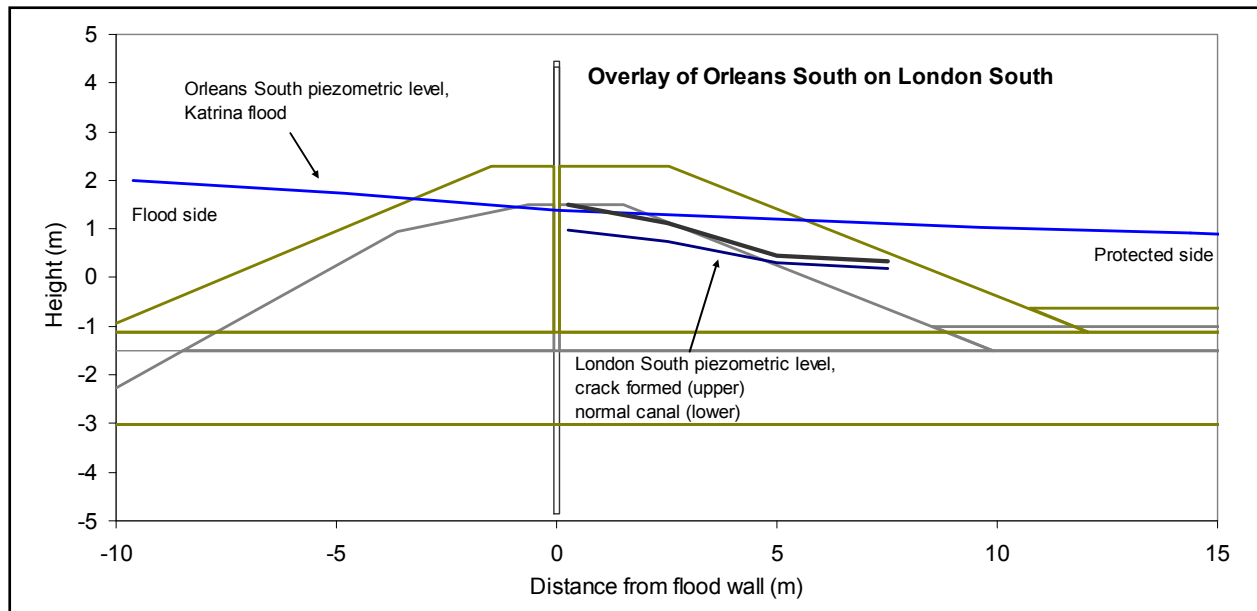


Figure 61. Comparison of piezometric levels in Orleans south (Katrina flood) and London south, with the base of the marsh layer assumed to be at a common elevation.

As the water level was raised above the Katrina flood level in the Orleans south model, a gap was seen to open at the toe of the floodwall, associated with small movements of the floodwall landward, as shown in Figure 62. Unlike the other models, this gap did not develop into a full failure condition; and no unstable movement of the floodwall was observed, despite the water level reaching the top of the floodwall. Translational movements were observed to be controlled by compression of the swampy marsh layer. Relative movement between the top of the sand and the swampy marsh was apparent, in a similar manner, to the uplift mechanism in the London Avenue models.

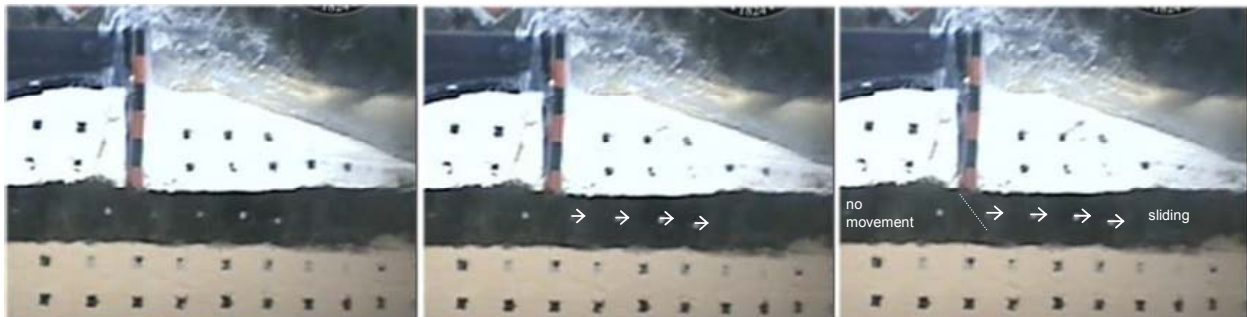


Figure 62. Small sliding movement of marsh as gap forms, Orleans south model

Comparison between the geometries of Orleans and London Avenue shows that the vertical effective stress in the sand foundation below the levee was considerably higher under the Orleans levee than under the London Avenue levees. Figure 63 shows the vertical effective stress on the underside of the marsh layer measured in the Orleans south and, for comparison, the London south models. The total stress for London south ranged from 1400 psf at the crest of the levee to 600 psf at the toe of the levee on the protected side, over a levee width of 25 ft. The total

stress for Orleans south ranged from 1700 psf at the crest of the levee to 650 psf at the toe of the levee on the protected side, over a width of 38 ft. The tendency of the floodwall to rotate is reduced by the height and weight of the landward section of the Orleans levee.

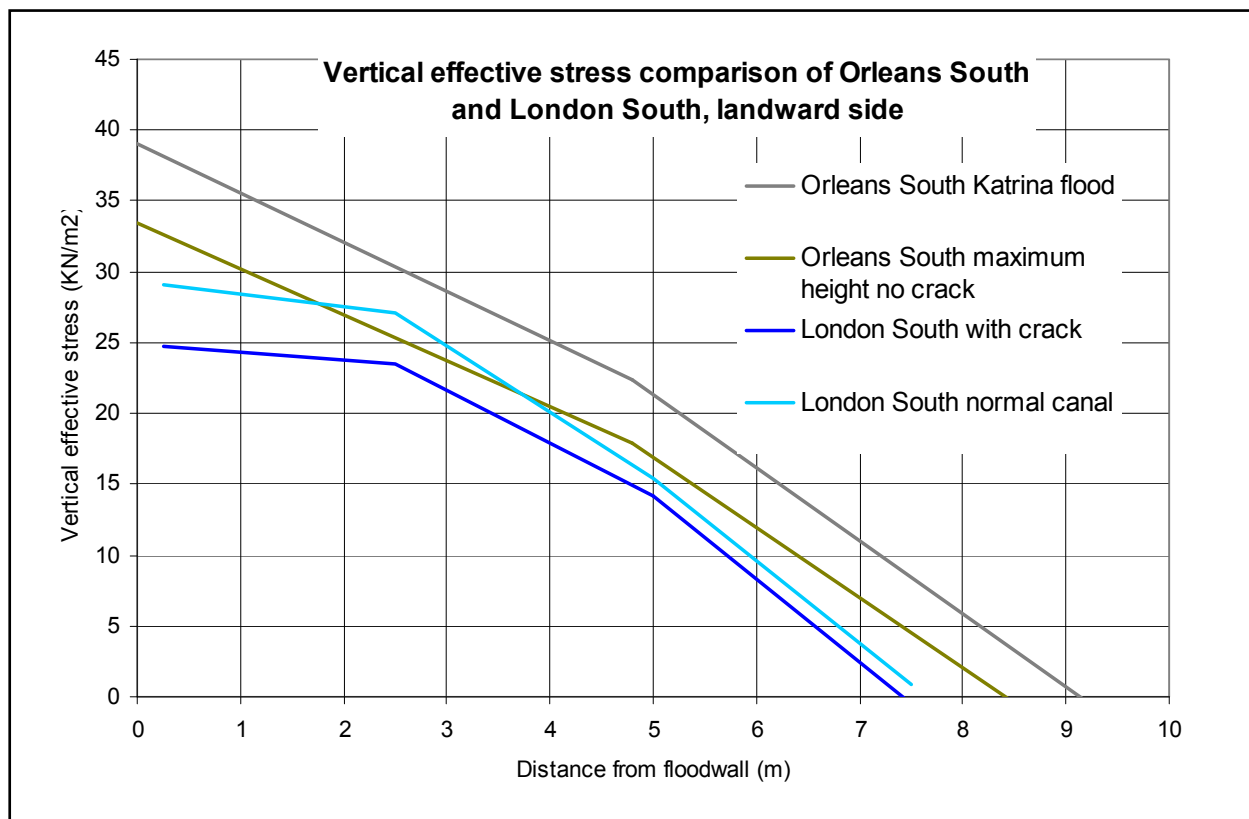


Figure 63. Vertical effective stress comparison between Orleans south and London south.

A more complete description of the centrifuge modeling effort is contained in Appendix 5, “IPET Centrifuge Model Test Report.”

### Analysis of the Performance of the Michoud Canal I-Walls

The purpose for this study of the Michoud Canal area is to compare the I-wall and embankment characteristics in this area, which did not fail, to other areas that experienced failure in order to better evaluate the Katrina-related failure mechanisms and analysis procedures. No levee or I-wall failures occurred in the Michoud Canal area during Hurricane Katrina.

The Michoud Canal area is protected by a series of I-walls constructed on top of a levee section. Construction of the Michoud Canal and the GIWW occurred in 1942. I-wall construction and capping occurred in the 1970s in response to Hurricane Betsy in 1965. The design water level was 3 ft below the top of the floodwall. The elevations of the top of the floodwall vary along the canal and are about 2 ft higher on the west side than on the east. Figure 64 is an aerial photograph showing the plan view of the Michoud Canal.

The post-Katrina reconnaissance revealed that overtopping by waves had eroded some soil adjacent to the wall on the protected side along some sections of the I-wall. Along a portion of the west I-wall is a series of sand drains that were installed to relieve the high pore pressures during high water events. Sections of the I-wall were overtopped by wave action, but this did not lead to breaching of the levee. Post-Katrina damage reports identify a section of I-wall along the west bank, approximately 200 ft south of the pump station, as leaning a few inches toward the canal side. It is uncertain whether this displacement occurred before or during Hurricane Katrina. A photograph showing this section of the I-wall is shown in Figure 65a. Figure 65b shows erosion that occurred on the protected side due to overtopping of the I-wall. Figure 65b shows some minor scour damage on the protected side of the levee on the west bank near the pump house area. It appeared that waves breaking over the top of the floodwall scoured and eroded the levee on the protected side of the I-wall, exposing the supporting sheet piles. This erosion was not severe enough to cause the sheet piles to lose their foundation support.

Other possible modes of failure considered were sliding instability and piping and erosion from underseepage. Piping and erosion from underseepage were unlikely problems because the I-walls were founded in a clay levee fill, a marsh layer made up of organics, clay, and silt, overlying a clay layer. Because of the thicknesses, the sufficiently low permeabilities of these materials, and the relatively short duration of the storm, the factors of safety for this failure mode were considered to be higher than for other conditions and were, therefore, not calculated. Global stability, determined by limit equilibrium analyses, was the primary focus of the investigation presented here.



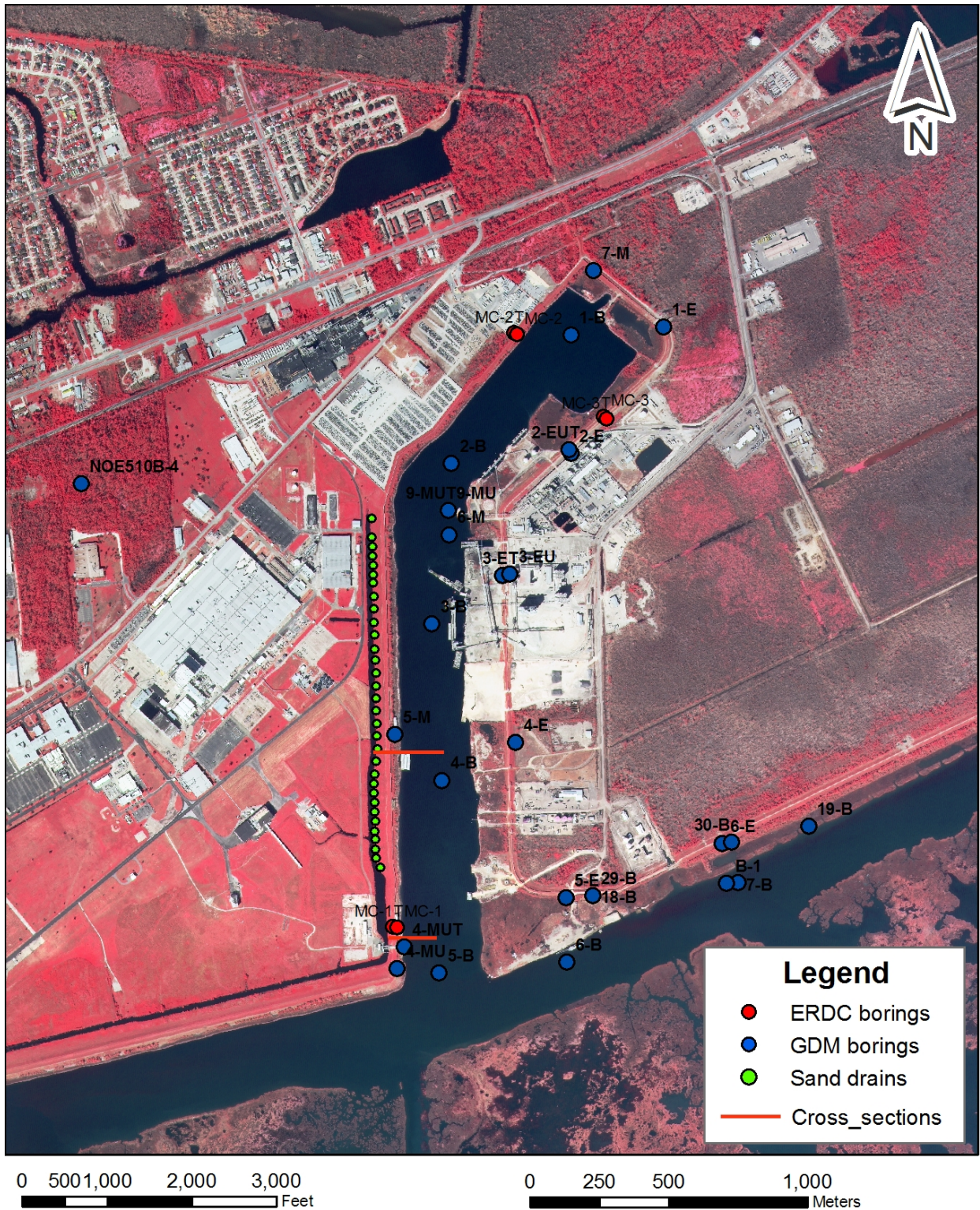


Figure 64. Aerial photograph of Michoud Canal.



Figure 65a. Post-Katrina photographs of Michoud Canal I-wall at pump station.



Figure 65b. Post-Katrina photographs of Michoud Canal I-wall showing erosion from overtopping waves.

The cross section developed for analysis, located on the west side of the Michoud Canal at Station 4+00, is shown in Figure 66. This cross section is approximately 100 ft north of the pump house, at the south end of the west wall. This section was selected for analysis because of the close proximity to existing exploratory borings. No sand drains were located at this section; therefore this section has the potential to be more unstable than I-wall sections to the north containing sand drains. The sand drains are located along the protected side of the levee near a drainage ditch to relieve pressures in the underlying foundation sands beginning at Station 11+00 and ending at Station 52+50.

The general stratigraphy at the site consists of six depositional units, listed in descending order as (a) levee fill, (b) marsh and swamp (termed marsh 1 and marsh 2), (c) interdistributary clay, (d) intradelta or relic beach sand, (e) nearshore gulf deposits, and (f) Pleistocene deposits. Specific engineering properties of these depositional units are described in greater detail in Appendix 23. The undrained strengths were used to characterize the levee fill, marsh 1, marsh 2, and interdistributary clay layers. However, the silty sand layer was treated as a drained material, and pore pressures in this layer were calculated using the finite element seepage analysis. None of the critical failure surfaces extended into the silty sand layer; therefore the undrained strengths of the cohesive soil layers above the silty sand layer controlled the stability of the section analyzed. The results of these analyses are presented in Table 3.

<b>Table 3 Results of Slope Stability Analyses for Michoud Canal Station 4+00.</b>						
<b>Case</b>	<b>Water Elevation (ft) NAVD88</b>	<b>Strength Model</b>	<b>Gap</b>	<b>Factor of Safety UTEXAS4 Non-Circular</b>	<b>Factor of Safety UTEXAS4 Circular</b>	<b>Factor of Safety SLIDE Circular</b>
1	15.5	IPET	No	1.243	1.357	1.368
2	15.5	IPET	Yes	1.023	1.100	1.099
3	19.7	IPET	No	1.098	1.179	1.182
4	19.7	IPET	Yes	0.835	0.919	0.924

The results of the analyses are consistent with the performance of the I-wall along the canal, indicating that the IPET strength model and method of stability analysis provide a suitable basis for evaluating the performance of the Michoud Canal I-wall during Hurricane Katrina. The Michoud Canal stability analysis followed the same general procedures used in the analyses of the 17th Street Canal, the London Avenue Canal, the Orleans Avenue Canal, and the IHNC flood control structures reported here.

The calculated factors of safety for Station 4+00 were about 20% lower for the gap condition compared to the no gap condition. The undrained strength of the interdistributary clay is important in the stability analyses since the majority of the failure plane is located in this layer. The beach sand layer, modeled as a drained material, did not influence the analysis because failure surfaces did not extend down to this layer.

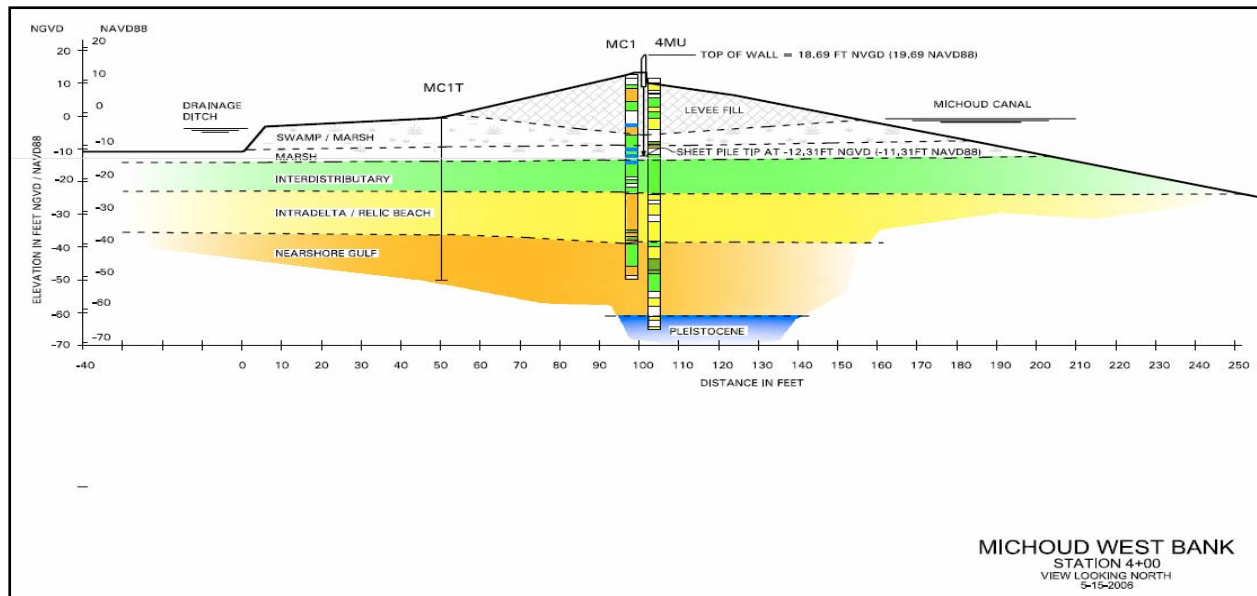


Figure 66. Geologic cross section of Sta. 4+00.

At Station 4+00, the top of the earthen levee was approximately 14.0 ft (NAVD 88). With the canal water level at the peak of the hydrograph (15.5 ft NAVD 88), only 1.5 ft of water acted on the cantilever I-wall. Since the factor of safety is greater than unity for the gap condition, it seems likely that the I-wall would have remained stable even if a gap had formed behind the wall. For the *no gap* case, the probability of failure was only 2%. For the case with a gap, the calculated probability of failure was much higher (40%).

If the static water level had reached the top of a wall and a gap did not form, the calculated factor of safety is still greater than unity, indicating that the wall would remain stable. However, had a gap formed under this high water level, the calculations indicate that the wall would have failed.

The true hydraulic loading of the I-wall at Station 4+00 may have been somewhere between Cases 2 and 4 (15.5 ft and 19.7 ft NAVD88). Evidence of scour on the protected side of the I-wall indicates that some overtopping due to wave action had occurred, but this loading by waves was apparently of too short a duration to be equivalent to the static water loading represented by Case 4 (19.7 ft NAVD88).

Similar to other cases analyzed as part of the IPET study, the use of non-circular failure surfaces resulted in factors of safety that were about 5% less than the values calculated using circular failure surfaces.

A significant effort was made to improve the stability of the pump station areas of the Michoud Canal after Katrina. The work was performed during the year 2006. These improvements include:

1. Installation of 19 relief wells between Stations 0+00 and 13+30 to relieve pore pressures in the sand layer.

2. An 80-ft-long sheet pile was installed from Station 0+05 to Station 13+00 to provide a deeper seepage barrier through the full thickness of the sand layer in this area.
3. The stickup height of the I-wall was reduced by rasing the top of the levee, and the levee slopes were flattened to improve stability. In addition, wave berms and riprap were added to improve erosion resistance.
4. The entire crest of the levee was paved to provide a greater level of protection against overtopping.

## **Levee Erosion and Scour from Overtopping**

Water overtopping the levees led to extensive scour and erosion in some locations, which ultimately resulted in breaches in the flood protection system. The performance of levees varied significantly throughout the New Orleans area. In some areas, the levees performed well in spite of the fact that they were overtopped. In other areas, the levees were severely eroded and completely washed away after being overtopped. Levee performance during Hurricane Katrina has highlighted the importance of the resistance of levees to overtopping, as an important factor determining the resilience of the flood protection system.

Lengthy reaches (miles) of earthen levees and capped levees were overtopped. Some reaches showed signs of initial erosion, others showed signs of progressive erosion, and other reaches contained significant breaching. Similar to levees, lengthy reaches of floodwall were overtopped and were left in various stages of damage, ranging from minor scour at the wall base to breaches where complete floodwall sections were flattened (Figure 67).

In the New Orleans East, Lakeshore, and St. Bernard Parish basins, approximately 50 miles of earthen levees overtopped but did not breach; approximately 20 miles of earthen levees overtopped and contained significant breaches; approximately 7 miles of floodwalls overtopped but did not breach; and approximately 2 miles of floodwalls overtopped and were breached. The majority of levees and floodwalls were damaged by overtopping, but did not breach.

In Plaquemines Parish, the combined length of the Mississippi River mainline levee and the back levee is about 162 miles. The length of I-walls and cantilever sheet-pile walls is about 7 miles. All of the levees in Plaquemines Parish sustained damage due to overtopping, and there was considerable crown and slope scour in all sections. The mainline levee riverside slope pavement sustained damage from numerous impacts from ships and barges. There were also several severe breaches, coinciding with pipeline crossings and with floodwalls. Five of the 7 miles of floodwall were damaged beyond repair. Major breaches occurred at sheet pile wing walls at two pump stations in the back levee. A major breach occurred at the Shell pipeline crossing near Nairn, and the West Pointe a la Hache pipeline crossing was severely damaged.

Several stages of erosion and scour progression were noted along numerous levee/floodwall reaches. Although conditions have been altered in many locations by construction of repairs, it is possible to infer useful information regarding soil erodibility from observations of performance during overtopping.

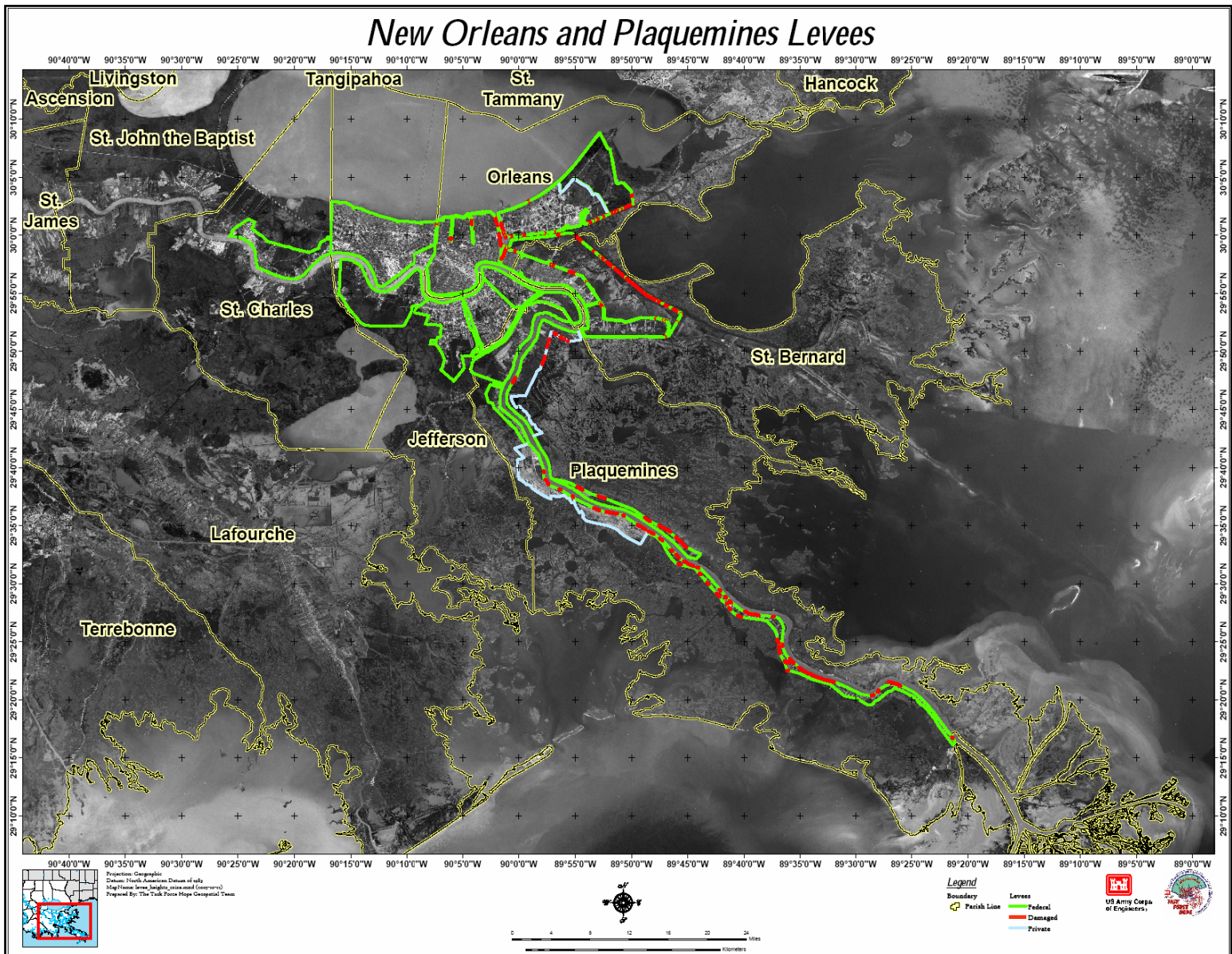


Figure 67. Locations (in red) of severe damage to hurricane protection structures resulting from Hurricane Katrina.

## Failure Patterns

The erosion of levees and floodwalls in the New Orleans area was predominantly due to overtopping. There are several locations along the levees adjacent to the MRGO facing Lake Borgne that show signs of some minor front side erosion from wave action, Figure 62. Figure 63 shows an aerial photograph of the area shown in Figure 62. Figure 64 shows the elevation of the levee before and after Katrina and the water levels due to the hurricane. The pre-Katrina levee elevations along this section where the front side erosion occurred are the highest along MRGO facing Lake Borgne and would have been the location with the longest period of time with the waves breaking on the front side of the levee. This may be the reason why there was erosion on the front side of the levee at this location.



Figure 68. Front side levee erosion along the Mississippi River Gulf Outlet.





Figure 69. Aerial photo of front side erosion on the MRGO.

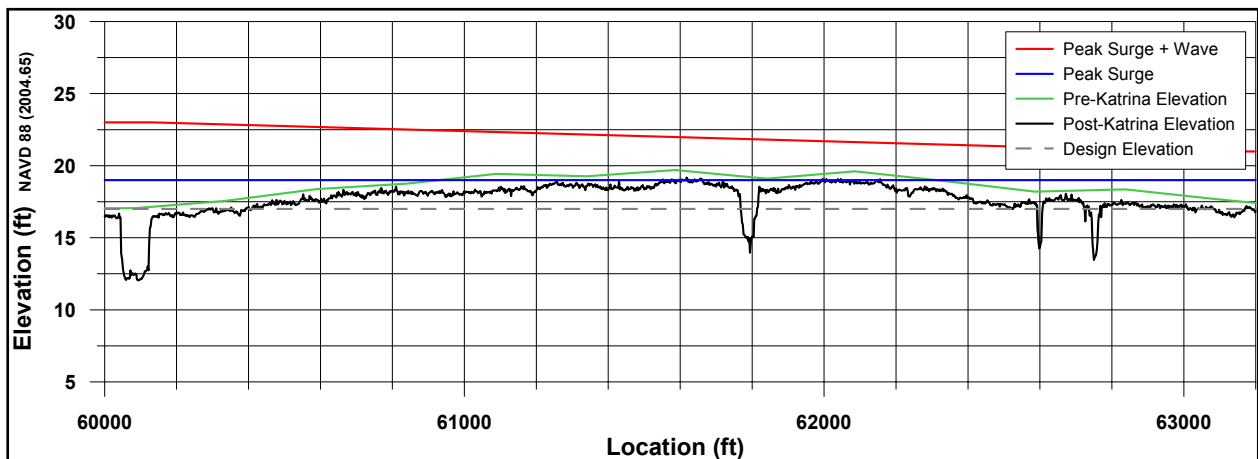


Figure 70. Pre- and post-elevation of the levee with water levels along the MRGO.

Protected side (backside or landside) erosion patterns were observed along the breached and unbreached levees and floodwalls in Orleans, St. Bernard, and Plaquemines Parishes. The following overtopping and breaching damage patterns were observed. Figure 71 shows a generalized cross section of a levee being overtopped by the storm surge. The water overtopping the levee increases in velocity as it flows down the protected side of the levee causing shear stresses to the levee surface. If the shear stresses are high enough, erosion will occur.

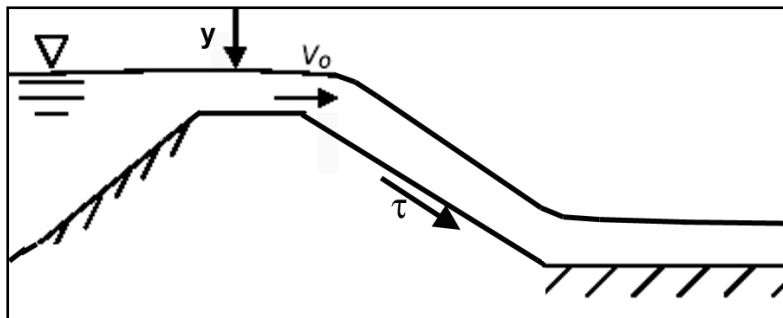


Figure 71. Conceptual diagram of water surge (without waves) overtopping an earthen levee.

As the earthen levee is overtopped, it will exhibit identifiable stages of progressive erosion on the protected side of the levee. The four stages of progressive erosion are illustrated in Figure 72.

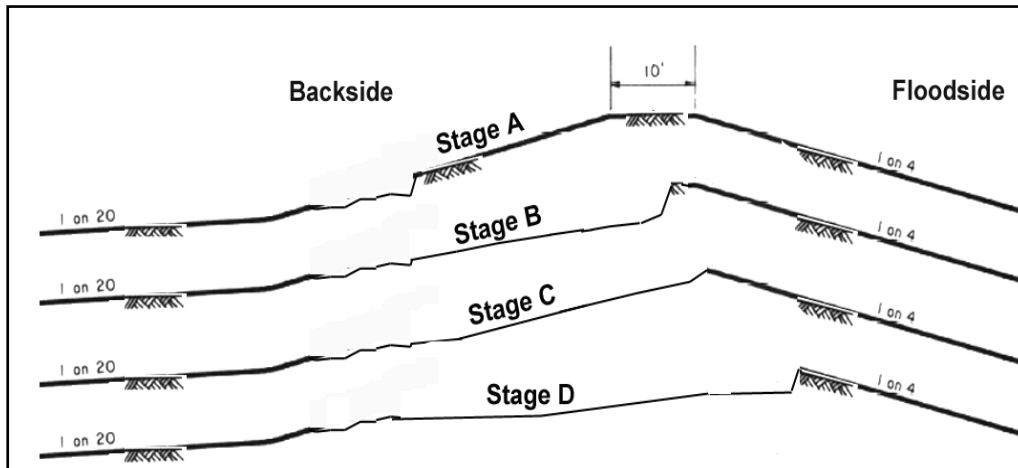


Figure 72. Erosion progression stages.

Figure 73 is a photograph that shows all four stages of progressive erosion:

**Stage A.** Initial overtopping causes surface sheet and rill erosion which develops into a series of cascading overfalls. The highest forces develop from the backside slope down to the backside toe, and the crown is not initially exposed to these large hydraulic forces. The cascading overfalls develop into one large headcut that migrates from the slope to the crest such that the erosion width approximately matches the overtopping width.

**Stage B.** The headcut continues to migrate from the backside crest (crown) to the floodside crest.

**Stage C.** The crest drops as a breach begins to develop.

**Stage D.** The breach opening erodes out to the toe and the breach widens.



Figure 73. Four stages of progressive erosion.

Figure 74 shows the observed failure progression for floodwalls. Scour pattern “A” indicates scour located on the protected side levee slope (or located immediately adjacent to the floodwall or sheet pile protected side); “B” indicates erosion on the protected slopes, including stabilizing transition slopes; “C” indicates erosion progressing to the levee crown adjacent to the floodwall or sheet pile protected side; “D” indicates scour on both the floodside and the protected side of the levee or floodwall; and “E” indicates that the original levee footprint has been significantly altered due to erosion, and the original foundation base may have scour holes or washouts.

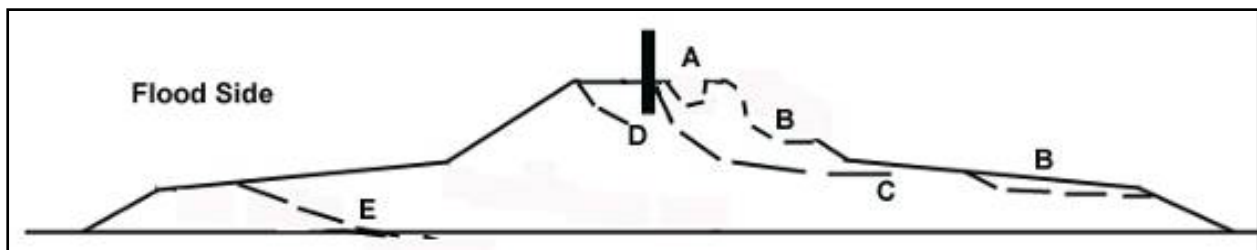


Figure 74. Erosion progression patterns for earthen levees, floodwalls, and exposed sheet pile.

Figure 75 shows a conceptual diagram illustrating the water overtopping plunging velocity and force of impact on the wall's backside. Figures 76 through 79 show the different stages of erosion as a result of floodwall overtopping along the Citrus Back Levee I-wall. Figures 80 through 83 show the different stages of erosion as a result of floodwall overtopping along the eastern side of the IHNC adjacent to the Lower Ninth Ward.

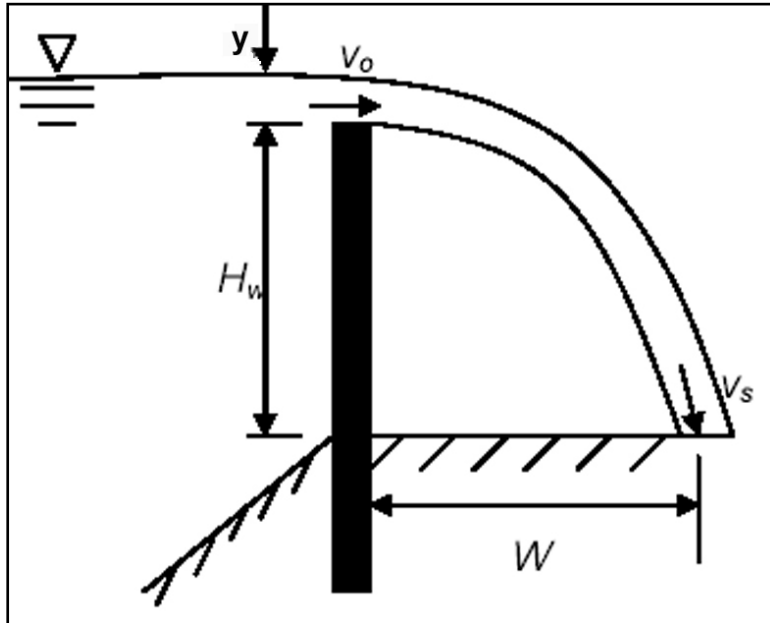


Figure 75. Conceptual diagram of water overtopping a floodwall or exposed sheet pile.



Figure 76. Aerial photo showing the deflection and tilting of the Citrus Back Levee I-wall.



Figure 77. Scour trench on the protected side of the Citrus Back Levee I-wall. (Figure 7.14, NSF-Berkeley report (ILIT Final Report, 31 July 2006).)



Figure 78. Another section of the Citrus Back Levee I-wall showing erosion of the levee, lateral deflection, and tilting from overtopping.



Figure 79. Deflection and tilting of the Citrus Back Levee I-wall.





Figure 80. Aerial photo of the breached floodwall along the eastern side of IHNC adjacent to the Lower Ninth Ward.



Figure 81. Displaced floodwall along the eastern side of the IHNC adjacent to the Lower Ninth Ward.



Figure 82. Stage A erosion along the eastern side of the IHNC adjacent to the Lower Ninth Ward.



Figure 83. Stage D erosion along the eastern side of the IHNC adjacent to the Lower Ninth Ward.

Water overtopping the floodwalls led to extensive scour and erosion in some locations, which ultimately resulted in breaches. This was most dramatic along the IHNC adjacent to the Lower 9th Ward where I-wall breaches were caused by overtopping erosion. It appeared that water flowing over the floodwall scoured and eroded the levee on the protected side of the I-wall, exposing the supporting sheet piles and reducing the passive resistance. The water flowing over the top of the walls may have scoured significant amounts of soil from the levee adjacent to the wall. Evidence of this scour can be seen along the unbreached reaches of the I-walls on the IHNC where U-shaped scour trenches could be found adjacent to the I-walls, as can be seen in Figure 82. As the scour increased, the I-wall may have moved laterally and leaned to the

protected side, causing the scour trench to grow as the water cascaded farther down the slope until sufficient soil resistance was lost and the wall failed, as shown in Figure 83. I-walls along the MRGO and the Mississippi River in Plaquemines Parish suffered similar damage due to overtopping where the greater the scour, the greater the lateral translation and tilting of walls.

It appears that the I-walls were not designed to withstand overtopping. The survivability of this type of wall could be significantly improved by providing erosion protection such as grouted riprap or concrete erosion mats running from the base of the wall down the face of the levee on the protected side.

While overtopping of the I-walls led to significant scour and damage in many cases, overtopping of T-walls did not lead to extensive scour and erosion. **In general, T-walls did not suffer severe scour on the protected side, likely because the base of the inverted T-wall section extends out on the protected side, preventing scour adjacent to the T-wall stem.**

## Levees

The performance of levees varied significantly throughout the New Orleans area. Lengthy reaches (miles) of earthen levees and capped levees were overtopped. Some reaches showed signs of initial erosion, others showed signs of progressive erosion, and other reaches contained significant breaching. Similar to levees, lengthy reaches of floodwall were overtopped and were left in various stages of damage, ranging from minor scour at the wall base to breaches where complete floodwall sections were flattened. Several stages of erosion and scour patterns were visually observed along numerous levee/floodwall reaches, and almost all patterns appeared to have been initiated on the protected side of the levee/floodwall.

Two variables played a major role in determining the extent and amount of levee damage. The hydraulic loading (storm surge and wave action) from the hurricane was the driving influence of course, but the levee damage was not a continuous function of overtopping surge and wave heights. The levee response (failure versus functional) was also determined by pre-Katrina geotechnical issues (soil type, soil layering, soil consistency, and levee construction methods).

Soil material properties greatly influence surface erodibility and erosion progression rate during overtopping. Cohesive (silt and clay) soils erode due to the formation and migration of a headcut perpendicular to the levee axis (i.e., across the levee section from the backside to the floodside). A headcut is a vertical or near-vertical elevation drop and migrates upstream due to hydraulic stresses at the overfall, base seepage, weathering, and gravity. Sandy (noncohesive) soil erosion involves a sediment transport process as the material is removed in layers. Cohesive soil erosion rates are more strongly influenced by soil material properties such as water content, density, erodibility, shear strength, and compaction effort during construction. For example, it was found that only a 5-point (5%) decrease in compaction water content caused a 100-fold increase in the breach widening rate for clay soil.

Characterizing soil erodibility is a complicated matter due to spatial non-homogeneity and variability in soil types, difficulty in selecting accurate engineering properties needed to

determine erodibility, and temporal effects during erosion progression such as surface roughness changes which, in turn, affect the hydraulic stress and turbulence conditions. Soil properties affecting erodibility are soil classification (gravel, sand, silt, clay proportions); water content (antecedent moisture); clay mineralogy and proportion; soil structure; Atterberg Limits; organic content; pore water chemistry (salinity, hardness, quality, pH); in situ density; erodibility parameters such as the critical shear stress required to initiate soil particle detachment, hydraulic shear stress, and erodibility coefficient; in situ shear strength, and compaction effort during construction (optimum moisture content and optimum dry density values both specified and as-built).

The rate of erosion is proportional to the applied shear stress in excess of a critical shear stress where erosion is initiated. Soils with a lower critical shear stress tend to be more erodible.

Levee geometry is important when investigating probability of erosion. A 1:3 side slope is steeper than a 1:4 slope, and a stabilizing berm slope acts as an overtopping energy dissipator. Water cascading down a 1:3 slope impacting a 1:20 berm slope would be more likely to initiate erosion than that on a 1:4 slope. Erosion would also depend on slope distance between the crest and the toe, surface roughness, and water depth.

The levees along the MRGO on the northeast side of St. Bernard Parish and the New Orleans East back levee, which fronts Lake Borgne, had numerous breaches and were washed out over considerable lengths. These levees were constructed using hydraulic fill that contains significant silt and sand, and they were subjected to large waves and significant depths of overtopping.

The New Orleans East back levee suffered considerable erosion. Figure 84 shows the major levee segments. The locations of the levee breaches caused by erosion are shown in Figure 85 and the hydraulic fill and hauled fill segments are indicated in Figure 86. It can be noted that the breaches are located in sections that were constructed of hydraulic fill. However, this is not an exact correlation, and other factors need to be considered. Figure 87 shows locations where the surge and wave hydrographs have been determined from calculations and high-water marks. Figure 88 shows a plot of pre-Katrina levee elevations and the surge height plus the peak wave height at these locations. It can be seen that the greatest erosion of the hydraulically filled levees occurs when the surge height plus the peak wave height had the greatest level above the crest of the levee. Examination of this information has shown that the peak wave height is the most important component of the surge. The figure also shows that levees constructed of rolled fill had equal to or greater surge plus the peak wave height over their crest, yet did not breach. Therefore, it is concluded that the combination of hydraulically filled levees and high surge and wave action leads to breaches by erosion.



Figure 84. General map of NOE basin. Major levee segments are Lakefront levees, NOE east levee (South Point to GIWW), NOE back levee, Citrus back levee, and IHNC levees.



Figure 85. NOE basin post-Katrina breaches.





Figure 86. NOE Levee construction materials.



Figure 87. Selected model data points for surge analysis.

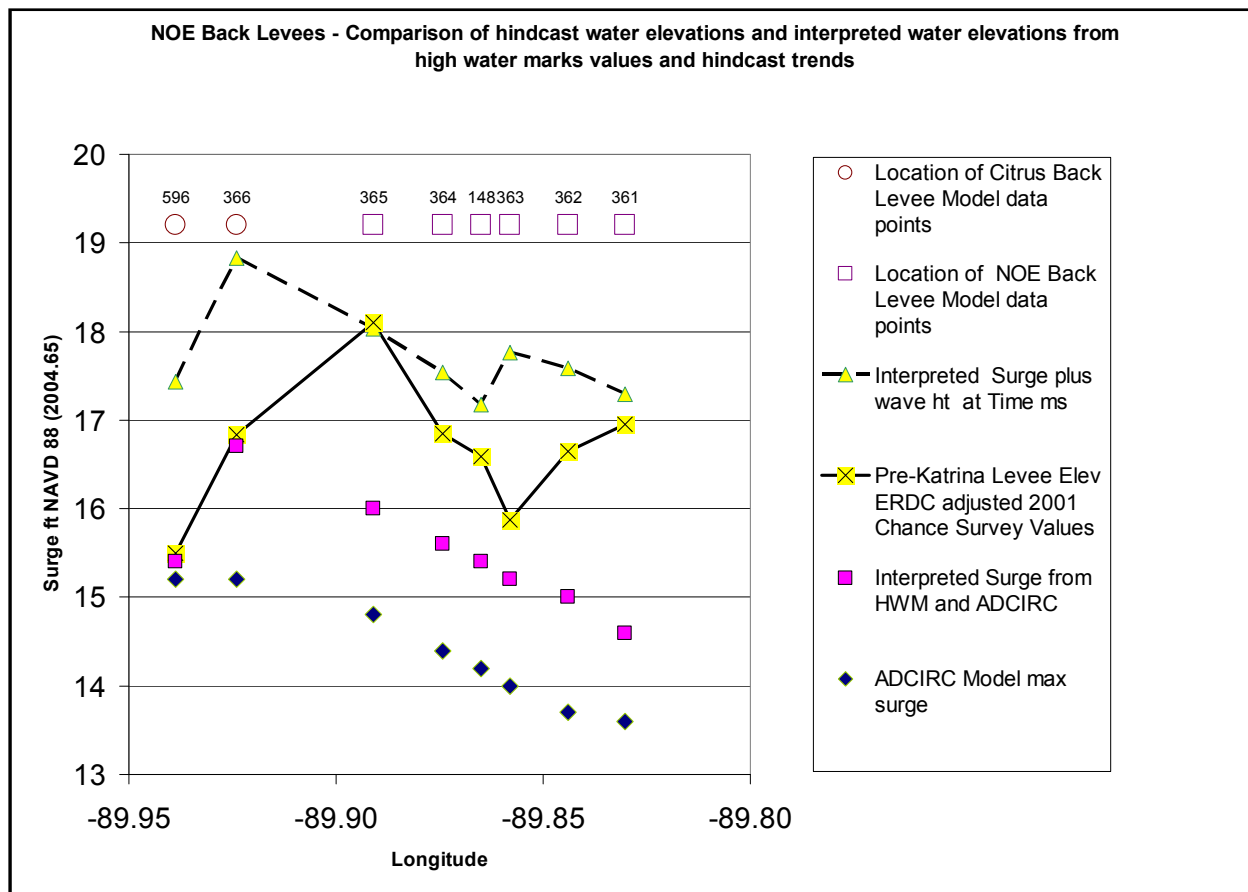


Figure 88. Levee elevations derived from pre-Katrina LIDAR for Citrus back levee and NOE back levee.

The LIDAR data along the levee crown can also be expressed as an elevation profile. Figure 89 is a plan view of the LIDAR stationing used in this investigation. Figures 90 through 94 show selected post-storm LIDAR survey data along the NOE BL. These data allow comparison of scour depths to construction methods and associated soil types, in addition to wave height and surge elevation.

Scour depths vary tremendously along the selected profiles starting at the Michoud Canal, moving east along the GIWW, and ending at the South Point levee. The average pre-storm elevation of the NOE BL was 16.0 ft (NVGD88, 2004.65) to the east of the pump station and 17.0 ft (NVGD88, 2004.65) to the west of the pump station. The average scour to the east of the pump station was 8 ft, with approximately 75% of the levee scoured to this depth. The maximum scour in this segment was approximately 15 ft. In contrast, the western portion of the NOE BL earthen levee performed well. Approximately 99% of the western NOE BL was scoured just 0.5 to 2.0 ft.

The variable levee performance in the NOE basin was most likely due to the differences in levee construction (hydraulic fill versus truck hauled), levee soil types (sandy versus clayey), and differences in surge and wave heights during the storm (hydraulic loading). The soil borings east of the Michoud Canal show that levee materials at the crown surface (the final soil construction lift) were silts, sands, and lean clays. Borings east of Pump Station 15 had more fat

clay layers in the top 10 ft than the other two borings west of Pump Station 15. The presence of fat clay layers is not necessarily the sole controlling factor leading to higher erosion rates, since the levees east of Pump Station 15 typically had higher erosion, scour, and breaching frequency than those on the west side. The hydraulic loading (surge and wave action) is greater east of Pump Station 15, which is consistent with the greater erosion. Figure 88 shows that Station 366 had a high hydraulic loading and was constructed by hauled compacted fill. The levee was constructed from fat clays and lean clays, with dry densities ranging up to 103 lb/cu ft and subsequently had minimal erosion damage.

Another example is the levee at the Entergy power plant in the New Orleans East area near the Paris Road Bridge. This overtopping can be seen in the widely circulated picture taken by Entergy personnel during the storm, shown in Figure 95. Preliminary results of Cone Penetrometer Tests taken on the levee at the Entergy power plant indicate that the levee was constructed of clay (CH) and later, erodibility tests showing it was resistant to erosion. Figure 96 shows that it suffered only minor erosion due to overtopping.



Figure 89. LIDAR stationing used in this report, starting at Lakefront levee and ending at the Michoud Slip along the GIWW.

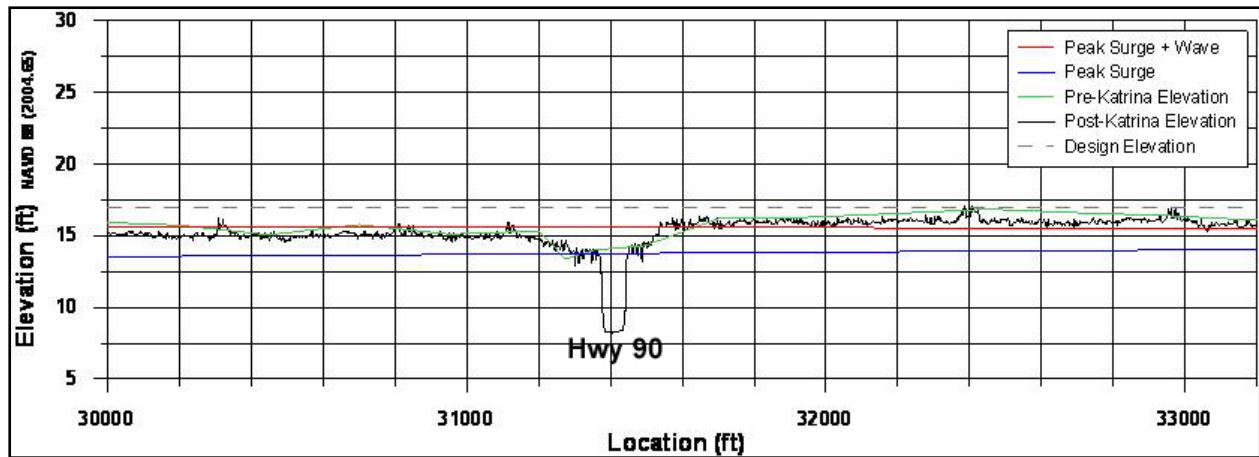


Figure 90. A typical post-Katrina LIDAR profile along the NOE back levee west of Michoud Canal.

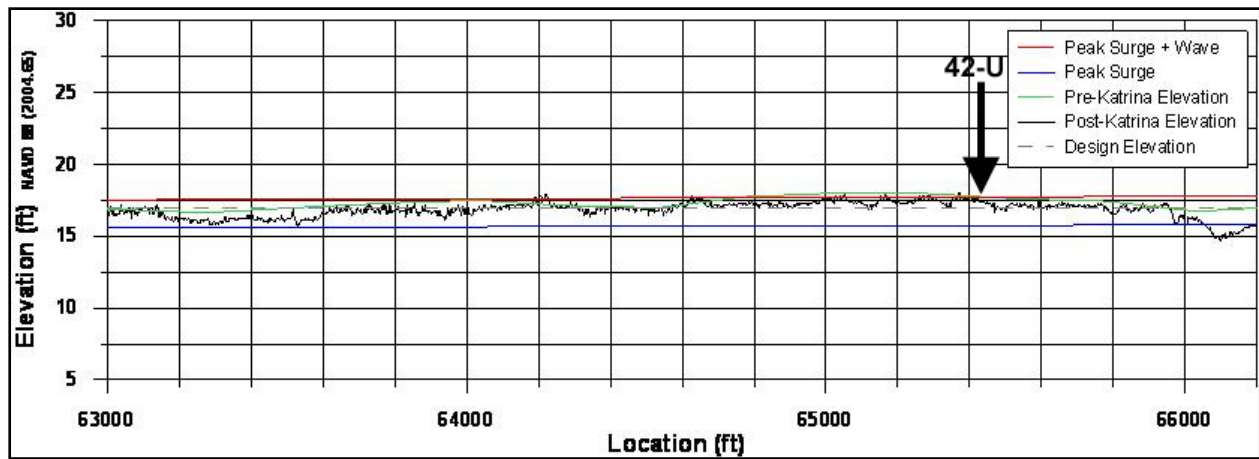


Figure 91. A typical post-Katrina LIDAR profile along the NOE back levee west of Pump Station 15.

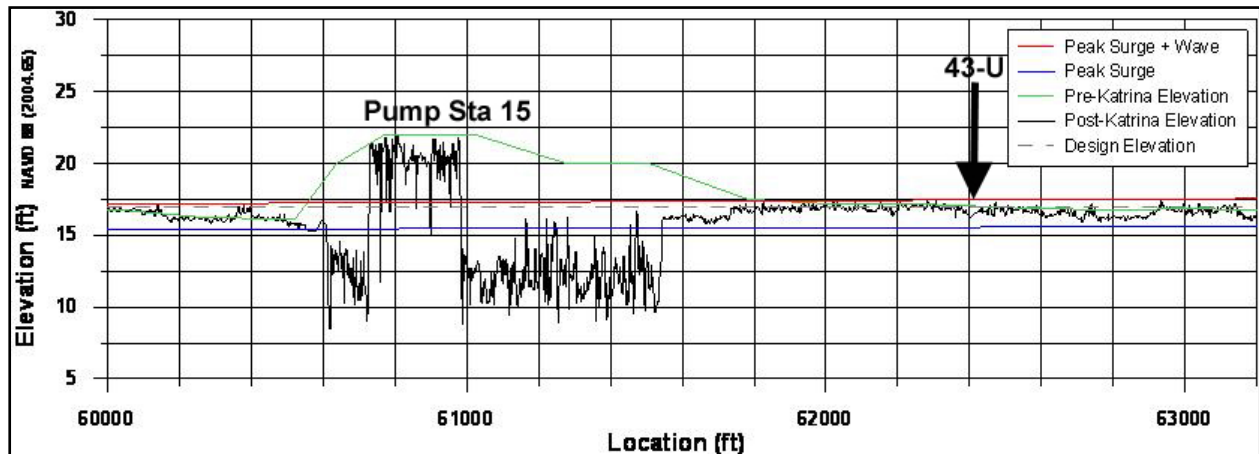


Figure 92. Another typical post-Katrina LIDAR profile along the NOE back levee west of Pump Station 15.

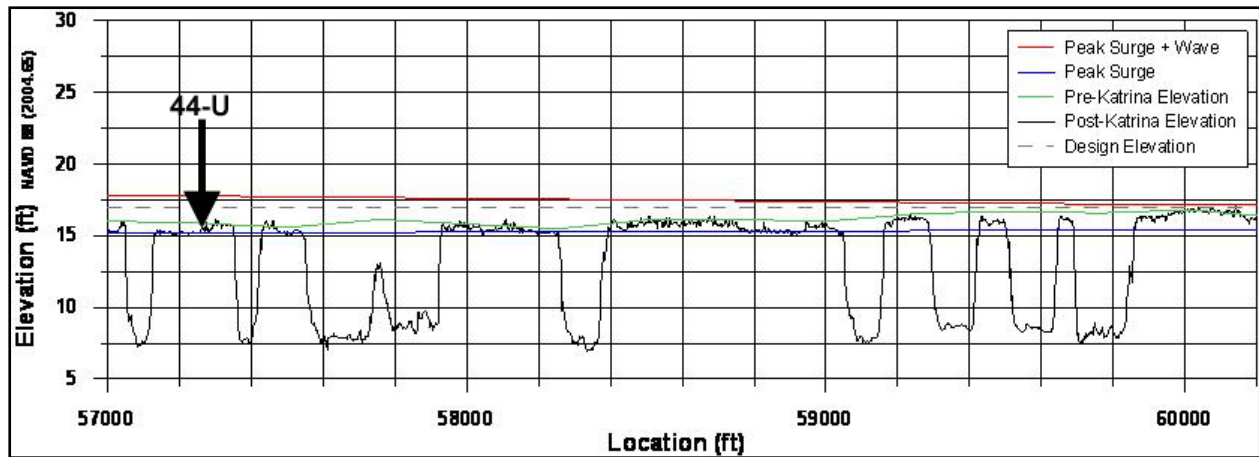


Figure 93. A typical post-Katrina LIDAR profile along the NOE back levee east of Pump Station 15.

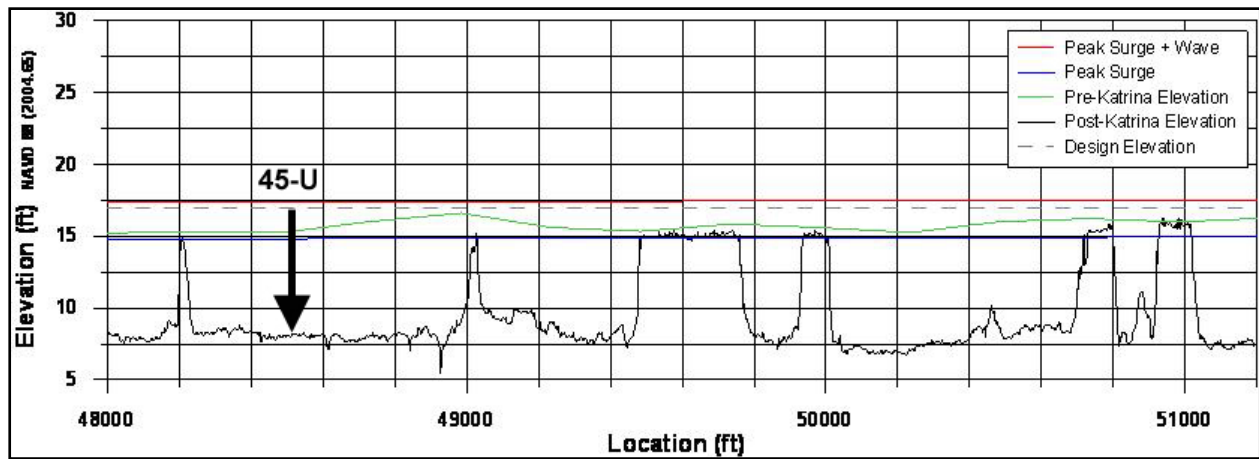


Figure 94. Another typical post-Katrina LIDAR profile along the NOE back levee east of Pump Station 15.



Figure 95. Overtopped levee under the Paris Road Bridge adjacent to the Entergy power plant in New Orleans East, during Hurricane Katrina.



Figure 96. Overtopping of the levee under the Paris Road Bridge adjacent to the Entergy power plant in New Orleans East after the storm.

Figure 97 shows the breach locations for St. Bernard Parish, which includes nearly 70% of the levee along MRGO. Figure 98 highlights the levee's construction methods, including hauled, hydraulically filled, and walled reaches. Note the breach locations in Figures 97 and 98 coincide with the reaches constructed using hydraulic fill.

Figure 99 shows a LIDAR stationing map for portions of the St. Bernard levee system. To establish possible correlations between soil type and erosion depth, the LIDAR data are plotted as levee profiles along 3,000-ft reaches (Figures 100 through 108). Levee reaches of high scour are easily identified using these profiles. The above boring locations are identified on the profiles to facilitate the correlation between soil and erosion. In addition, Figure 106 shows the location of one set of erodibility tests, the ASTM Jet Index Test. The tests indicated high resistance to erosion at this site, and the LIDAR also shows little scour at this location. The existing levee at this location was constructed with a fat clay (CH) surface as noted by the test engineers.





Figure 97. St. Bernard Parish breach locations.

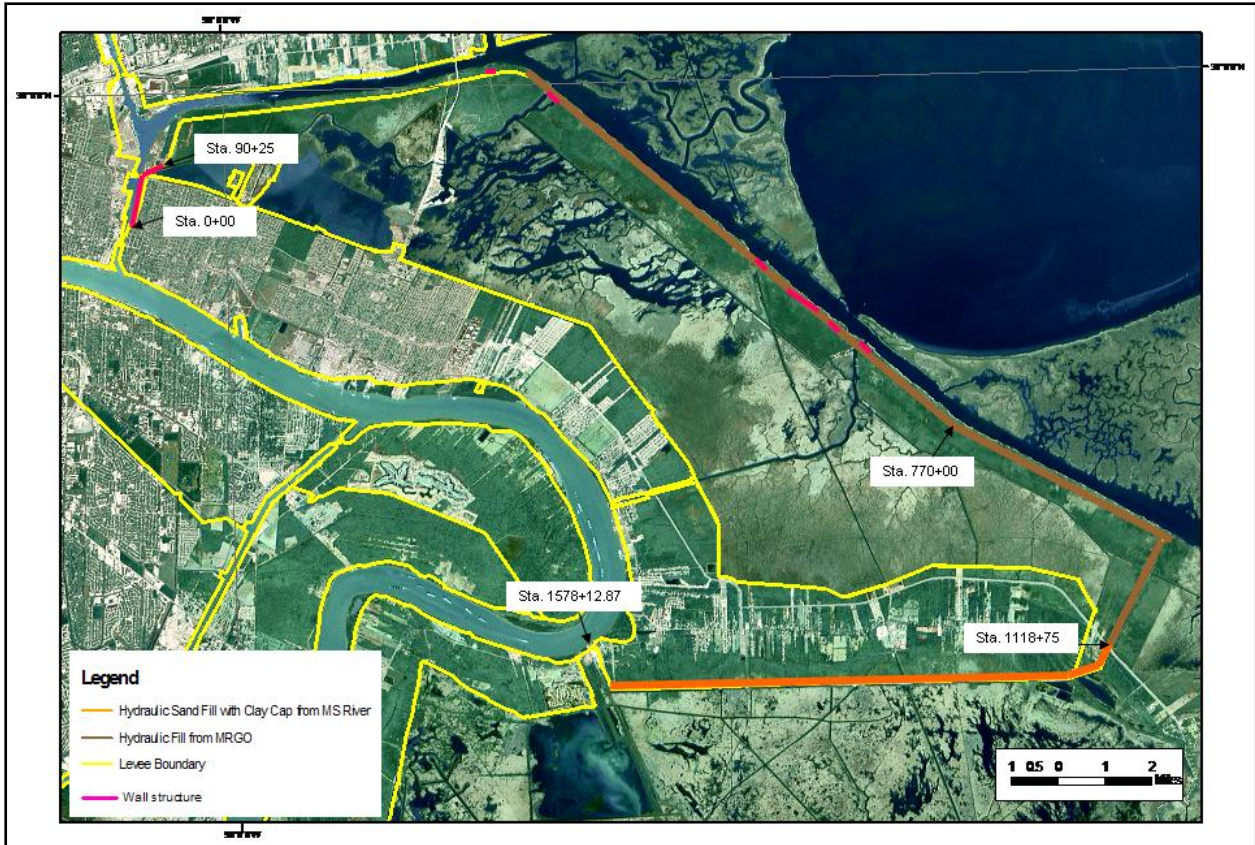


Figure 98. Constructed levee soil sources.

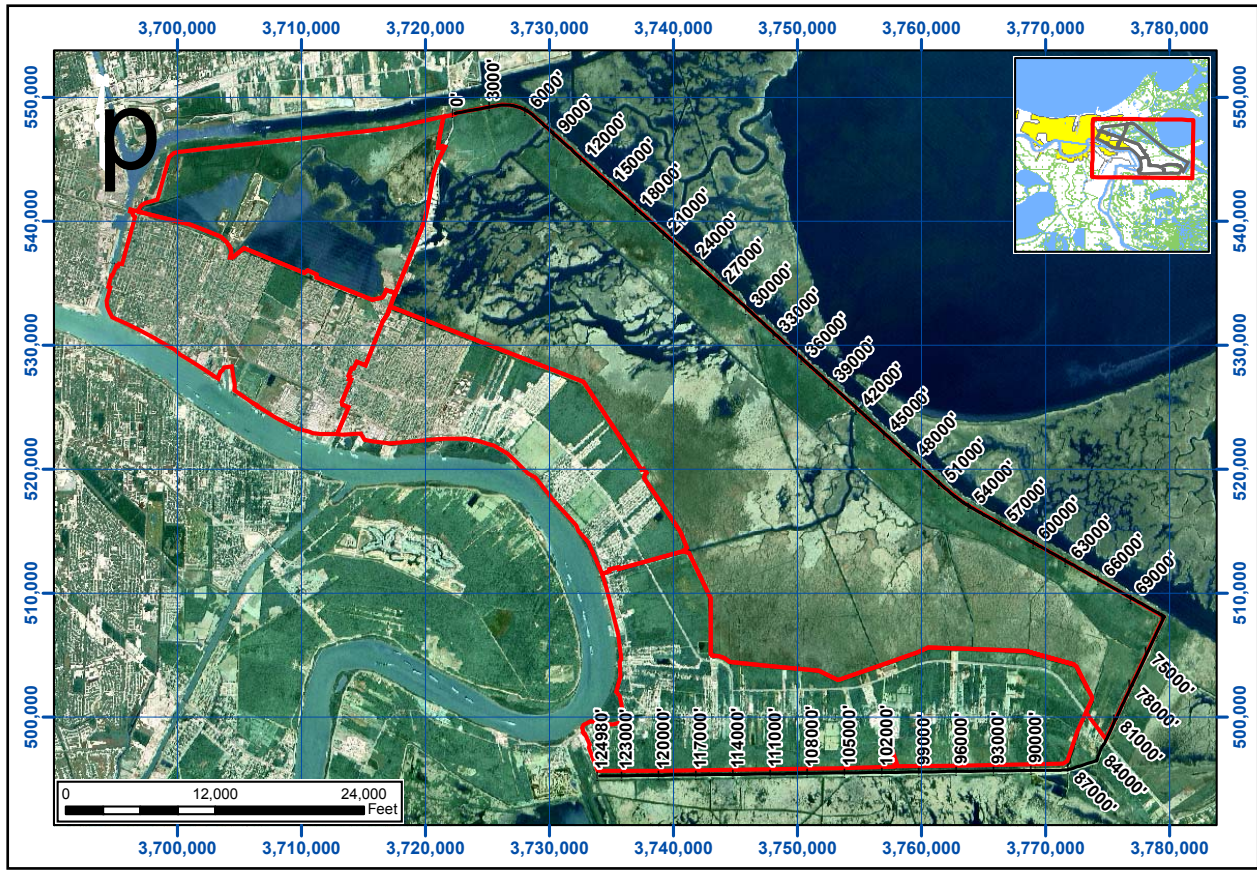


Figure 99. St. Bernard Parish LIDAR stationing map with ERDC erosion test locations.

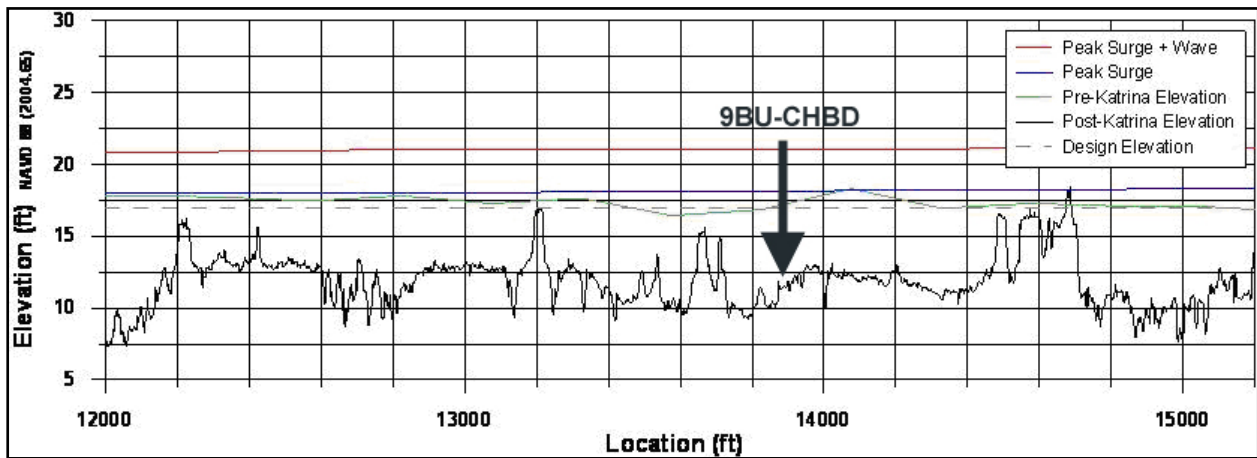


Figure 100. LIDAR plot showing soil boring 9BU-CHBD approximate location. Erosion depth was approximately 5 ft.

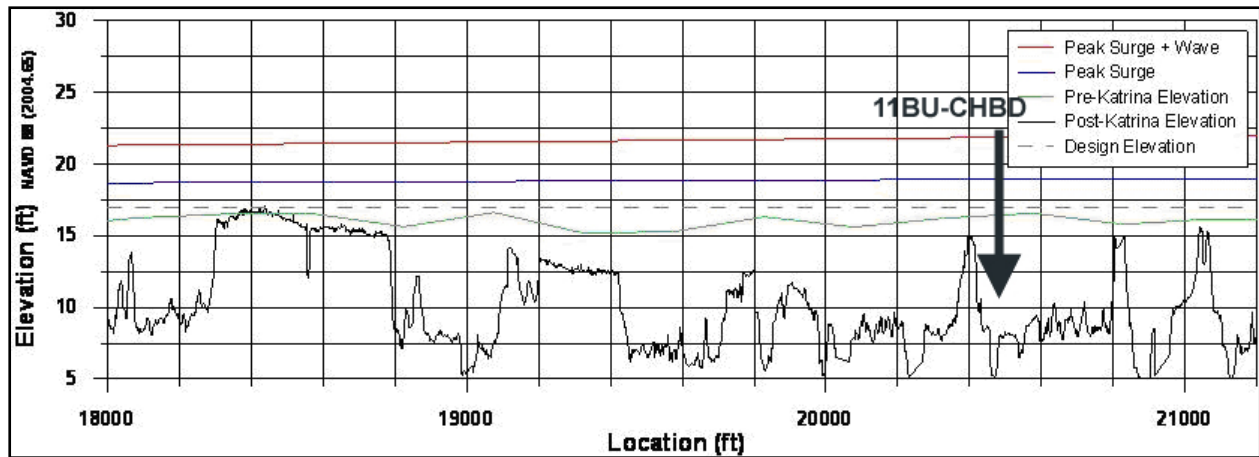


Figure 101. LIDAR plot showing soil boring 11BU-CHBD approximate location. Erosion depth was approximately 10 ft.

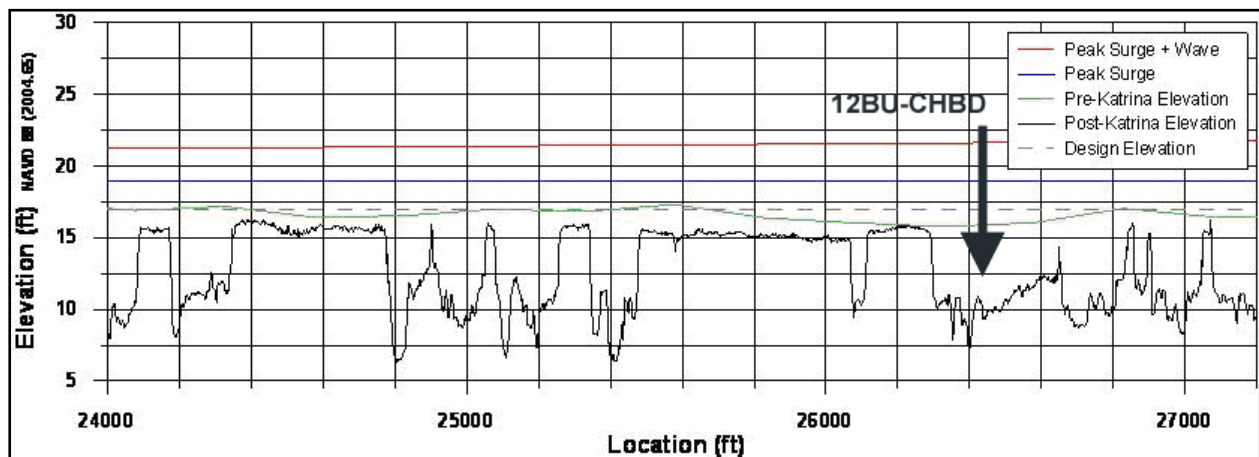


Figure 102. LIDAR plot showing approximate location of soil boring 12BU-CHBD. Approximate erosion depth was 6 ft.

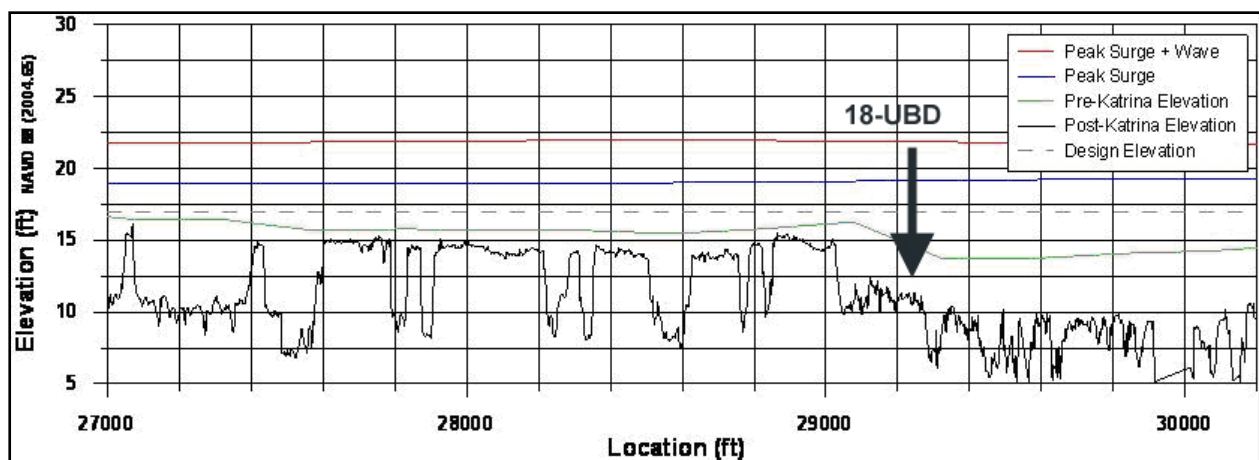


Figure 103. LIDAR plot showing approximate location of soil boring 18-UBD. Approximate erosion depth was 6 ft.

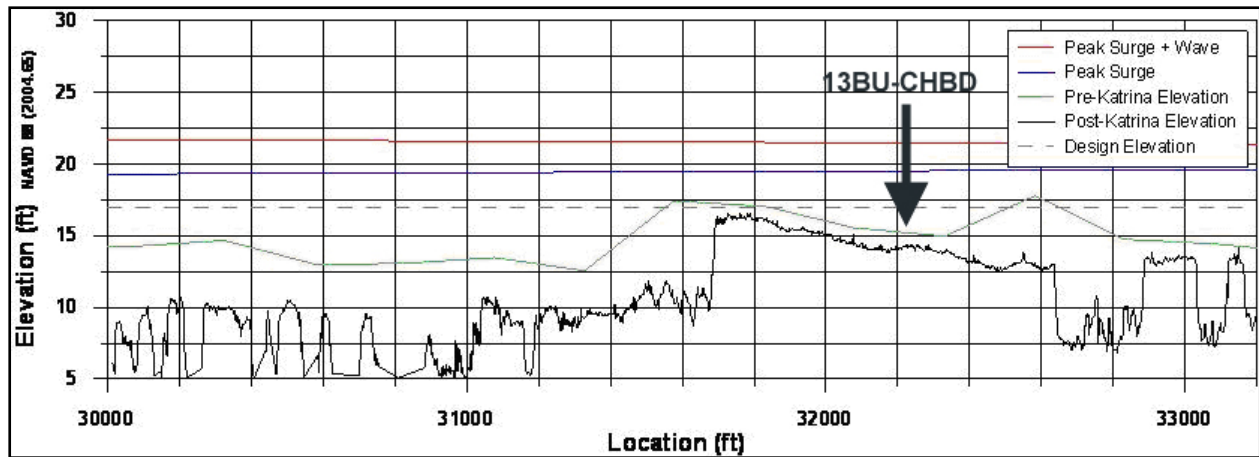


Figure 104. LIDAR plot showing soil boring 13BU-CHBD approximate location. Erosion depth was approximately 1 ft.

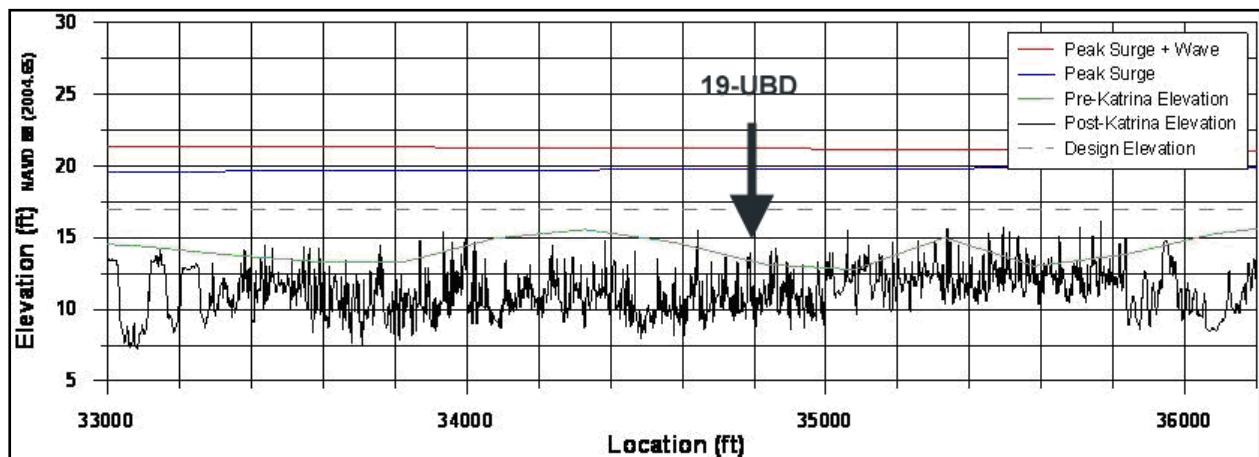


Figure 105. LIDAR plot showing soil boring 19-UBD approximate location. Sheet piling was present at this location as indicated by the LIDAR signature.

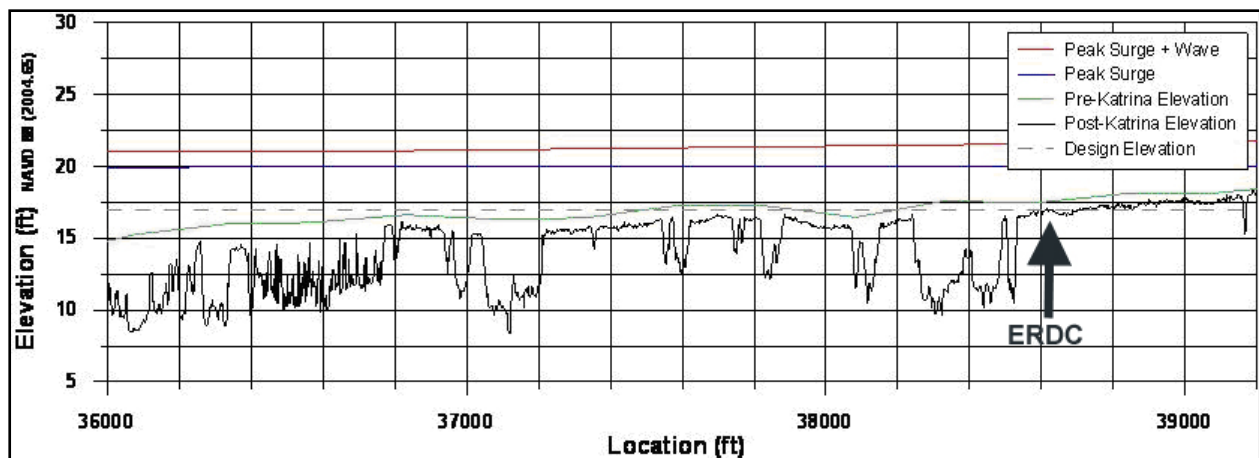


Figure 106. LIDAR plot showing approximate location of erosion tests (ERDC) on the crown of the surviving post-Katrina levee.

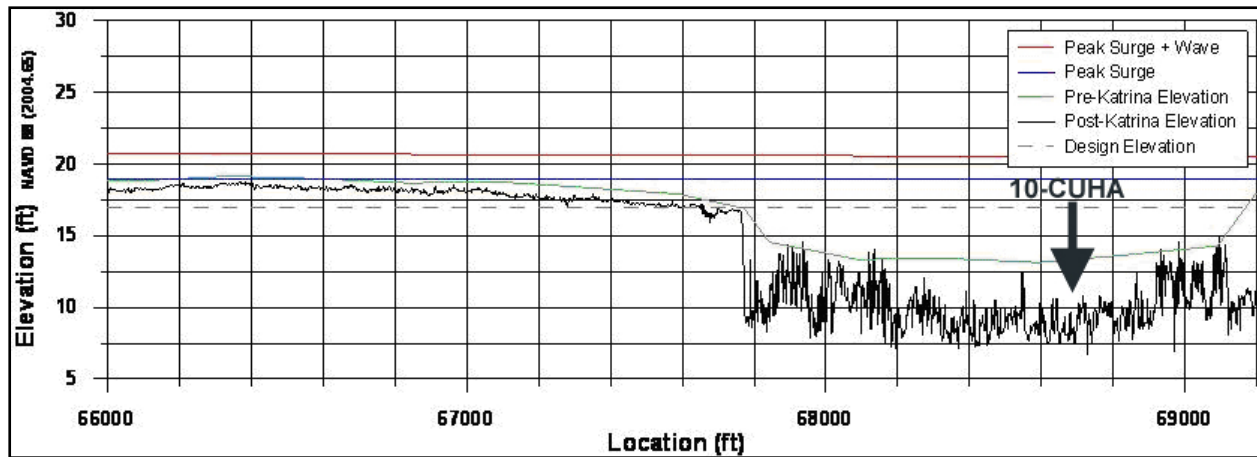


Figure 107. LIDAR plot showing approximate location of soil boring 10-CUHA. Sheet piling was present at this location as indicated by the LIDAR signature.

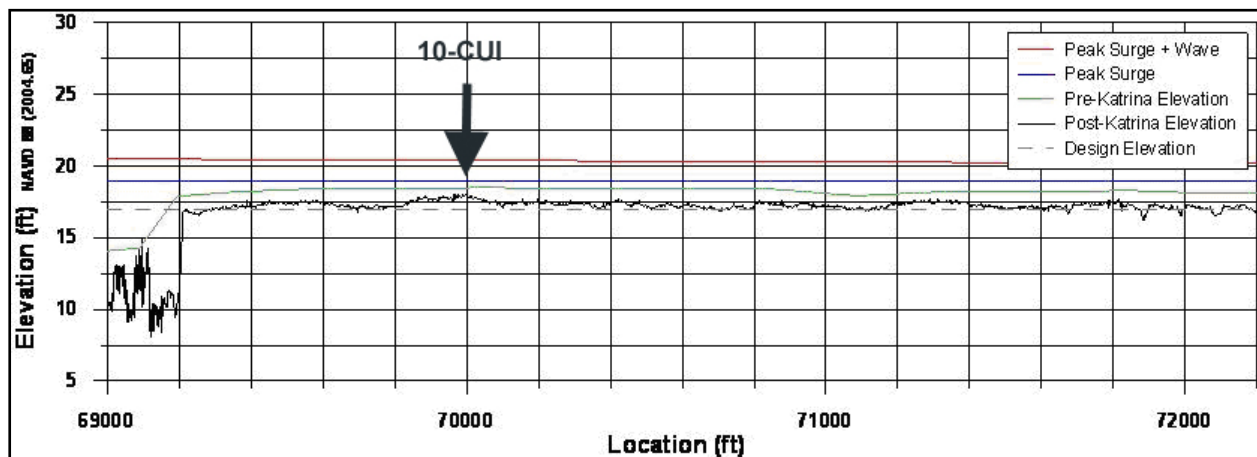


Figure 108. LIDAR plot showing approximate location of soil boring 10-CUI drilled in 1985. Erosion damage was minimal.

The soil type, scour depth, and hydraulic loading data from the above figures (Figures 100 through 108) are generalized in Table 4. The levee crown surface soil types and consistencies (strengths) are shown with approximate scour depths and approximate surge plus wave heights. Figure 109 is a plot of the Table 4 data and shows the relations between soil type, soil strength, hydraulic loading, and erosion depths at selected points along the levee crown. Note that no strong correlation between erosion depth and hydraulic loading was observed. From these selected points (Table 4), it appears that soil consistency (strength) and soil type correlate with erosion depth and hydraulic loading. The soil consistency is correlated in that soft fat clays performed poorly (i.e., had deeper erosion) compared to medium fat clays, and the medium fat clays performed better than the medium lean clays. The soil strengths (consistencies) are directly comparable to the construction compaction effort. For example, a compacted clayey soil will have higher density and strength than an uncompacted clayey soil at the same water content.

**Table 4  
Surface Soil and Scour Versus Hydraulic Loading.**

Boring	Surface Soil Type	Scour Depth, ft	Overtop Crest, ft
9BU	med CL	5	2
11BU	soft CH	10	5
12BU	med CL	6	7
18UBD	SM	6.2	7
13BU	med CH	1	7
ERDCM3	med CH	0.7	7
10-CUI	med CH	0.5	6
9-CUA	stiff CL	7	5
44-U	med CH	0.5	1
45-U	med CL	8	2
5A-CAU	stiff CL	0	1

Strengths (consistencies) are soft, medium (med), and stiff.  
Soils are lean clay (CL), fat clay (CH), and sandy silt (SM).

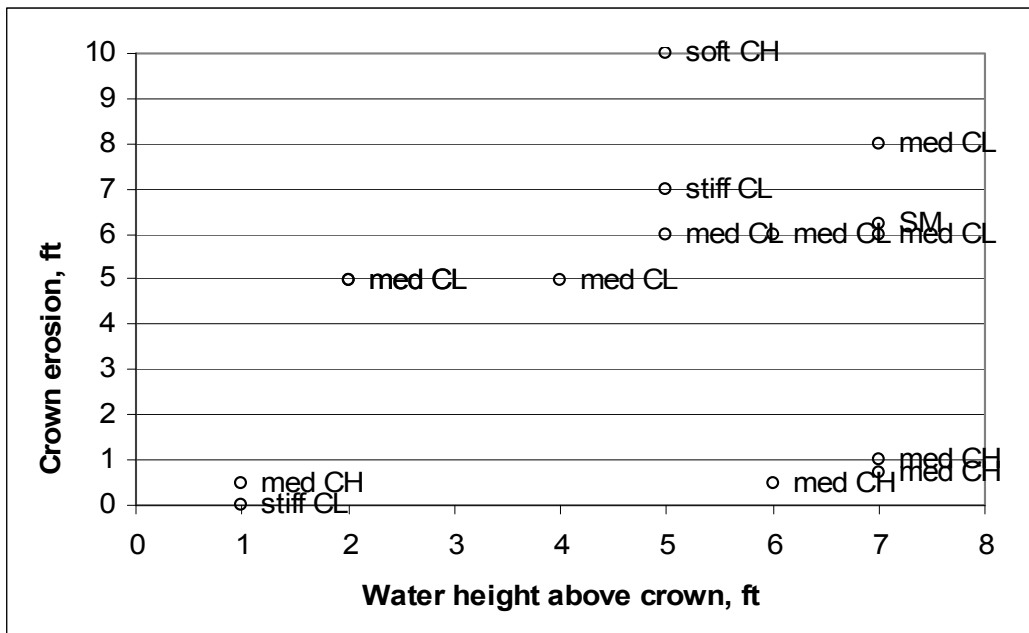


Figure 109. Scour depths versus surge/wave loading from soil borings and LIDAR data plotted from Table 4 levee surface soil stiffness (strength) and soil type are labeled. Note that medium-strength fat clay (med CH) had the least amount of erosion as the hydraulic loading increased.

## Transitions

A common problem observed throughout the flood protection system was the scour and washout found at the transition between structural features and earthen levees. In many cases, the structural features were at higher elevations than the adjacent earthen levee, resulting in scour and washout of the levee at the end of the structural feature. At these locations, the dissimilar

geometry concentrates the flow of water at the intersection of the levee with the structure, causing high flow velocities and turbulence that resulted in the erosion of the levee soil. The performance at transitions could be improved by fully embedding the structural walls within the levee fill and using the levee to transition the difference in elevation from the structure to the main section of the levee. In a few cases, observations indicated that this type of transition performed successfully. The embedded area and the transition to the main section of the levee should have erosion protection such as grouted riprap or concrete erosion mats.

In some cases, the structures were lower than the connecting earthen levees. At these sites, the flow of the water is channeled over the structural feature, causing erosion of soil on the protected side of the structure. The performance in these cases can be improved by providing erosion protection on the protected side of the structures and along the transition section.

## **Floodwall and Levee Performance Findings and Lessons Learned**

### **Findings**

The majority of approximately 50 levee and floodwall breaches resulted from overtopping and subsequent erosion, or from erosion-induced instability of I-walls.

A single design cross section was used for long sections of the I-walls and was applied in areas where the protected side ground elevation was lower than considered in the design analysis.

Four major floodwall breaches, three in the outfall canals and one on the IHNC, resulted from shear failure or erosion and piping through the foundation soils at water elevations below the original design elevations. The foundation-induced breaches had the common element that a gap opened between the levee and floodwall, on the canal side of the wall, as the water rose against the wall. Water entering these gaps imposed increased loads on the walls.

Where the foundation soil was permeable sand, water flowing down through the gaps increased the water pressure in the sand, reduced the capacity of the foundation to resist load, and increased the likelihood of erosion and piping.

In sections where the foundation soils were clay, the shear strength of the clay was smaller beneath the levee slopes and beyond the toe than beneath the crest where the clay was compressed under higher pressures and was, therefore, stronger.

No levee breaches occurred without overtopping. The degree of erosion and breaching of overtopped levees was directly related to the character of the in-place levee materials and the severity of the surge and wave action. Hydraulically filled levees with higher silt and sand content in the embankment material that were subjected to high overtopping surge and wave action suffered the most severe damage. Rolled clay levees performed well, even when overtopped.



I-walls throughout the HPS that were subjected to overtopping suffered extensive erosion and scour of the foundation of the wall on the protected side. The only exceptions were walls that had paved surfaces adjacent to the walls on the protected side.

Significant scour and erosion occurred at many transitions between concrete structures and earthen levees.

While overtopping of the I-walls led to significant scour and damage in many cases, overtopping of T-walls did not lead to extensive scour and erosion, because the base of the inverted T-wall sections extended over the protected side.

T-walls performed well during Katrina. Because of their pile foundations, they are better able to transfer high lateral water loads into stronger underlying foundation materials.

Many of the levees in the New Orleans Hurricane Protection System had numerous encroachments ranging from trees growing on the protected side slope of levees to swimming pool at the toe of the protected side of the levees. While none of the breaches were attributed to these encroachments, they can adversely affect the stability of a levee section and should be controlled.

## **Lessons Learned**

A broad range of potential failure modes should be considered for the floodwall design criteria.

I-walls should be designed to be stable, with a gap between the wall and the levee on the water side of the wall, with hydrostatic pressure acting through the depth of the gap.

Both horizontal and vertical variation of the strengths of clay foundation soils with overburden pressure should be considered in evaluations of levees and I-walls.

Water pressures in sand foundations beneath levees and I-walls should be evaluated by means of seepage analyses that reflect very conservative assumptions regarding hydraulic boundary conditions, and seepage control measures should be included in the design, as needed, to reduce the potential for erosion and piping.

Rolled clay-fill embankments are generally able to withstand overtopping without erosion for many hours and should be used to construct levees wherever possible. Armoring can augment existing levee materials to provide improved erosion resilience.

Improved resistance against erosion at transitions between earthen levees and structures can be achieved by embedding the structural walls within the levee fill, and protecting the transition by armoring.

Design methods should be updated periodically to include the review of recent research and case histories.

## Other Studies

There were a number of other studies conducted within the time frame of the IPET activities. Perhaps the most publicly recognized of these are the efforts of the Independent Levee Investigative Team led by the University of California at Berkeley (UCB) and Team Louisiana led by the Louisiana State University (LSU). It was important to have multiple teams examining the post-Katrina situation in New Orleans.

These efforts differed dramatically in their scope, resources, and levels of effort. The IPET was comprised of over 150 experts and another 150 support personnel with resources exceeding \$22 million and direct access to the unique experimental facilities of the U.S. Army Engineer Research and Development Center, as well as those of the eight major government agencies, 23 private sector firms, and 25 universities that composed the task force. In addition, the IPET efforts have been continuously peer-reviewed by the ASCE External Review Panel and strategically reviewed by the NRC Committee on New Orleans Regional Hurricane Protection Projects. Team Louisiana and the UCB Teams were much smaller in all dimensions and did not have the benefit of real time or strategic peer review. While the IPET effort was highly focused on in-depth analyses of the engineering and system-wide performance issues, the UCB effort was divided between work on the engineering aspects and some on the organizational and human factors. Team Louisiana also examined a broad spectrum of topics but in less detail. To date, there has not been a formal report published by Team Louisiana; however, some of their information was incorporated into the UCB report.

Following release of the IPET Draft Final Report on 1 June 2006, review comments were provided by the ASCE External Review Panel and the NRC Committee on New Orleans Regional Hurricane Protection Projects. In an endeavor to respond to their feedback and to ensure that the IPET Final Report contained the best information possible, IPET teams reviewed in some detail the work of the other studies. The objective was to incorporate, as appropriate, any information that would enhance the value of final IPET findings, lessons learned, and analytical processes documented in the report. It was also important to provide feedback to engineers and organizations engaged in the planning, design, and construction of flood risk-reduction structures in New Orleans and elsewhere. There were a number of issues that have been published by the media, as well as the study reports that deserve some specific mention here.

There were two major differences in the findings between the IPET investigation and the other efforts. The first deals with the failure modes of the floodwalls for the 17th Street breach site and for one of the breach sites on the IHNC. This is significant for the future planning and design of these structures, as well as understanding appropriate remedial measures to strengthen existing structures. The Team Louisiana assessment of the 17th Street Canal breach was superficial and lacked any realistic representation of the site conditions, observed failure surface, and shear strength of the soil. Both the IPET and UCB Team investigations are in agreement that the excessive deflection of the floodwall structures was a major component of the failure mode for the levee and I-wall system at the 17th Street Canal breach. Both assessments have identified weak subsurface soils as the other major culprit in the failure mode. They differ in which subsurface layer was the culprit. The IPET investigation placed the failure plane at the top of a

weak clay layer underlying the persistent layer of peat in the region. This location of the failure plane was based on the elevation and shape of the failure plane from profiles of the breach area obtained from underwater surveys conducted before emergency repairs were initiated (Figures 10 through 13), and site geotechnical investigations that included excavating the actual failure plane with a backhoe (Figures 16 and 17). These physical observations are fully supported by detailed numerical modeling by two independent teams and physical modeling by two independent centrifuge teams. The UCB Team hypothesized that a thin 1-in.-thick sensitive clay layer within the peat layer (overlying the weak clay) is the location of the slip plane that caused the failure. The UCB Team based this on small diameter Shelby tube soil samples and limited numerical analyses using a suspect geology profile and unrealistic soil properties (see Appendix 22). IPET has not been able to detect a widespread thin (inch or less in thickness) layer within the peat layer, in spite of having physically harvested large volumes of peat for use in centrifuge testing and acquisition of significant additional subsurface soils data. The UCB has not been able to explain the clay layer imbedded in the peat exposed when the slide block excavated with a backhoe. The clay layer, which was initially located beneath the marsh layer, was displaced upward and over a portion of the marsh layer by the lateral displacement that occurred during the failure (Figures 17 and 18).

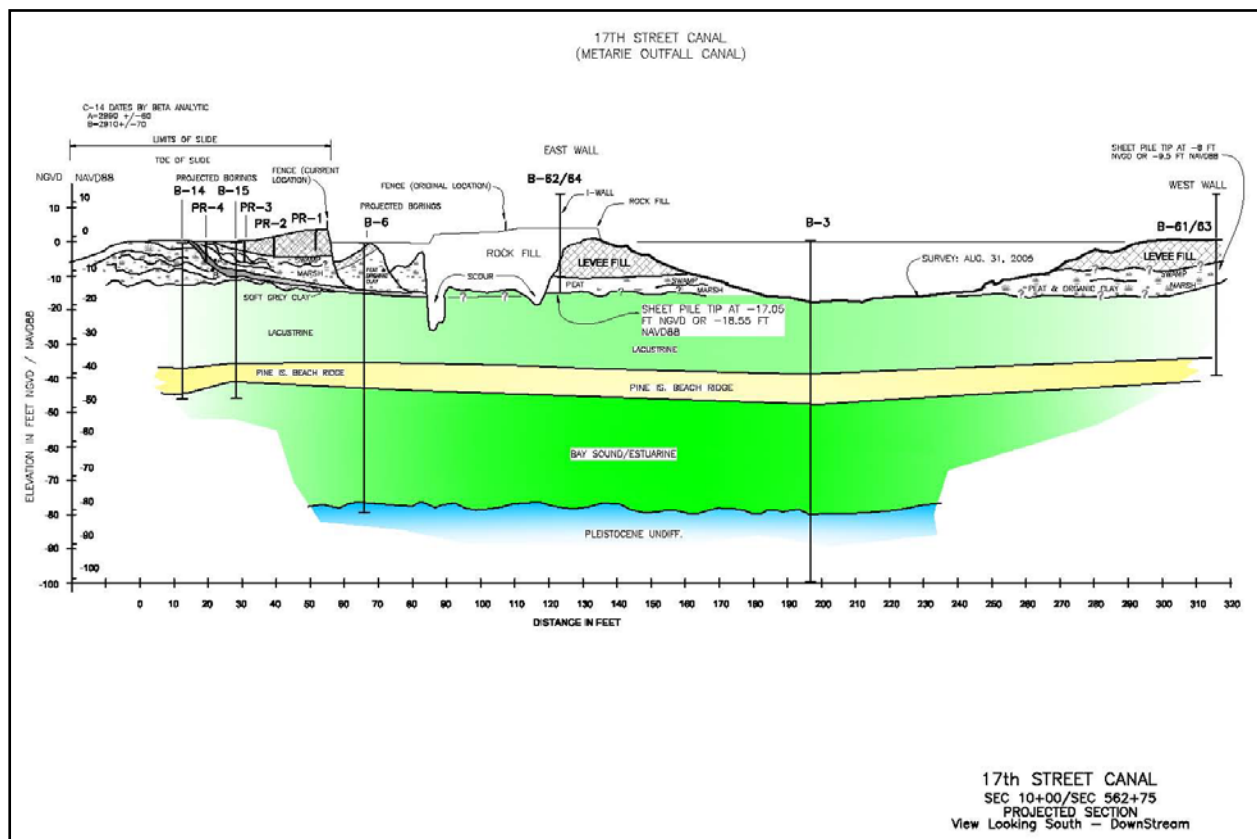


Figure 110. Cross section through the slide block based on continuous soil borings.

The IPET investigation of the northern IHNC breach adjacent to the Lower 9th Ward revealed a failure mode similar to that experienced at the 17th Street breach, deflection of the wall and failure within the underlying weak clay layer, with additional influence of the local

topography. The elevation of the land on the protected side of the floodwall was significantly less than shown in the original design documents, which would have decreased the ability of the levee to withstand the high forces it experienced. The UCB speculation focused on seepage as an issue at this site. Since the geology of the site is similar to that at the 17th Street breach, with weak clay under the pervasive peat layer, it is difficult to find evidence of major seepage through the clay or the peat (Appendices 11 and 17). UCB's assumptions for permeability of the peat were far higher than any measured for the actual materials or published values for similar materials. While these values of permeability would indicate seepage, IPET has found no justification for these assumptions and no physical evidence of seepage being a systemic performance issue at this site.

The second area of significant difference dealt with the performance of the levees, specifically along the MRGO. The UCB report and numerous media accounts attributed to these teams hypothesized that these levees "crumbled" prior to water levels reaching the crest of the levees. There was also stipulation of wave action causing high pore pressures within the levee materials leading to deterioration by slumping and seepage-induced erosion. An analytical basis for these hypotheses has not been presented to date by the UCB Team. The IPET investigation has shown that even if the levees along MRGO were totally constructed of a clean sand, which they were not, the time that the water remained on the unprotected side of the levees due to the Hurricane Katrina surge before it overtopped the levees was not sufficient to establish through seepage and cause erosion of the levees (Appendix 17).

It is true that the relatively permeable and erodible materials of the levees constructed by hydraulic fill did contribute to their ultimate breaching. However, analysis and field observations demonstrate that the UCB/LSU hypothesis was not the systemic process leading to breaching. IPET's analysis of this phenomenon included regional analysis of the surge and wave hydrographs along the levee sections, detailed modeling of wave action and currents in proximity to the levees, and analysis of the erosion process for the materials comprising the levees. The IPET analysis and physical evidence at the sites show that the systemic issue for levee performance was overtopping, and the subsequent erosion from waves and ultimately surge. Where waves were incident perpendicular to the levees, the overtopping waves created velocities on the protected side of the levees up to three times those experienced on the front (water) exposed sides. This created a potential for erosion 27 times more severe on the crest and protected sides of the levees. In addition, claims of wave action increasing pore pressures within the relatively permeable materials of the interior of the levees leading to seepage-induced erosion do not stand the "test of time." The permeability of the materials was not sufficient to allow this process to take place in the time frame of the exposure to high waves and surge.

For levee sections that experienced waves traveling more aligned with their orientation, velocities on the protected sides were significantly lower, and significantly less erosion occurred.

There are meaningful lessons learned in the above examples. In an environment as complex and heterogeneous as this, there are many possible failure modes. It is critical to consider them all in any analysis, planning, or design activity. To do so requires detailed and comprehensive information and analyses with cross checks from independent sources, not always feasible when resources and time are limited. It is particularly important to determine if an anomaly, observed

locally, is just that or a component of a widespread characteristic that represents a systemic performance issue.

Another major lesson learned is that it is not likely that all possible failure modes have been identified or observed for structures in complex geological environments such as in New Orleans. The engineering community should continuously seek additional insights on potential performance for wide ranges of conditions and incorporate as often as possible potential non-traditional behavior modes in their analyses.